The distribution of different fluorescence dyes in the egg and embryo of the zebrafish (*Danio rerio*)

Diplomarbeit

vorgelegt der Fakultät für Biowissenschaften der
Ruprecht-Karls-Universität Heidelberg

Britta von der Goltz

2009

Die vorliegende Arbeit wurde am Institut für Zoologie der Universität Heidelberg in der Zeit vom 15. November 2008 bis 18. August 2009 unter Anleitung von Herrn Professor Dr. Thomas Braunbeck ausgeführt.

Referent: Prof. Dr. Thomas Braunbeck
Institut für Zoologie der Universität Heidelberg

Korreferent: Prof. Dr. Stefan Frings
Institut für Zoologie der Universität Heidelberg

Hiermit erkläre ich, dass ich die vorliegende Diplomarbeit selbständig unter Anleitung verfasst und keine anderen Hilfsmittel als die angegebenen Quellen benutzt habe.

Ort/Datum	Unterschrift

Acknowledgements

I would like to thank everyone who contributed to the completion of my thesis, with special thanks to:

Prof. Dr. Thomas Braunbeck, my first referee, for the possibility to prepare this thesis in his research group and for his suggestion and support.

Prof. Dr. Stefan Frings for the acception to function as second reviewer.

The Nikon Imaging Center for the uncomplicated collaboration and mutual assistance, special thanks to Christian Ackermann for his broad support and his patient training on the confocal microscope.

Dipl. Biol. Kirsten Wendler, for mentoring and introduction into procedures and methods, for the inspiring discussions and proofreading.

Erik Leist for the technical support and the maintenance of the test animals.

Special Thanks to my proof-readers Susanne Keiter, Franziska Förster and Anna von der Goltz who had a really hard job with my excellent English skills.

The working group “Aquatische Ökotoxikologie”, for the nice working atmosphere and teamwork: Cleo, Christopher Fassbender, Franziska Förster, Florian Schmidt, Kirsten Wendler, Lisa Baumann, Nadja Schweizer, Ruben Strecker, Raoul Wolf, Sarah Schnurr, Shoui, Susanne Keiter, Susanne Faltermann, Susanne Knoerr.

My family and friends (especially Vicky von Mach) for all their appreciation and support.

Finally, the line on page 9 which escorted me from the first hour of this document and does not leave my side. Furthermore, Microsoft Word 2007 for the bond of friendship that developed out of this thesis …..

Table of contents

1 Introduction

Aquatic toxicology is the qualitative and quantitative study of adverse or toxic effects of chemicals and other anthropogenic materials or xenobiotics on aquatic organisms (Rand, 1985). Historically, fish have always been used for evaluating acute and chronic toxicity. The scientific community, regulatory bodies and chemical industries have accepted them as representatives of the aquatic environment. The acute fish test has thus long been a mandatory component of initial toxicity testing. However, a closer inspection of existing acute fish data reveals differences in orders of magnitude not only between species, but also within the same species between different laboratories (Braunbeck, 2005). Furthermore, the significance of the death of individual fish after short-term exposure to high toxicant concentrations for environmental risk assessment is low – except in case of accidental spills (Nagel, 2002). In addition to these scientific considerations, ethical concerns have grown, because fish exposed to acutely toxic concentrations of chemicals are likely to suffer severe distress and pain, which is not compatible with current animal welfare legislation. The idea to reduce, refine and replace animal testing by alternative test methods was created as early as 1959 by Russel und Burch (1959) and has now become an inherent part of the new European Chemical Legislation REACH (Registration, Evaluation, Authorisation and Restriction of Chemicals). One alternative to the acute fish toxicity test is the fish embryo test. In 2005, the 48 h toxicity test with fertilized eggs of the zebrafish (*Danio rerio)* (DIN 2001) became mandatory for the routine testing of whole effluent discharges in Germany and, thus, replaced the conventional 96 h acute fish test. Recently, a proposal for a new guideline on fish embryo toxicity for the testing of chemicals has been submitted to the OECD by the German Federal Environment Agency (Braunbeck et al. 2006). Furthermore, Braunbeck et al. (2005) provided data substantiating that an optimized test protocol can equally be applied to the early embryonic stages of other OECD species such as the fathead minnow (*Pimephales promelas*) and the Japannese medaka (*Oryzias latipes*). Lammer at al. (2009) documented that the correlation between the fish embryo test and the acute fish toxicity test is just as good as the correlation between conventional acute fish toxicity tests with different species. However, a small number of substances were identified to differ significantly with respect to in embryonic *versus* adult toxicity. Despite repeated speculations, it could not be clarified unequivocally whether the chorion represents an effective barrier and, thus, protects the embryo from exposure to distinct chemicals.

The chorion surrounds the embryo and is a 1.5 - 2.5 µm thick acellular envelope. Rawson (2000) studied the structure of the chorion of *Danio rerio* by using field emission scanning electron microscopy (FE-SEM) and transmission electron microscopy (TEM). This study confirms the outer chorion membrane complex to consist of three layers: electron-dense outer and innermost layers (thickness: 0.2 - 0.3 and 1.0 -1,6 µm, respectively) and an electron-lucent intermediate layer (thickness: 0.3 - 0.6 µm) (Fig. 1.1). The middle and inner layers are pierced by pore canals. The diameter of the outer opening of the pore canals is 0.5 - 0.7 µm and the centre-to-centre distance 1.5 - 2.0 µm. The pores are cone-shaped with a larger diameter at the inner surface and display a corkscrew-like ridged wall with lamellae ringing the inner surface of the pore canal. These pores have been reported to potentially restrict the uptake of compounds depending on their size. Therefore, an essential aspect of the permeability of the chorion is the molecular weight. Polymers and high molecular weight surfactants (~ 40 000 – 100 000 g/mol) are suspected to be blocked by the chorion, since comparison between embryo, eleutheroembryo toxicities (Leonard et al. 2005), and dechorionated embryos (Wendler et al., in prep. 2009) resulted in considerably higher sensitivity of both the latter. Creton (2004) investigated the inhibition of the ER Ca^{2+} pump in zebrafish embryos and established that the chorion is permeable to fluorescent dextrans of 3000 Da, but is not permeable to fluorescent dextrans of 10.000 Da (data not shown). To locate a "critical molecular size", which would not allow a substance to pass the chorion, polymers present themselves to be an ideal test substance: a polymer is a macromolecule composed of repeating identical structural units typically connected by covalent chemical bonds, which are available in various molecular weights. Since the basic unit is always the same, no additional functional groups which might interact with the chorion are introduced.

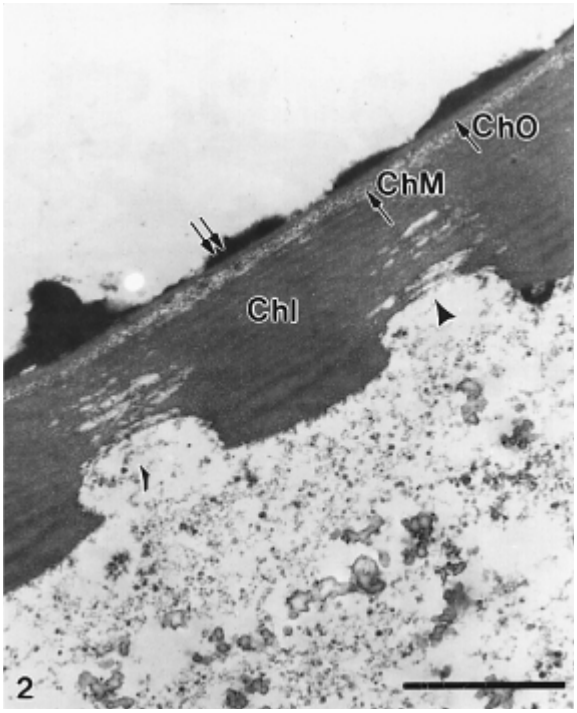

Figure 1.1: TEM view of gastrula-stage embryo showing the chorion consisting of three layers. The outer (**ChO**) and innermost layers (**ChI**), 0.2-0.3 µm and 1.0-1.6 µm in thickness, respectively, are electron dense and separated by a 0.3-0.6 µm thick, low-contrast middle layer (**ChM**). The middle and inner layers are pierced with pores (▲). The outermost layer of the chorion is visible as distinctive projections (↑↑); Bar = 1 µm (Rawson 2000)

Due to the size evidences of between 3 kDa and 10 kDa (Creton 2004), in this study Dextran fluorescein of between 3 and 40 kDa are tested on their ability to pass the chorion.

Moreover, there is limited evidence that the permeability of the chorion changes during the embryonic development and that, after hardening, the chorion is less permeable (Gellert el al. 2001) and might then function as a barrier for even smaller molecules. Ozoh (1980) found dechorionated zebrafish embryos to be more sensitive against copper intoxication than non-dechorionated embryos, which corroborated several other studies with different teleost species showing accumulation of different heavy metals at or within the chorion (Wedemeyer 1968; van Leeuwen et al. 1985; Stouthart et al. 1994). Only few studies indicated a weak barrier function of the zebrafish chorion for lipophilic substances such as γ-hexachlorocyclohexane (lindane; Braunbeck et al. 2005) and small substances such as dimethylsulfoxide (DMSO; Harvey 1983). The same seems to hold true for substances like cypermethrine and thiobencarb in other teleost species like the medaka (*Oryzias latipes*; Villalobos et al. 2000; Gonzalez-Doncel et al. 2004).

The fish embryo test is a promising choice for future toxicological routine testing; therefore, the knowledge of the distribution of substances with different physical and chemical characteristics is a crucial prerequisite for the application of this method. Different parameters such as lipophilicity, molecular weight, different substituents and different charging, are important for distribution and for ecotoxicological issues. This study focuses on a selection of some of these parameters; their specific importance for the aquatic toxicology is explained briefly.

The usage of fluorescence dyes allows the visualization of test substances and, thus, their uptake into the egg as well as its accumulation can be followed. Wavelength and amount of the emitted energy depend on both the fluorophore and the chemical environment of the fluorophore (Tsien, 1995). The two well-known classes of highly fluorescent dyes, rhodamines and fluoresceins, are derivatives of xanthenes and belong to heterocyclic compounds.

Heterocyclic compounds are organic compounds containing at least one atom of carbon, and at least one element other than carbon, such as sulfur, oxygen or nitrogen within a ring structure (Eicher, 2003). Therefore, the structure of rhodamine and fluorescein is similar to that of polycyclic aromatic hydrocarbons (PAHs), which are chemical compounds consisting of fused aromatic rings and do not contain heteroatoms or carry substituents (Fetzer, 2000). PAHs are some of the most widespread organic pollutants. Polycyclic aromatic hydrocarbons are lipophilic. Water solubility and P_{ow}, the partition coefficient for octanol and water, are core parameters due to their importance for the quantitative description of many processes in the environment, and they are the basis for the estimation of toxicological parameters and, in particular, biological parameters such as bioaccumulation (Fiedler & Lau 1998). Octanol provides a reasonable surrogate for biota lipid in most situations. Thus, bioconcentration behavior with aquatic organisms can generally be predicted by relationships such as the octanol/water partition coefficient (Connell, 1998). In most risk assessments, substances with a log $P_{ow} > 3$ are considered to have a high potential for causing harm (Fiedler & Lau 1998). Chemicals most susceptible to bioaccumulation are those chlorohydrocarbons and polyaromatic hydrocarbons with log P_{OW} values between 2 and 6.5 (Connell, 1998).

In addition to their similarity to PAHs, rhodamine and fluorescein are ecologically relevant by themselves. Uranin is the water-soluble sodium salt of fluorescein and has been used in river systems, most notably in the case of the Chicago River, where fluorescein was the first substance used to dye a river green on St. Patrick's Day in 1962. In industrial applications, it is used to color automotive coolants (anti-freeze), for dying wool and silk, as an Air-Sea rescue marker, as ground water tracing dye, soap solutions and for the coloring of agrochemicals and fertilizers. Rhodamines are used as dyes for paper and textiles, also in luminous pigments, in dye lasers, as well as in cell biology, where they have served as markers in fluorescence microscopy.

Apart from water solubility and the partition coefficient, there are also other parameters, which have to be considered, like the Topological Polar Surface Area (TPSA), which is an estimation of the polar fraction of the molecular surface area (Ertl, P, 2000). Similar to the physicochemical parameters, such as the influence of the particular structure and its complexity, it affects the environmental impact and toxicological potential. The complexity rating of the compounds is a rough estimate of how complicated a structure is, in terms of both elements and the displayed structural features including symmetry. Generally, larger

compounds are more complex than smaller ones, but highly symmetrical compounds or compounds with few distinct atom types or elements are downgraded (PubChem).

Substituents are another important feature for ecotoxicological aspects. They have different characteristics and cause specific chemical reactions. Organochlorines are typically nonaqueous and are usually denser than water due to the presence of heavy chlorine atoms. Some types of organochlorines exert significant toxicity to plants or animals, including humans, such as dioxins, produced when organic matter is incinerated in the presence of chlorine, and some insecticides such as DDT are persistent organic pollutants which pose danger when they are released into the environment. Chlorinated organics belong to the persistent organic pollutants (POPs), which are resistant to environmental degradation through chemical, biological and photolytic process (Ritter, 2007). One important aspect of their chemical properties, namely lipid solubility, results in the ability to pass biological phospholipid membranes and bioaccumulate in the fatty tissues of living organisms. Therefore substances of low biological degradability tend to accumulate throughout trophic levels of the food chain (Ritter, 2007). The behavior of substituents with charged moieties, such as sulfo groups or other functional groups like carboxylic acid (COOH), also known as carboxyl group, is also of interest.

The present study investigates the mechanism of the uptake and distribution of fluorescent dyes with different chemical characteristics. As mentioned above, lipophilicity, molecular weight, different substituents, as well as different charging are important issues for ecotoxicological questions. Rhodamine b and sulforhodamine b were representatives for good water solubility and low log P_{ow}. Fluorescein is a small molecule and is regarded as a basic molecule. This study investigates how the chemical behavior of fluorescein might change with the insertion of two chlorine atoms or with an additional carboxy-group. In addition, the solvent behavior of dimythyl sulfoxide (DMSO) in different concentrations was investigated separately. The eggs and embryos were examined after 24 h and 48 h in the standard fish embryo toxicity test (FET) according to DIN 38415-T6 and ISO 15088 (DIN 2001; ISO 2007). The time between 26 h and 48 h (called pre-hatching) is especially important for the question of distribution, given the fact that the structure of the chorion changes during this time. The experimental results of Kim (2004) quantitatively describe “chorion softening” which is mostly due to the proteolytic activity at the pre-hatching stage.

2 Material & Methods

2.1 Test substances

Fluorophores are components of molecules which render other molecules fluorescent. It is a functional group in a molecule, which will absorb energy of a specific wavelength and re-emit at a longer wavelength (e.g. Fig. 2.1.1). This difference in wavelength between the positions of the band maxima of absorption and emission spectra is called stokes shift, named after the Irish physicist George G. Stokes.

All test substances are characterized by molecular weight, log P_{ow}, water solubility, excitation maximum, emission maximum, topological polar surface area (TPSA) and complexity (Tab. 2.1-2.5). TPSA is a simple method, only nitrogen and oxygen are considered (3d coordinates are not used) and there are various precomputed factors for different hybridizations, charges and participation in aromatic systems. The complexity is computed using the Bertz/Hendrickson/Ihlenfeldt formula (Hendrickson, J.B 1987 and Ihlenfeldt 1991). A scaling factor for aromaticity is used, so that the complexity of benzene is the same as that of cyclohexane. The scaling factor is a floating point value ranging from 0 (simple ions) to several thousand (complex natural products). As mentioned, larger compounds are more complex than smaller ones, but highly symmetrical compounds or compounds with few distinct atom types or elements are downgraded. However, neither stereochemistry nor isotope labeling are used as auxiliary criteria. (PubChem, data from National Cancer Institute (NCI) open database).

2.1.1 Test substances with high water solubility

Water solubility and P_{ow}, the partition coefficient for octanol and water, are core parameters for aquatic toxicology, because they may be used as predictors for the behavior of chemicals in water and biological systems. Test substances with good water solubility have a low log P_{ow} and a smaller topological polar surface area (TPSA).

Rhodamine b

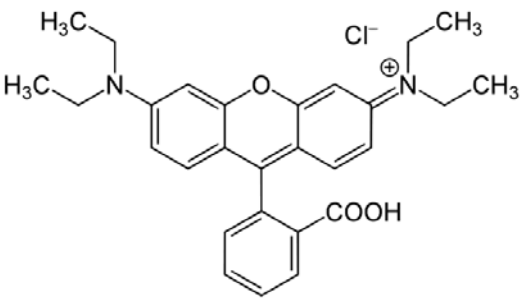

Figure 2.1.1: Chemical structure of rhodamine b

Rhodamines (Fig. 2.1.1) are derivatives of xanthenes and were among the first fluorescent dyes to be used as laser dyes. Their absorption and emission spectra are quite narrow and the maximum emission is at ca. 566 nm (Fig. 2.1.2). They have good water solubility, a relatively small polar surface area and average complexity (Tab. 2.1).

Table 2.1: Physical and chemical characteristics of rhodamine b

CAS number:	81-88-9	Excitation max.[4]:	545 nm
Molecular weight[1]	479,01 g/mol	Emission max.[1]:	566 nm
log P_{ow}[2]:	2.28	Polar Surface Area[5]	52.8
Water solubility[3]:	15.8 g/L	Complexity[5]	811

[1]Sigma Aldrich; [2]Calculated with software from LOGKOW© provided by Sangster Research Laboratories; [3]Merck Index; [4]Sigma Aldrich (Excitation in 0.1 M Tris by pH 8.0); [5]PubChem

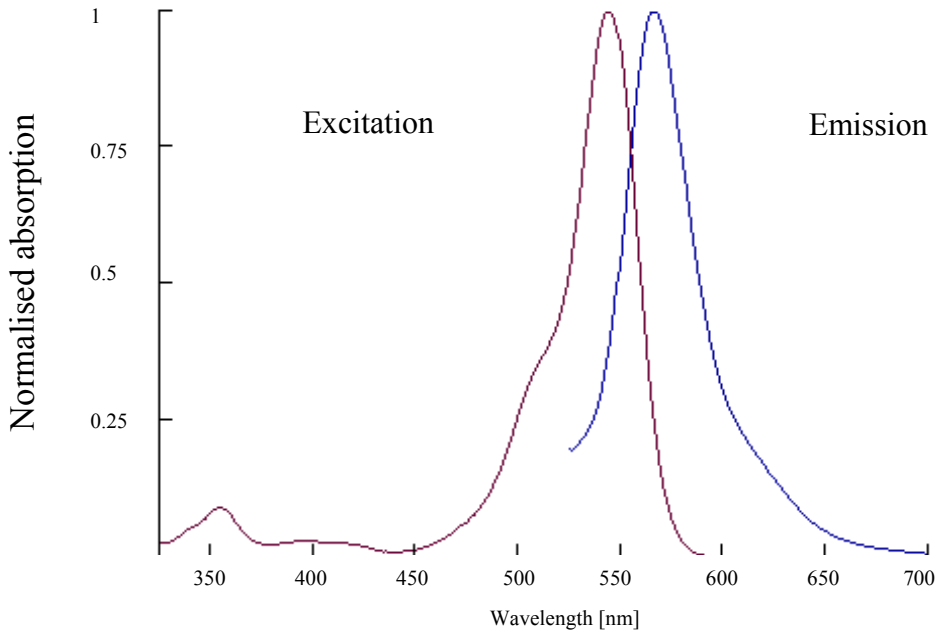

Figure 2.1.2: Absorption and fluorescence emission spectra of rhodamine b; wavelength in nm

Sulforhodamine B

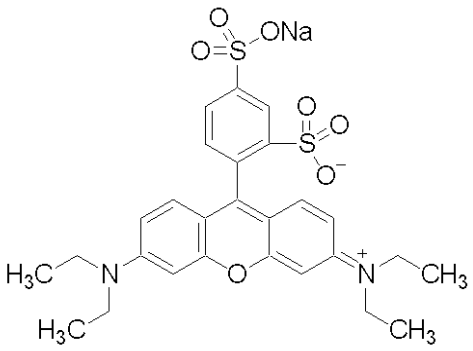

Figure 2.1.3: Chemical structure of sulforhodamine b

If compared to rhodamine b, sulforhodamine b has two sulfo groups (Fig. 2.1.3), derived from sulfuric acid. Sulfuric acid has a log P_{ow} of - 0.5; therefore, the log P_{OW} of sulforhodamine b is lower than the log P_{ow} of rhodamine b. As a result of increased polar surface area, the complexity of the whole molecule increases, whereas the water solubility decreases (Tab. 2.2) The dye absorbs 566 nm and emits 584 nm light (Fig. 2.1.4). Sulforhodamine b is primarily used as a polar tracer. Absorption or fluorescence is not pH-dependent over the range of 3 to 10 (Coppeta 1998).

Table 2.2: Physical and chemical characteristics of sulforhodamine b

CAS number:	3520-42-1	Excitation max.[3]:	566 nm
Molecular weight[1]:	580.65 g/mol	Emission max.[1]:	584 nm
log P_{ow}[2]:	1.44	Polar Surface Area[4]	130
Water solubility[2]:	4.45 g/L	Complexity[4]	1150

[1]Sigma Aldrich; [2]Calculated with software from LOGKOW© provided by Sangster Research Laboratories; [3]Sigma Aldrich (Excitation in 0.1 M Tris by pH 8.0); [4]PubChem

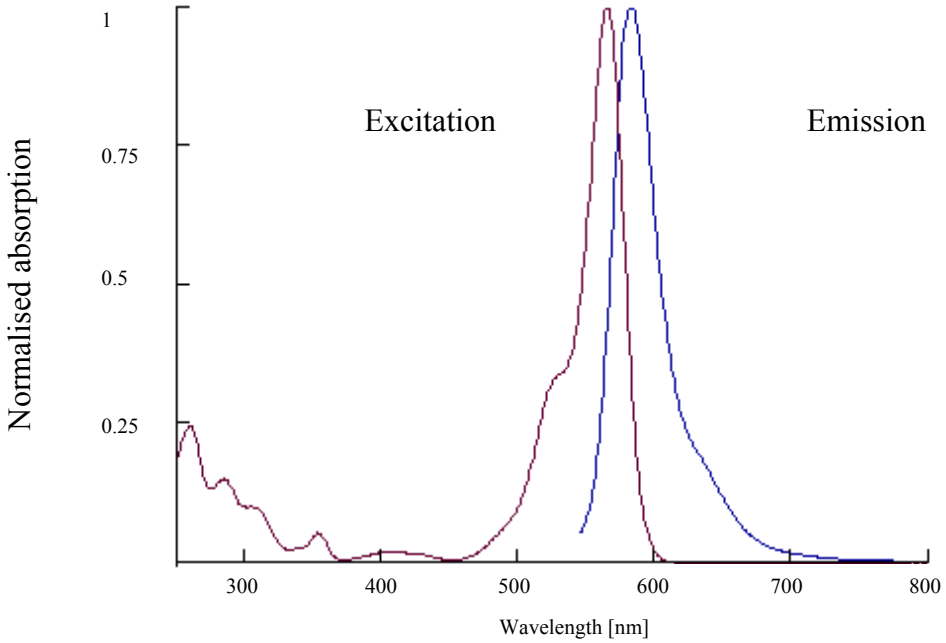

Figure 2.1.4: Absorption and fluorescence emission spectra of sulforhodamine b

2.1.2 Test substances with a low water solubility

Low water solubility correlates with a high partition coefficient for octanol and water (log P_{ow}).

Fluorescein

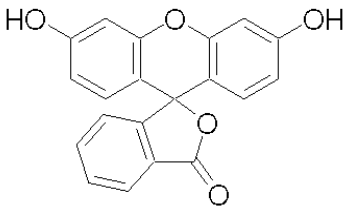

Figure 2.1.5: Chemical structure of fluorescein

The second family of xanthene dyes consists of fluorescein and its derivatives. Fluorescein (Fig. 2.1.5), the smallest molecule tested in this study with log P_{ow} of 3.4 (Tab. 2.3). Fluorescein, itself is only slightly fluorescent in alcoholic solutions. In contrast, the alkali salt obtained by addition of alkali exhibits the well-known yellow-green fluorescence characteristic of the fluorescein to dianion (uranin). Fluorescein and its derivatives are known to be very sensitive to pH and can thus be used as pH-dependent fluorescent probes. Therefore, the absorption (and excitation) spectrum depends on pH in the investigated range. Fluorescein has an excitation maximum of 490 nm and emission maximum of 514 nm (in 0.1 M Tris by pH 8.0) (Fig. 2.1.6). Using fluorescein has a few disadvantages: the fluorescence lifetimes of the protonated and deprotonated forms of fluorescein are approximately 3 and 4 ns, respectively. The reduction of fluorescence emission intensity is known as photobleaching phenomenon. Photobleaching is an irreversible degradation of the fluorescent molecule in the excited state, caused by the interaction with molecular oxygen before emission. To reduce these phenomena, some safety precautions must be taken: the time frame for investigation should be identical; the stock solution must be kept in the dark and should not be used if it is older than one week (Harris & Mutz 2006). It is also important that the microtiter plates are protected from light throughout the test period, e.g. with aluminum foil.

Table 2.3: Physical and chemical characteristics of fluorescein

CAS. Nr.:	2321-07-5	Excitation:[3]	490 nm
Molecular weight[1]:	332.30 g/mol	Emission max.[1]:	514 nm
log P_{ow}[4]:	3.4	Polar Surface Area[4]	76
Water solubility[2]	25 mg/L	Complexity[4]	522

[1]Sigma Aldrich; [2]Calculated with software from LOGKOW© provided by Sangster Research Laboratories; [3]Sigma Aldrich (Excitation in 0.1 M Tris by pH 8.0); [4]PubChem

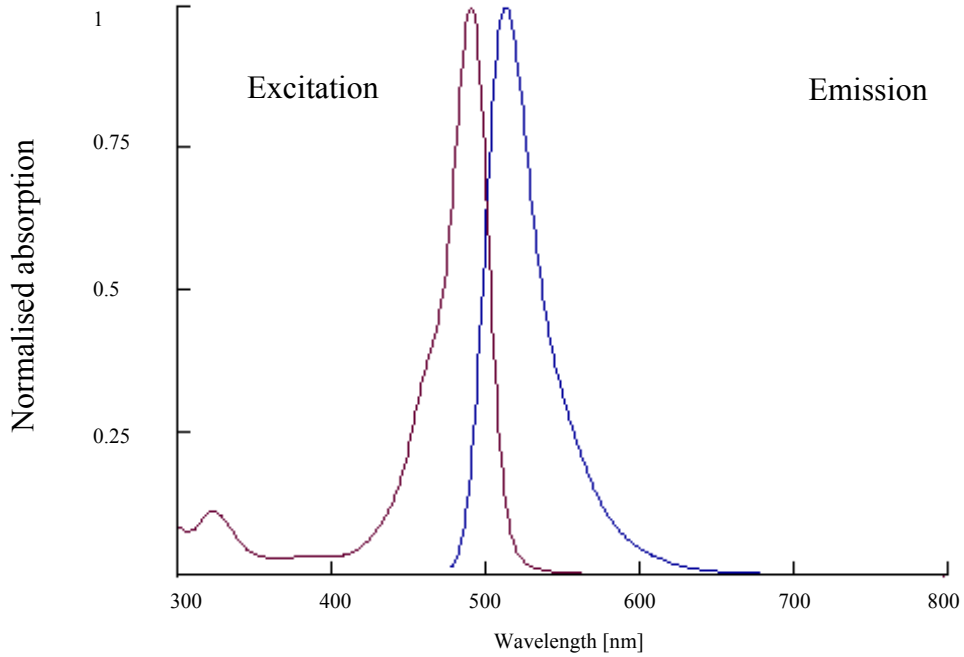

Figure 2.1.6: Absorption and fluorescence emission spectra of fluorescein

2,7-Dichlorofluorescein (DCF)

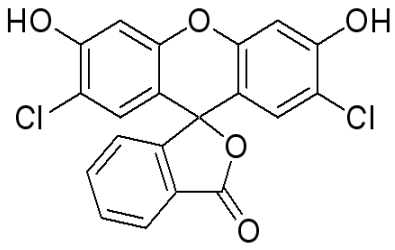

Figure 2.1.7: Chemical structure of 2,7-dichlorofluorescein

In comparison to fluorescein, 2,7-dichlorofluorescein is additionally chlorinated (Fig. 2.1.7). The lipophilicity of DCF is correlated to a high log P_{ow} (1.3 times higher than for fluorescein); therefore, its water solubility is much lower than that of fluorescein. However, the polar surface from fluorescein and DCF is exactly the same, whereas the complexity of DCF is about 12 % higher (Tab. 2.4). DCF has an excitation maximum of 504 nm and an emission maximum of 529 nm (in 0.1 M Tris at pH 8.0) (Fig. 2.1.8). The photobleaching of DCF is not as fast as that of fluorescein.

Table 2.4: Physical and chemical characteristics of 2,7-dichlorofluorescein

CAS. Nr. :	76-54-0	Excitation[1]:	504 nm
Molecular weight[1]:	401.20 g/mol	Emission max.[3]	529 nm
log P_{ow}[4]:	4.7	Polar Surface Area[4]	76
Water solubility[2]:	2.34 mg/L	Complexity[4]	585

[1]Sigma Aldrich; [2]Calculated with software from LOGKOW© provided by Sangster Research Laboratories; [3]Sigma Aldrich (Excitation in 0.1 M Tris by pH 8.0); [4]PubChem

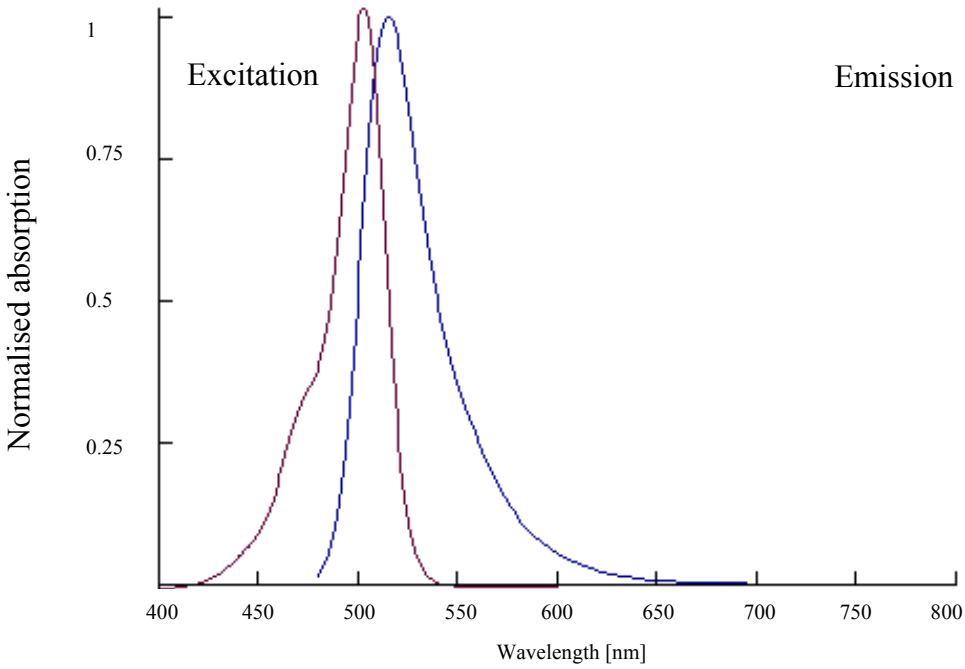

Figure 2.1.8: Absorption and fluorescence emission spectra of 2,7-dichlorofluorescein

5-(and-6)-Carboxy-2,7-Dichlorofluorescein (CX-DCF)

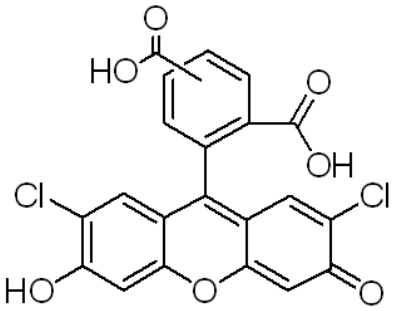

Figure 2.1.9: Chemical structure of CX-DCF

Compared to 2,7-dichlorofluorescein, CX-DCF has a second carboxy group (Fig. 2.1.9); therefore, its complexity and polar surface area are about three times higher. The high log P_{ow} and the low water solubility indicate increased lipophilicity (Tab. 2.5**).** CX-DCF has the same excitation and emission maxima as DCF (Fig. 2.1.10).

Table 2.5: Physical and chemical characteristics of 5 (and-6)-Carboxy-2,7-dichlorofluorescein

CAS. Nr. :	111843-78-8	Excitation[1]:	504 nm
Molecular weight[1]:	890 g/mol	Emission max.[3]	529 nm
log P_{ow}[2]	5.51	Polar Surface Area[4]	242
Water solubility[2]:	0.54 mg/L	Complexity[4]	1780

[1]Sigma Aldrich; [2]Calculated with software from LOGKOW© provided by Sangster Research Laboratories; [3]Sigma Aldrich (Excitation in 0.1 M Tris by pH 8.0); [4]PubChem

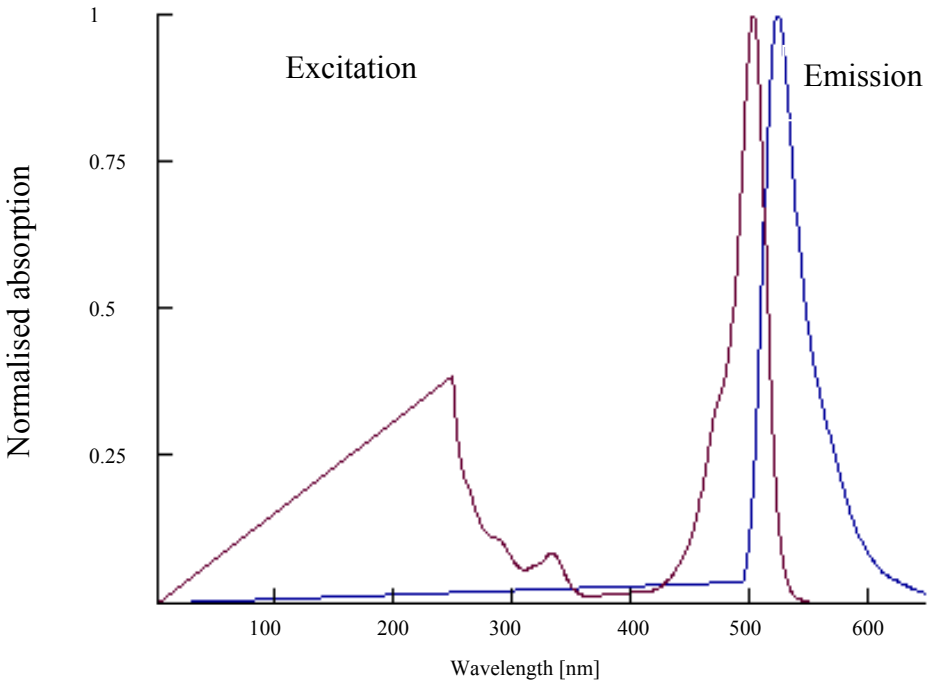

Figure 2.1.10: Absorption and fluorescence emission spectra of 5-(and-6)-carboxy-2,7-dichlorofluorescein

2.1.3 Test substances with different molecular weights

Dextran- fluorescein 3000 Da and 40.000 Da, anionic

Dextran conjugates are hydrophilic polysaccharides synthesized by *Leuconostoc* bacteria. They are characterized by their high molecular weight, good water solubility, low toxicity, and relative inertness. Moreover, their biologically uncommon α-1,6-polyglucose bonds are resistant to cleavage by most endogenous cellular glycosidases; therefore dextran, conjugates represent ideal long-term tracers for the uptake and internal processing in fish eggs. The solubility of dextran conjugates decreases with increasing molecular weight; thus, the maximum solubility in aqueous buffers is about 100 mg/mL for 3 kDa and about 36 mg/mL for 40 kDa. Invitrogen™ supplies dextrans with nominal molecular weights (MW) of 3 kDa and 40 kDa. Since unlabeled dextrans are polydispers (and may become even more so during the chemical processes required for their modification and purification), the actual molecular weights present in a particular sample may have a broad distribution. Therefore, Invitrogen specifies that dextran-fluorescein 3 kDa contains polymers with molecular weights predominantly in the range of ~ 1.5-3 kDa and the 70 kDa dextran preparations contain polymers with molecular weights ranging from 60 to 90 kDa, so that the dextran- fluorescein 40 kDa will also have a broad distribution. Dextran labeled with fluorescein has an excitation maximum of 494 nm and an emission maximum of 521 nm (Invitrogen™, Product information, 2006) (Fig. 2.1.11).

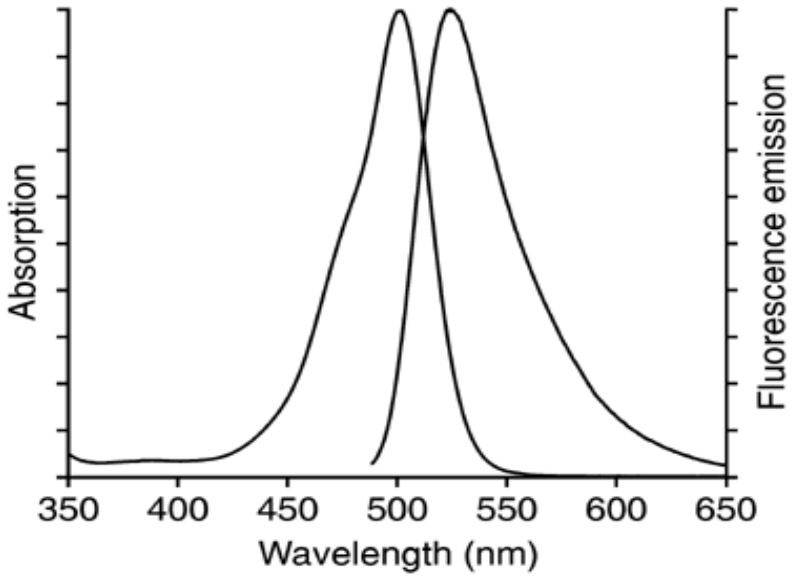

Figure 2.1.11: Absorption and fluorescence emission spectra of dextran- fluorescein

2.2 Fish embryo toxicity test (FET)

2.2.1 Materials

The polystyrene 24-well microtiter plates were provided by Renner (TPP; Dannstadt, Germany), and the self-adhesive foil (clear polyester sealing tapes) was purchased from Nunc (Langenselbold). Agarose was provided by SeaKem (HGT Agarose, Cambex BioScience Rockland, ME, USA; gelling temperature: 40.5°C - 43.5°C). DMSO (Sigma Aldrich, Deisenhofen, Germany) was tested at 24 hours post fertilization (hpf) and 48 hpf at exposure concentrations of 0.01 %, 0.1 %, and 1 %. The positive control, 3,4-dichloroaniline (p.a.) and all chemicals were of highest analytical standard available and were purchased from Sigma-Aldrich, unless noted otherwise. The artificial water corresponded to reconstituted water according to ISO 7346/3 (ISO 1996; conductivity: 700 µS/L, NO_3^-: < 4.5 µg/L, NO_2^- < µg/L, NH_4^+: < 1.9 µg/L, PO_4^{3-}: < 50 µg/L; Fe^{2+} and Fe^{3+} not detectable; chemical oxygen demand (COD): < 4 mg/L), which was diluted 1:5 using double-distilled water. Before use, the pH was adjusted to 7.8 ± 0.2.

2.2.2 Test organism system

Fish maintenance

For egg production, a brood stock of zebrafish aged between 6 and 24 months was used. All fish were free of externally visible symptoms of disease and did not receive any pharmaceutical (acute or prophylactic) treatment for 6 months before spawning. For housing, fish were kept in glass aquaria providing sufficient space for swimming (i.e. ≥ 1 L per fish). For both housing and breeding, standardized dilution water as specified in ISO 7346-1 and ISO 7346-2 (294.0 mg/L $CaCl_2 \cdot 2\ H_2O$; 123.3 mg/L $MgSO_4 \cdot 7\ H_2O$; 63.0 mg/L $NaHCO_3$; 5.5 mg/L KCl) or suitable drinking water with ≥ 80 % oxygen saturation was used. Constant filtering or permanent flow-through conditions guaranteed that ammonia, nitrite, and nitrate were kept below detection limits. Temperature was maintained at 26.0 ± 1.0 °C, and fish were kept under a constant artificial dark:light cycle of 16:8 hours. Fish were fed commercially available artificial diets (e.g., TetraMin™ flakes; Tetra, Melle, Germany) twice daily; especially the day before breeding, food was supplemented with *Artemia* nauplii or small daphnids of appropriate size obtained from an uncontaminated source. Overfeeding was strictly avoided to ensure optimal water quality; remaining food and feces were removed daily.

Egg production

The evening before a test, males and females in a ratio of 2:1 were transferred into breeding chambers immediately before artificial sunset (Braunbeck et al., 2005). Breeding chambers were coated with black silicone except for the front to block sight to neighboring tanks and top-coated with a grid to prevent fish from jumping out of the tank. The bottom was replaced by a stainless steel grid with a mesh size of 1.25 mm to prevent the spawn from being eaten by the adult fish. As a special stimulant, a green plastic plant dummy was used. Mating, spawning and fertilization took place within 30 min after the onset of light in the morning. Eggs dropped into rectangular full-glass dishes placed underneath the spawning tanks. About 30-60 min. after spawning, the spawning dishes were removed, and the eggs were transferred to a dissecting microscope. After determining the overall egg number, viable (i.e. fertilized) eggs were selected for testing.

Standard fish embryo toxicity test (FET) with fluorescent dyes

The standard FET with fluorescent dyes was conducted according to DIN 38415-T6 and ISO 15088 (DIN 2001; ISO 2007): Embryo tests were initiated 3 h after fertilization (~128 cell stage) at the latest. In order to start exposure to the fluorescent dyes with minimal delay, at least 20 freshly-spawned zebrafish eggs were selected per concentration and transferred to 60 mm crystallization dishes containing 20 mL of the different test concentrations, the positive control and the negative control, respectively. As a negative control, artificial water was used and as a positive control 3,4-dichloroaniline at 3.7 mg/L was tested. To identify the spectrum of suitable concentrations, in which LOEC (lowest observed effect concentration) and NOEC (no observed effect concentration) (48 hours) could be determined, it was necessary to conduct a screening test. The LOEC is defined as the concentration at which at least 20 % of the embryos showed an effect and the NOEC shows the concentration at which ≤ 10 % of the embryos showed effects. As endpoints for effects, the following lethal and sublethal effects (Table 2.6) were used according to DIN (2001) as well as to Bachmann (2002) and Nagel (2002). For finding the EC_{10}, different concentrations of the fluorescent dyes were tested (Tab. 2.7). Additionally, eggs exposed to 1 % DMSO were used as a solvent control.

Table 2.6: Endpoints for evaluating the toxicity of chemicals on embryos of *Danio rerio* (according to Bachmann (2002), Nagel (2002) and DIN 38415-6 (DIN 2001))

Toxicological endpoints	Exposure time [hours]	
	24	48
Coagulation	#	*
Retarded somite stage	#	*
Tail not detached		*
Lack of heartbeat	#	*
Lack of spontaneous movement		
Failure of hatching		
Reduced heartbeat rate		+
Lack of blood circulation		+
Reduced blood circulation		+
Tail/spine deformation		+
Underdevelopment	+	+
Oedema formation		+
Malformation in general	+	+

*****lethal endpoint according to DIN 38416-6; **#** lethal endpoint;
+ sublethal endpoint

Table 2.7: Concentrations of fluorescence dyes tested (results are listed in the appendix)

Fluorescent dye	Test run	concentrations tested [mg/L]
Rhodamine b	V_1	5, 75, 150, 225, 300, 400, 500
	V_2	5, 45, 90, 130, 170, 215, 300
	V_3	5, 45, 90, 130, 170, 215, 300
Sulforhodamine b	V_1	5, 10, 50, 100, 500, 1000
	V_2	50, 125, 200, 275, 350, 425, 500
Fluorescein	V_1	1, 5, 10, 50, 100, 500, 1000
	V_2	25, 50, 100, 200, 300, 400, 500
	V_3	50, 100, 200, 300
2,7- Dichlorofluorescein	V_1	5, 10, 25, 50, 100, 200, 300
	V_2	50, 65, 85, 100
5-(and-6)-Carboxy-2,7-dichlorofluorescein	V_1	10, 25, 50, 80

Subsequently, 10 fertilized eggs were selected for each test concentration and transferred to 24-well plates filled with 2 ml freshly prepared test solutions and controls or dilution water per well. For pre-saturation, 24-well plates had been pre-treated with the respective concentrations 24 h prior to the exposure of the embryos. The 24-well plates were then covered with self-adhesive foil and incubated at 26.0 C ± 1.0°C. The embryos were examined after 24 h and 48 h following the standard FET. Evaluation of the development was done according to DIN 38415-T6 and ISO 15088 (DIN 2001; ISO 2007). The EC_{10} was determined graphically by linear interpolation. Embryo tests were classified as valid, if the mortality in the negative control was ≤ 10 %, and the positive control showed mortalities between 20 % and 80 %.

2.3 Measurement of fluorescence

Experimental design

The suitable concentration of fluorescence dye is a compromise between EC_{10} (criteria see Tab. 2.6) and a good fluorescence signal. Table 2.8 shows the concentrations, which were chosen for the observation. The concentrations represent the EC_{10}-EC_{20} values (results of the pre-tests, see appendix)

Table 2.8: Concentrations of the fluorescence dyes used

Fluorescence dye	concentration [mg/L]
Rhodamine b	100
Sulforhodamine b	200
Dextran 3000 Da	50
Dextran 40000 Da	50
Fluorescein	100
DCF	50 und 65
CX-DCF	80

In the first test series, the eggs were not dechorionated after 24 hours; therefore, only those larvae which hatched after 48 hours were investigated. The second test series was a

combination between epi-fluorescence microscopy and confocal laser scanning microscopy (CLSM). The eggs were always compared with dechorionated embryos after 24 h and 48 h. Parallel to each observation, a negative control not exposed to the fluorescence dye was analyzed, for background fluorescence of the egg and the embryo. In addition, the background fluorescence of eggs and embryos exposed to DMSO (Sigma Aldrich, Deisenhofen, Germany) at concentrations of 0.01 %, 0.1 % and 1 %, were tested at 24 and 48 hpf.

Dechorionation

One half of 24 hpf and 48 hpf eggs, which had been exposed to fluorescent dyes, were transferred to agarose-coated petri dishes, and their chorions were removed with sharp forceps (Dumont No. 5). After dechorionation, embryos were carefully transferred by means of pipettes to wells of 24-well microtiter plates filled with 2 ml of dilution water. Hereby, care should be taken to avoid air contact, since the embryos tend to inflate upon air contact.

In each test, two fluorescence dyes were compared; rhodamine b with sulforhodamine b and dextran 3 kDa with dextran 40 kDa. Fluorescein as well as DCF was dissolved in different DMSO concentrations of 0.01 %, 0.1 % and 1 %. CX-DCF was observed separately without a comparative fluorescence and in a DMSO concentration of 0.01 %.

Additionally to the described method, the test was extended to determine the permeability of the chorion after 24 hpf. After exposure of 24 hours, two eggs and two dechorionated embryos were transferred to artificial water, so that they were unexposed over the next 24 hours. For comparison, two 24-hours-old dechorionated embryos were transferred directly into fluorescence dye in order to see if an increased uptake of dye is possible. In this way, it was also possible to determine whether there is an uptake of dye from the chorion, since an increase in signal intensity can only be due to additional dye uptake from the chorion. This extended determination was done with dextran fluorescein with 3 kDa, dextran fluorescein with 40 kDa, fluorescein (in 0.01 % and in 1 % DMSO) and DCF (65 mg/L).

2.3.1 Epi-fluorescence microscopy

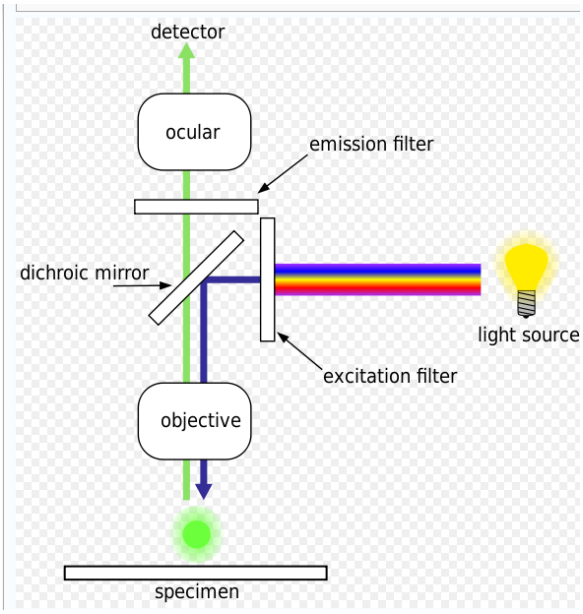

Figure 2.3.1: Schematic of a fluorescence microscope (Blachnicki 2006; polish orginal, derivative work: Mühlpfordt 2008)

The basic function of a fluorescence microscope is to irradiate the specimen with a desired and specific band of wavelengths, and then to separate the much lower emitted fluorescence from the excitation light. In a properly configured microscope, only the emission light should reach the eye or detector so that the resulting fluorescent structures are represented with high contrast against a very dark (or black) background (Fig. 2.3.1).

The limits of detection are generally governed by the darkness of the background, and the excitation light is typically several hundred thousand to a million times brighter than the emitted fluorescence. Wavelengths passed by the excitation filter reflect from the surface of a dichromatic (also termed a dichroic) mirror or beamsplitter through the microscope objective to bath the specimen with intense light. If the specimen fluoresces, the emission light gathered by the objective passes back through the dichromatic mirror and is subsequently filtered by a barrier (or emission) filter, which blocks the unwanted excitation wavelengths.

The common terminology applied to fluorescence microscopy filter combinations has become confusing as a result of the various initials and codes utilized by different manufacturers to identify their filters. Basically, there are three major categories of filters: excitation (often referred to as exciters), barrier (emission), and dichromatic beamsplitters (or dichroic mirrors).

Rhodamine b and sulforhodamine b were filtered by TxRed Chroma 31004 with an excitation spectrum of 560 nm (+/- 40), an emission spectrum of 630 nm (+/- 60) and with a dichromatic beamsplitter of 595 nm. Fluorescein, DCF and CX-DCF were filtered by FITC 31001 with an excitation spectrum of 480 nm (+/- 30), an emission spectrum of 535 nm (+/- 40) and with a dichromatic beamsplitter of 505 nm.

All specimens were imaged with the epi-fluorescence microscope (AZ100 Multizoom microscope, Nikon Instruments Inc., New York, USA) with a 5x-objective (Nikon Plan Flour, NA 0.3, WD 16.0 m). To guarantee comparability, camera and microscope settings were used with fixed values to be the same (Tab. 2.9).

Table 2.9: Camera and microscope settings

Camera Settings:	Microscope Settings:
Format: 1280x1024 no binning	Shutter (EPI) state: Opened
Exposure: auto	Shutter (EPI) mode: Fast
Gain: 1.00x	Light (EPI) Iris intensity: 100.0
Noise Reduction: Off	Condenser: 2 (Low)
Offset: 0.00	Zoom: 2.00x
Contrast: Linear	

Preparation for epi-fluorescence microscopy

The exposed embryos and eggs were washed for three hours; meanwhile, the artificial water was changed three times to avoid external signals. For observation, the eggs and dechorionated embryos were transferred with 1 ml artificial water in a block-glass square bowl with a 2 mm indentation in the middle, ensuring that the pictures of the eggs were always taken in the same position. Eggs and embryos were immobilized with 0.1 % benzocaine.

Distribution in the embryo

Plot Profile

The plot profile is a two-dimensional graph of the intensities of pixels along a line across the image. Image analysis was done with the imaging software imageJ 1.40g (Image Processing and Analysis in Java). The x-axis represents the distance along the line and the y-axis is the pixel intensity. The higher the gray value, the higher the fluorescence is (Handbook, ImageJ Analyze Menu).

ROI manager

The ROI (Region of Interest) manager is a tool for analyzing multiple selections. The selections are from different regions of the embryo and provide an opportunity to compare these inside the embryo. The measured data of mean gray value are exported to Excel™ and can there be analyzed further. The mean gray value is the sum of the gray values of all the pixels in the selection divided by the number of pixels, i.e. an average grey value. It is calculated by converting each pixel values to a single grayscale value using the formula *gray=(red+green+blue)/3*. The intensity of the gray value is determined by the analog to digital converter (ADC) of the camera. An analog to digital converter is a device which converts continuous signals to discrete digital numbers. The digital output uses the gray code scheme. Therefore, the units are non-dimensional (Handbook, ImageJ Analyze Menu).

2.3.2 Confocal laser scanning microscopy (CLSM)

The key feature of confocal microscopy is its ability to produce in-focus images of thick specimens, a process known as optical sectioning. Images are acquired point-by-point and reconstructed with a computer, allowing three-dimensional reconstructions of topologically complex objects. In a confocal laser scanning microscope, a laser beam passes through a light source aperture and is then focused by an objective lens into a small (ideally diffraction limited) focal volume within a fluorescent specimen (Fig. 2.3.2). A mixture of emitted fluorescent light and reflected laser light from the illuminated spot is then recollected by the objective lens. A beam splitter separates the light mixture by allowing only the laser light to pass through and reflecting the fluorescent light into the detection device. After passing a pinhole, the fluorescent light is detected by a photodetection device (a photomultiplier tube (PMT) or avalanche photodiode), transforming the light signal into an electrical impulse that is recorded by a computer (Fellers TJ, Davidson MW, 2007). Image processing was accomplished with the imaging software NIS-Elements 3.0 (Nikon™).

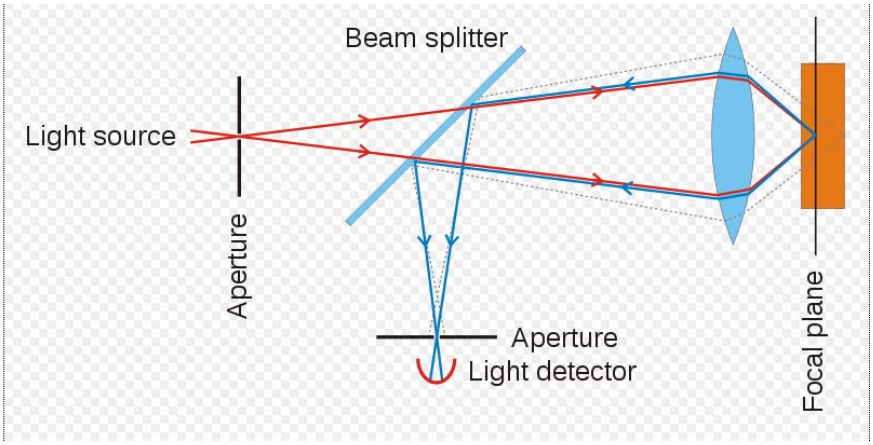

Figure 2.3.2: The principle of confocal microscopy (Haertle 2006)

The detector aperture obstructs the light that is not coming from the focal point, as shown by the dotted gray line in Figure 2.3.2. The out-of-focus light is suppressed, i.e., most of the returning light is blocked by the pinhole, which results in sharper images than those from conventional fluorescence microscopy techniques and permits to obtain images of planes at various depths within the sample (Inoué 2006).

The pictures were described with the laser power (L) and the high voltage (HV) of the photomultiplier for example: L: 15; HV: 14. The highest laser power is 100 which also enables fluorescence dyes with a low brightness to be imaged. Photomultipliers are detectors

which multiply the current produced by incident light by as much as 100 million times. It enables individual photons to be detected when the incident flux of light is very low. Therefore, the higher the high voltage of photomultiplier, the weaker the fluorescence signal is.

Preparation for the confocal laser scanning microscopy (CLSM)

The washing steps of the eggs and embryos followed the same procedure as previously described under "Preparation for the epi-fluorescence microscopy". The CLSM is an inverse microscope, therefore the eggs and dechorionated embryos were transferred into glass bottom culture dishes™ (MatTek Cooperation) for observation. The embryos were embedded in 3 % methylcellulose (viscosity 400, Sigma Aldrich). In contrast, the eggs were transferred only into artificial water for observation, because they would lose water in methylcellulose and would begin to shrivel. Eggs and embryos were immobilized with 0.1 % bezocaine.

3 Results

The aim of this study was to determine the uptake and distribution of fluorescent dyes with different chemical characteristics in eggs and embryos of the zebrafish. The following section will give a short impression of the embryonic development after 24 and 48 hours according to Kimmel et al. (1995) and Westerfield (2000).

Fig. 3.1-H shows the development stage with the most prominent organs after 24 hours post fertilization (hpf). The length of the embryo is 1.9 mm and there are about 30 somites, 13 of them located in the tail. This stage is called the straightening period. The final body shape of the fish larva can already be recognized, since the tail has detached completely from the yolk, the caudal fin enlarges and the pectoral fins develop. The embryo performs spontaneous movements like contractions of the tail and the trunk. The anlagen of the eyes are visible, and the iris can be differentiated from the rest of the eye. The heart is formed and detectable as a cone-shaped tube. The heart begins to beat just prior to this stage. The heart beat first lacks a definite direction of beat, and the rhythm may interrupt. After 26 hpf, the heart tube is elongated and the blood cells begin to circulate.

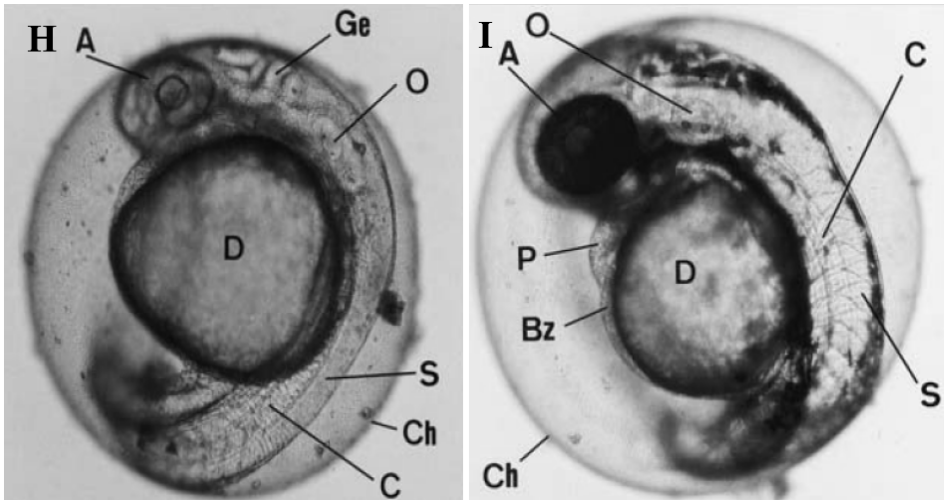

Figure 3.1: 24 hpf (H) and 48 hpf (I) selected stages of the embryonic development of *Danio rerio* (pictures: Marc Rudolf (Rudolf, 2000))

A: eye anlage/eye; **Bz**: blood cells; **C**: chorda; **Ch**: chorion; **D**: yolk sac; **Ge**: brain anlage; **O** ear bud; **P**: pericardium; **S**: somites

Fig. 3.1-I shows the stage of development after 48 hpf. At the age of 30 hours, the embryo is about 2.5 mm long and the growth rate is reduced. The tail has nearly reached end of morphogenesis, and the tail bud is no longer present. Cells throughout the pigmented layer of the retina develop visible pigment granules, and melanophores begin to migrate into the different regions of the body and form star-shaped melanocytes. Heart beat is becoming more prominent and rhythmic. The blood slowly circulates. In the period between 48 and 72 hpf, the embryo grows in size and uses up most of the remaining yolk. Pectoral fin rays develop and become vascularized. The pigmentation pattern becomes more and more distinct and spreads all over the body. The heart beat becomes continuous and levels off at 3 beats per second. Blood circulation becomes prominent in all arches and becomes visible in the pectoral fin. Also, intestinal tract and liver are developed.

3.1 Rhodamine b

3.1.2 Pre-test

To identify suitable test concentrations at which on the one hand the fluorescence signal was strong, but on the other hand an effect level of 10 % was not exceeded, it was necessary to conduct a screening test. Based on little fish (*Lepomis macrochirus*, *Oncorhynchus mykiss*, *Oryzias latipes*) toxicity data (Marking 1969; Tonogai 1982; Svobodova 1986; Baldwin 1994), a range of 5 to 500 mg/L was tested (see appendix). Concentrations of 90 and 100 mg/L were chosen for further testing.

Even with the light microscope, the accumulation of rhodamine b could clearly be visualized, especially in the yolk sac (Fig. 3.3.1).

Figure 3.1.1: 48 hpf embryo exposed to 90 mg/L Rhodamine b

3.1.2 Epi-fluorescence microscopy – Rhodamine b

Due to high brightness of the fluorescence signal of rhodamine b, the iris intensity was reduced to 75 %. The 24 hpf embryos showed an accumulation especially in yolk and yolk extension (Fig. 3.1.2). The chorion and the rest of the body gave no signal. However, after 48 hpf, the fluorescence signal weakened and spread throughout the whole body (Fig. 3.1.3).

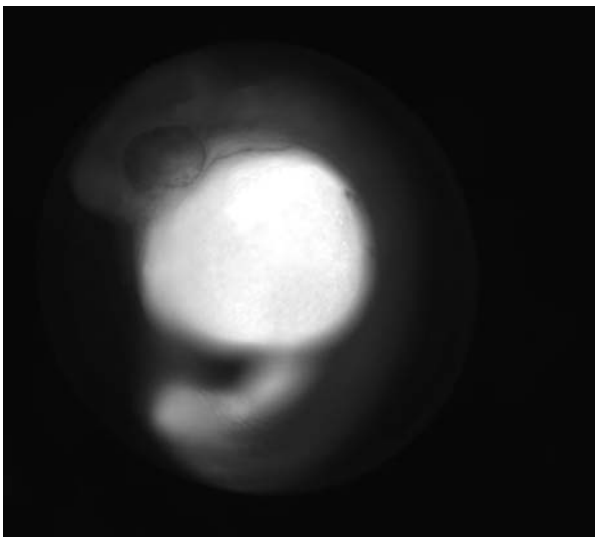

Figure 3.1.2: 24 hpf embryo exposed to rhodamine b (90 mg/L) showed an accumulation in yolk; shutter speed: 2 ms; zoom: 2

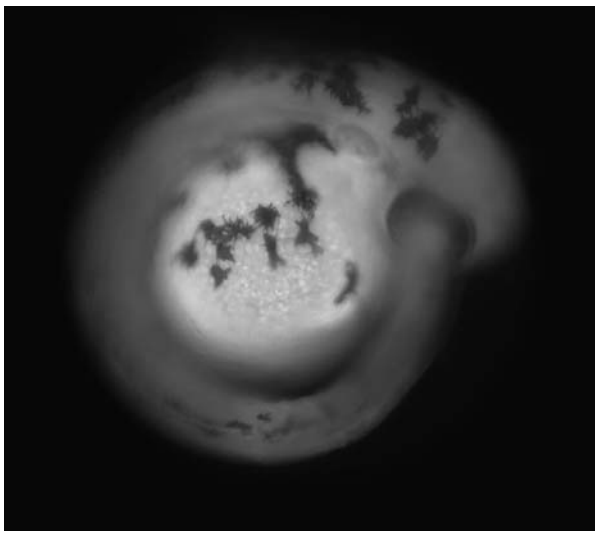

Figure 3.1.3: 48 hpf embryo exposed to rhodamine b (90 mg/L), fluorescence signal spread throughout the body; shutter speed: 2 ms; zoom: 2

In the hatched embryos, the accumulation was still detectable, but the brightness decreased with time (Fig. 3.1.4), even when considering the smaller zoom of 1, which needs in general a higher shutter speed (Fig. 3.1.5).

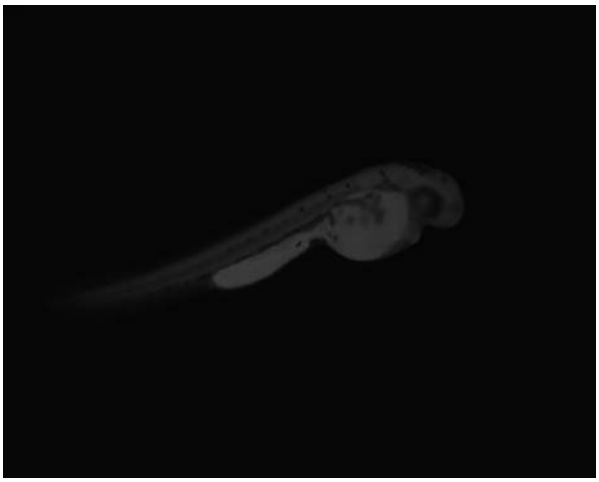

Figure 3.1.4: 48 hpf larva exposed to rhodamine b (90 mg/L) fluorescence dye decreased with hatching; shutter speed: 2 ms; zoom: 1

Figure 3.1.5: 48 hpf larva exposed to rhodamine b (90 mg/L); with an increased shutter speed: 7 ms; zoom: 1

Micrographs (Fig. 3.1.6-9) were taken in a total of 56 eggs exposed to different concentrations of rhodamine b (5 mg/L, 45 mg/L, 90 mg/L, 130 mg/L, 170 mg/L). Except for a weakening signal with lower concentrations, no differences in the distribution of rhodamine b were detected (Fig. 3.1.6-9). All images had a shutter speed of 2 ms. The control group demonstrated a weak auto-fluorescence or refraction (Fig. 3.1.10).

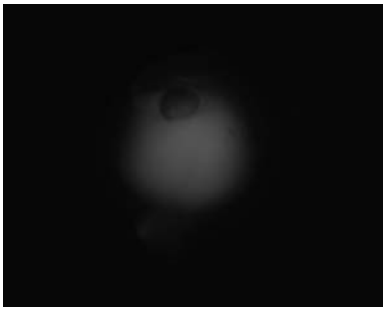

Figure 3.1.6: 24 hpf embryo exposed to rhodamine b (**5** mg/L)

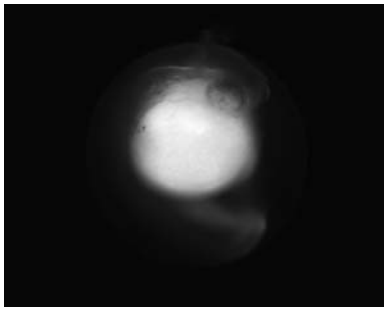

Figure 3.1.7: 24 hpf embryo exposed to rhodamine b (**45** mg/L)

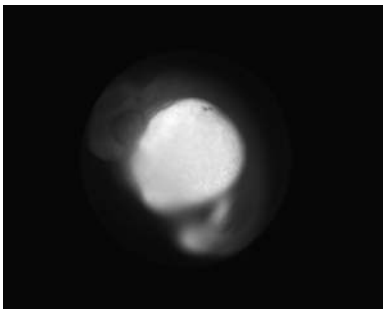

Figure 3.1.8: 24 hpf embryo exposed to rhodamine b (**90** mg/L)

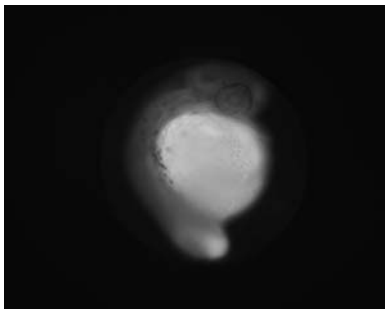

Figure 3.1.9: 24 hpf embryo exposed to rhodamine b (**130** mg/L)

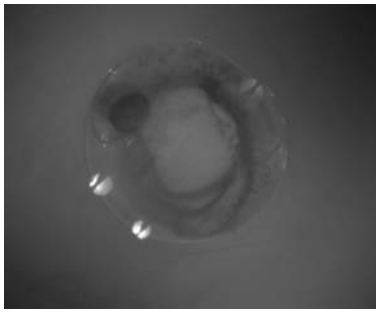

Figure 3.1.10: 24 hpf embryo exposed to artificial water (**control** group); shutter time : 1.63 s

Dechorionation

A separate investigation into dechorionated zebrafish showed in addition a signal in embryo (Fig. 3.1.12) and also a weaker signal in the chorion (Fig. 3.1.11). However, the intensities of the signals could not be compared, since there were big differences in volume, position and surfaces between chorion and embryo. Comparing embryo and chorion of the control by using the auto shutter speed as a measurement for intensity of the fluorescence signal, the auto fluorescence of chorion (Fig. 3.1.13) and embryo (Fig. 1.3.14) are almost identical with a shutter speed of approximately 1.7 sec.

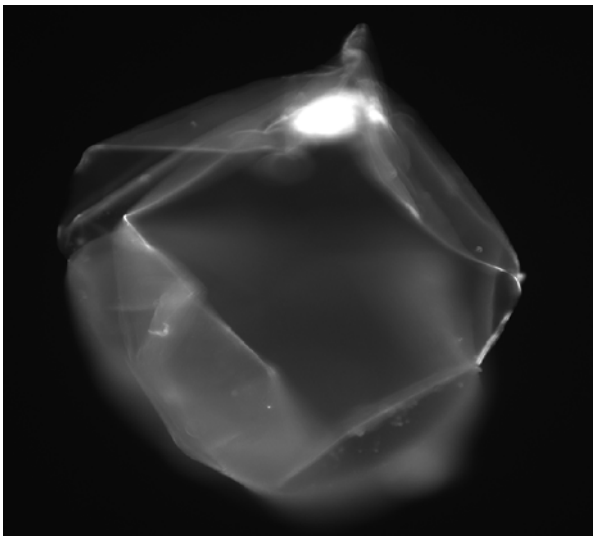

Figure 3.1.11: Fluorescence signal of the chorion of the 24 hpf embryo (of Fig. 3.1.12); shutter speed: 40 ms

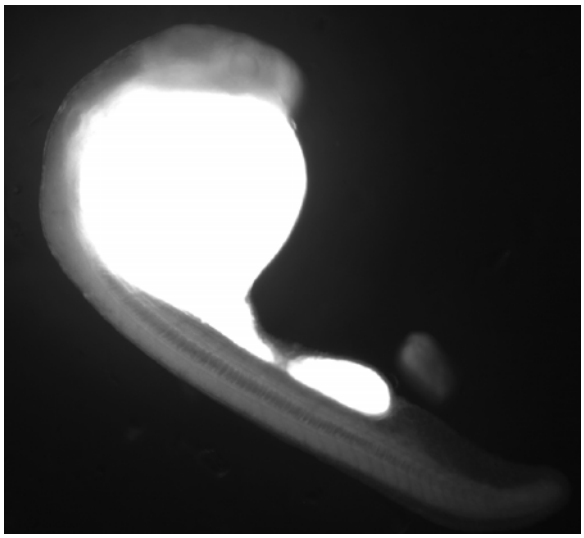

Figure 3.1.12: High fluorescence signal in the 24 hpf dechorionated embryo; shutter speed: 1 ms (full iris intensity)

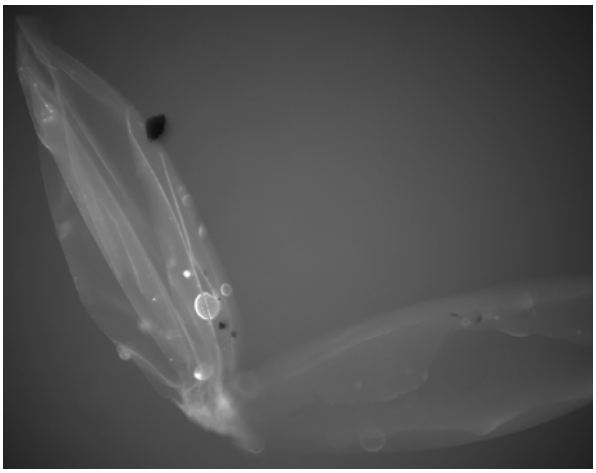

Figure 3.1.13: control group, chorion of 24 hpf embryo (of Fig. 3.1.14); with high shutter speed: 1.67 sec

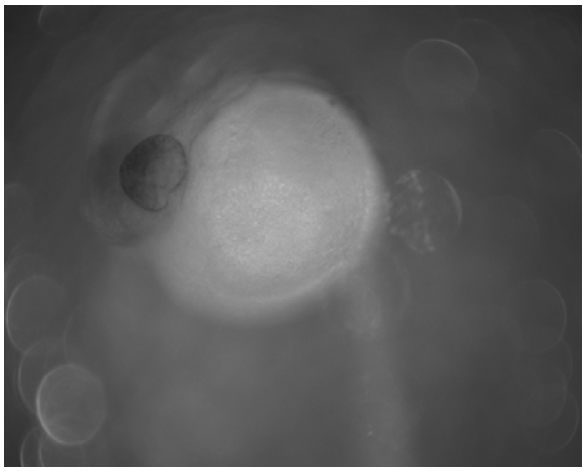

Figure 3.1.14: control group, 24 hpf embryo; with high shutter speed: 1.7 sec

Distribution in the embryo

Plot Profile

Figure 3.1.15 shows the plot profile of a 24 hpf embryo exposed to rhodamine b (90 mg/L). The plateau reflects a constant high gray value in the area of the yolk and demonstrates the accumulation of rhodamine b.

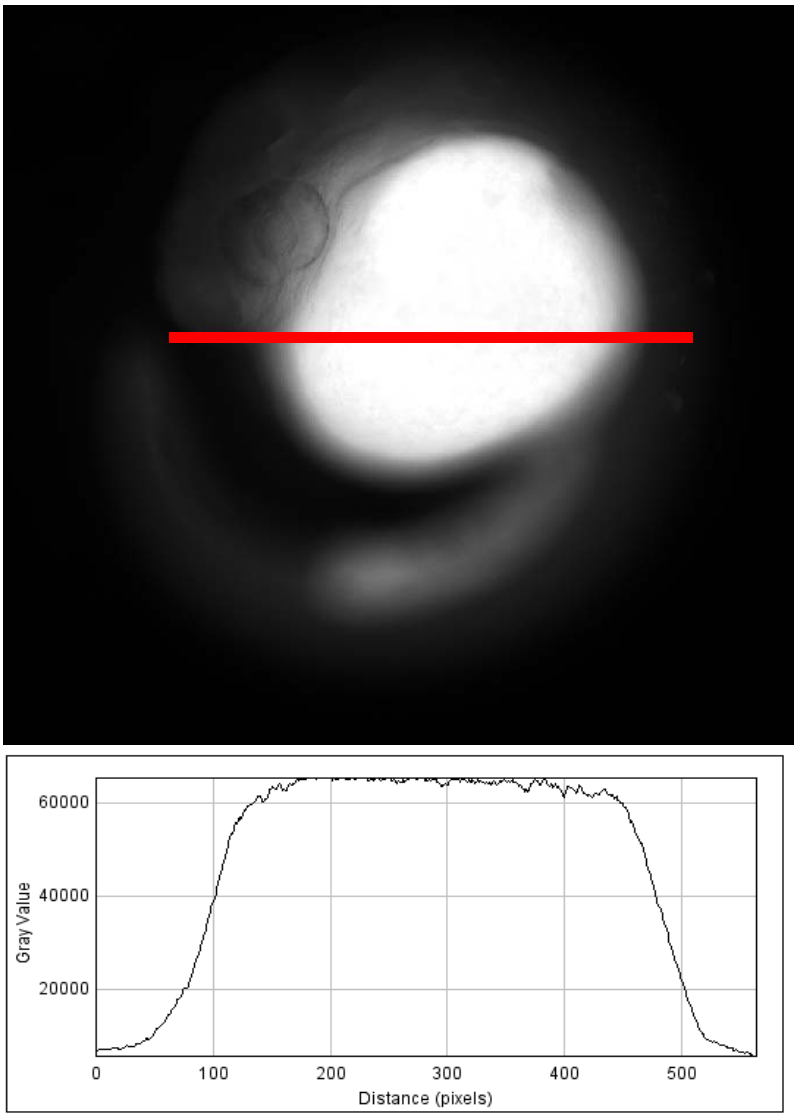

Figure 3.1.15: Plot profile of 24 hpf embryo exposed to rhodamine b (90 mg/L). The plateau reflects a constant high gray value in the area of the yolk; shutter speed of 2 ms

ROI manager

Figure 3.1.16 shows a 24 hpf embryo exposed to rhodamine b (90 mg/L) with selected regions of interest (ROI): yolk, brain and background fluorescence. In total, 32 images were analyzed with two ROIs (yolk, background fluorescence) and five with three ROIs.

The highest fluorescence signal was detectable in the yolk with a mean gray value of 60.000.000 (Fig. 3.1.7). The fluorescent signal in the brain was about five times smaller than in the yolk. However, it should be noted that the evaluation was based only on five images. The small gray value of 2.500.000 in background demonstrates that there were no interference signals in the background.

Figure 1.3.18 confirms the impression that the signal vanishes with time, e.g., the intensity in the yolk was decreased approximately by 30 %. After 48 hours the difference between yolk and brain became smaller. The fluorescent signal in the brain was only two times weaker than in the yolk. All differences in distribution of rhodamine b are significant (Dunn's test, $p<0.05$).

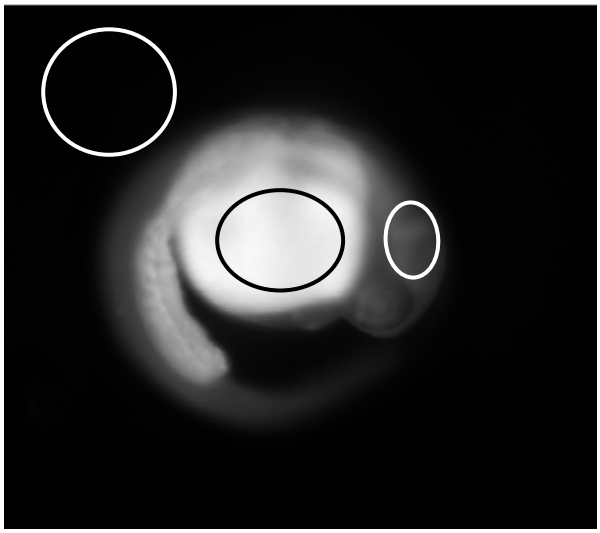

Figure 3.1.16: 24 hpf embryo with the selected regions of interest: brain, yolk and background fluorescence; shutter time of 2 ms

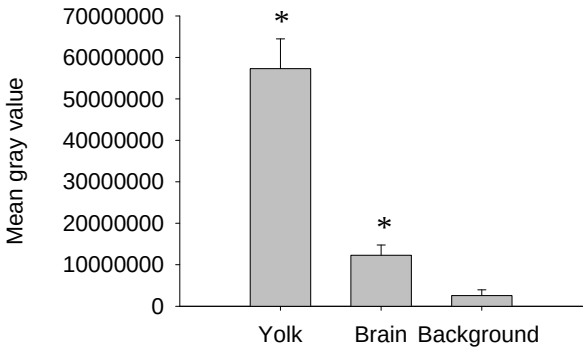

Figure 3.1.7: Distribution of rhodamine b (90 mg/L) in 24 hpf embryos (significant (*), Dunn's test, $p<0.05$)

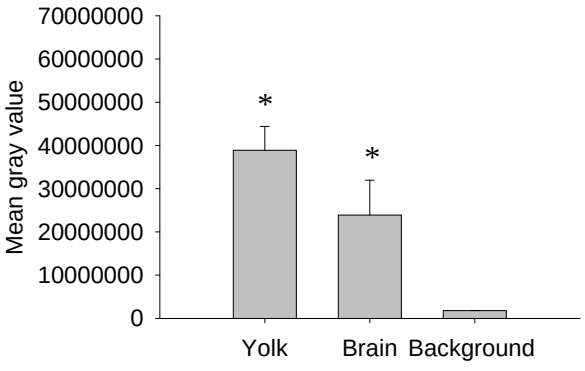

Figure 3.1.8: Distribution of rhodamine b (90 mg/L) in 48 hpf embryos (significant (*), Dunn's test, $p<0.05$)

3.1.3 Confocal laser scanning microscopy (CLSM) – Rhodamine

Figure 3.1.19 illustrates an embryo at 24 hpf with a clear accumulation of rhodamine b in the yolk and a weak signal in the chorion.

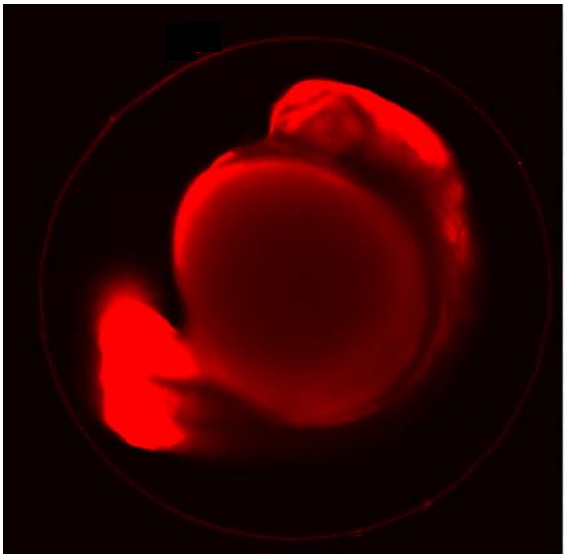

Figure 3.1.19: 24 hpf embryo exposed to rhodamine b (100 mg/L); L: 15; HV: 14

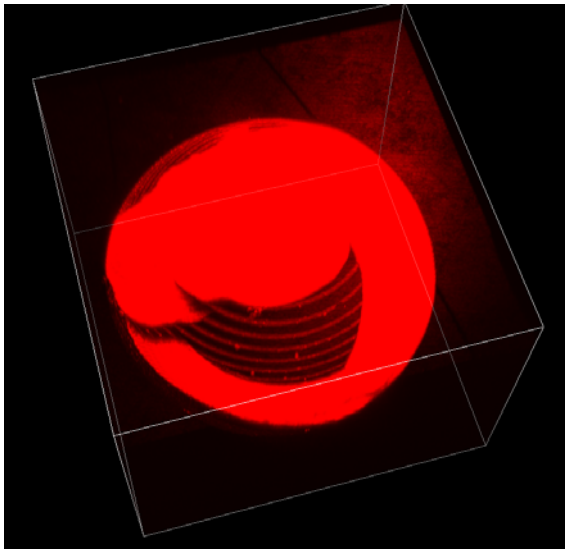

Figure 3.1.20: 48 hpf embryo exposed to rhodamine b (100 g/L); L: 15; HV: 14

Figure 3.1.20 illustrates an embryo at 48 hpf reproduced in the 3d version with the same distribution in the egg as in the embryo at 24 hpf. The red shadow in the background demonstrates an interference signal, since rhodamine b still diffused out of the egg. Both pictures were taken with laser power (L) of 15, and the photomultiplier works with high voltage (HV) of 14.

3.2 Sulforhodamine b

3.2.1 Pre-test

Due to the lack of existing fish toxicity data, it was necessary to conduct a screening test to identify the spectrum of suitable concentrations of sulforhodamine b. The results of two range-finding tests (see appendix p. II) show that sulforhodamine b is not as toxic as rhodamine b. The brightness of sulforhodamine b was much lower than rhodamine b, therefore concentrations of 100-200 mg/L were chosen for the measurement of fluorescence. Even though sulforhodamine b was less toxic than rhodamine b, toxic effects could be seen at high concentrations. Figure 3.2.1 already shows necrotic cells after 4-5 hours at an exposure concentration of 1000 mg/L.

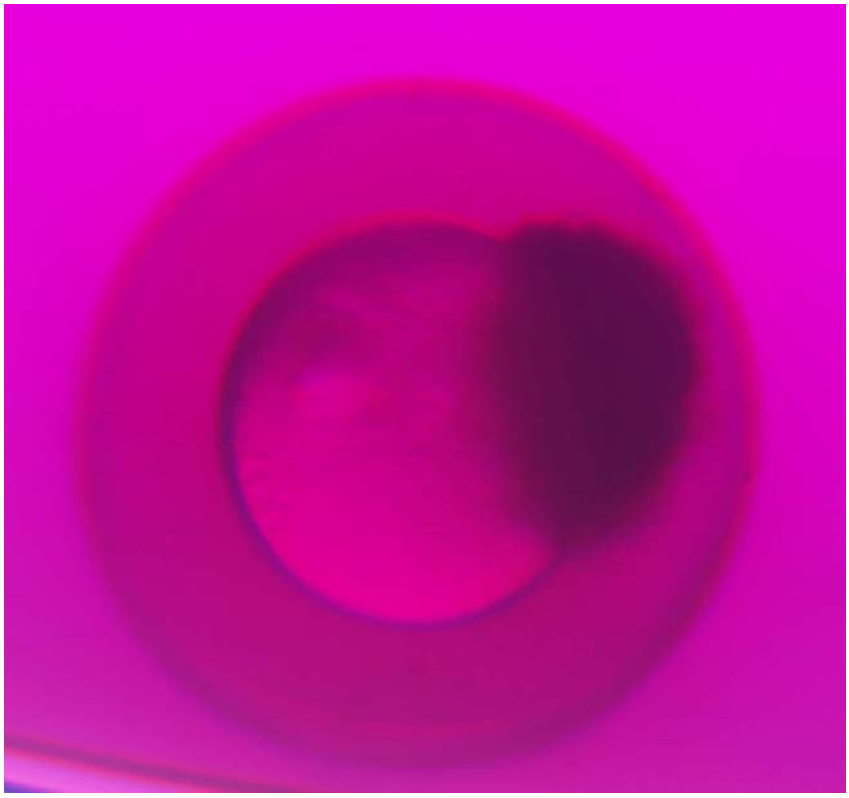

Figure 3.2.1: 4 hpf embryo exposed to sulforhodamine b (1000 mg/L), necrotic cells after 4 hours exposition

3.2.2 Epi-fluorescence microscopy – Sulforhodamine b

Comparing the images (Fig. 3.2.2 and Fig. 3.2.3) with the ones of rhodamine b (Fig. 3.1.2 and Fig. 3.1.3, p. II), it is evident that the pictures are blurry and the embryos are not clearly detectable. The 24 hpf embryos showed low accumulation in the vascular system in the area of the heart (Fig. 3.2.2); whereas after 48 hours the signal in the whole egg increased and sulforhodamine b accumulated predominantly in the yolk (Fig. 3.2.3).

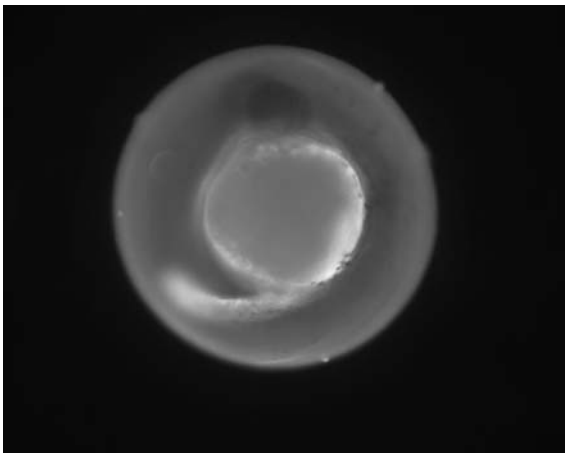

Figure 3.2.2: 24 hpf embryo exposed to sulforhodamine b (100 mg/L); shutter speed: 80 ms

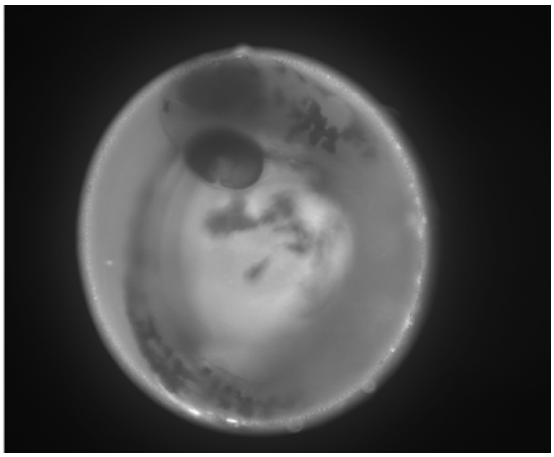

Figure 3.2.3: 48 hpf embryo exposed to sulforhodamine b (100 mg); shutter speed: 80 ms

Dechorionation

The 24 hpf embryos (Fig. 3.2.4) showed a weaker signal than their chorions (Fig. 3.2.5), but, as previously mentioned, a comparison of the two intensities in embryos and chorions is difficult, since the structure is quite different. Nevertheless, Fig. 3.2.4 and Fig. 3.2.5 were both imaged with the same shutter speed of 80 ms and demonstrate that the fluorescence dye was located at the surface of the chorion.

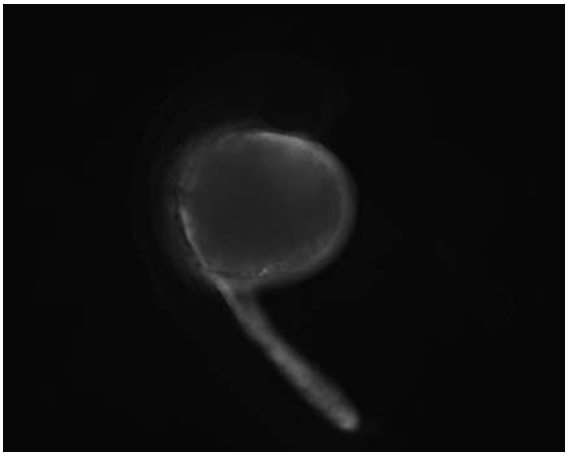

Figure 3.2.4: 24 hpf dechorionated embryo; shutter speed: 80 ms

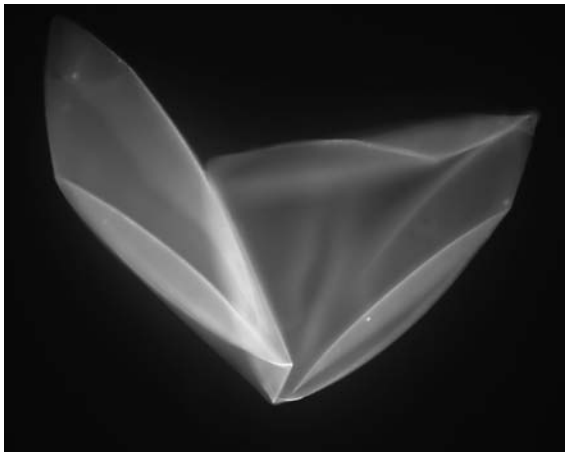

Figure 3.2.5: Chorion of the embryo (Figure 3.2.4); shutter speed: 80 ms

Embryos dechorionated and washed for 24 hours after 48 hours exposure

In order to check if there is an uptake of sulforhodamine b into the embryo after 48 hours from the chorion, one group of the dechorionated embryos was washed for 24 hours in artificial water after 48 hours of exposure (Fig. 3.2.6). The control group was also rinsed for 24 hours with chorion in artificial water (Fig. 3.2.7). Figure 3.2.6 and Figure 3.2.7 show no detectable differences in their intensities of fluorescence signal between the two groups. Both groups were imaged with a shutter speed of 80 ms.

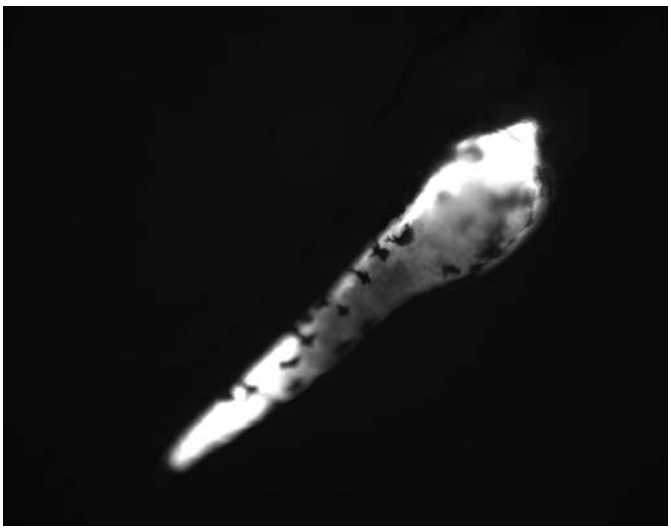

Figure 3.2.6: 72 hpf embryo exposed to sulforhodamine b, dechorionated at 48 hpf, washed for 24 hours in artificial water; shutter speed: 80 ms

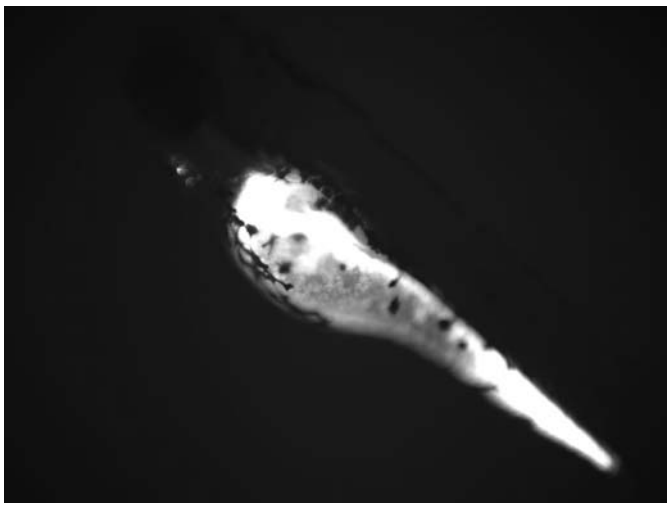

Figure 3.2.7: 72 hpf embryo exposed to sulforhodamine b, 48 hpf chorionated embryo washed for 24 hours in artificial water; shutter speed: 80 ms

Distribution of sulforhodamine b in the embryo

Plot profile

Figure 3.2.8 shows the plot profile of a 24 hpf embryo exposed to sulforhodamine b with a concentration of 100 mg/L. Given the evenly distributed signal, the plot profile confirms the assumption that sulforhodamine b was attached to the chorion. The highest peak is in the area of vascular system (black circle). Lawson & Weinstein (2002) investigate the circulatory system of a zebrafish embryo at 30 hpf (Fig. 3.2.9). Blood leaves the heart (H) and enters the lateral dorsal aortae (LDA), which converge into the dorsal aorta (DA). The circulation progresses into the caudal artery (CA), where blood empties into the caudal vein (CV) and returns through the common Duct of Cuvier (DC) (Fig. 3.2.9, black circle), returning to the heart.

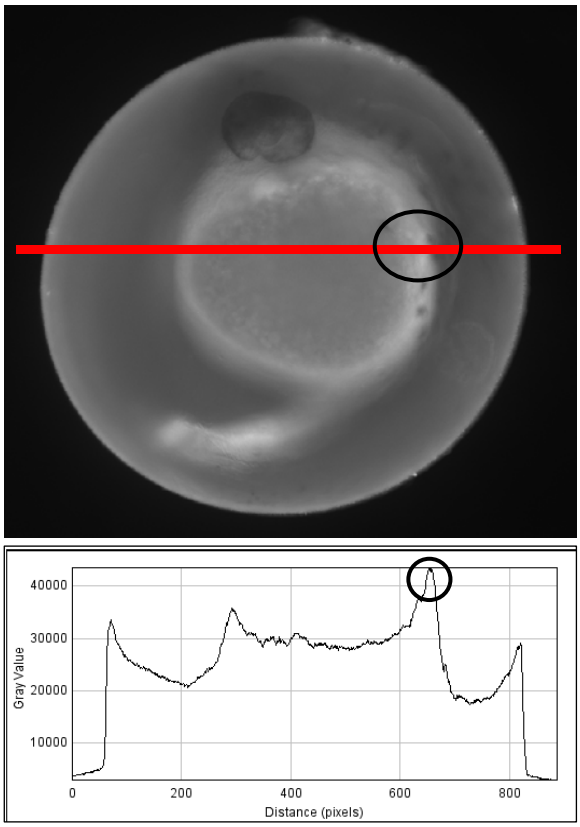

Figure 3.2.8: Plot profile of 24 hpf embryo exposed to sulforhodamine b (100 mg/L) **black circle**: vascular system with a high fluorescence signal; shutter speed of 80 ms

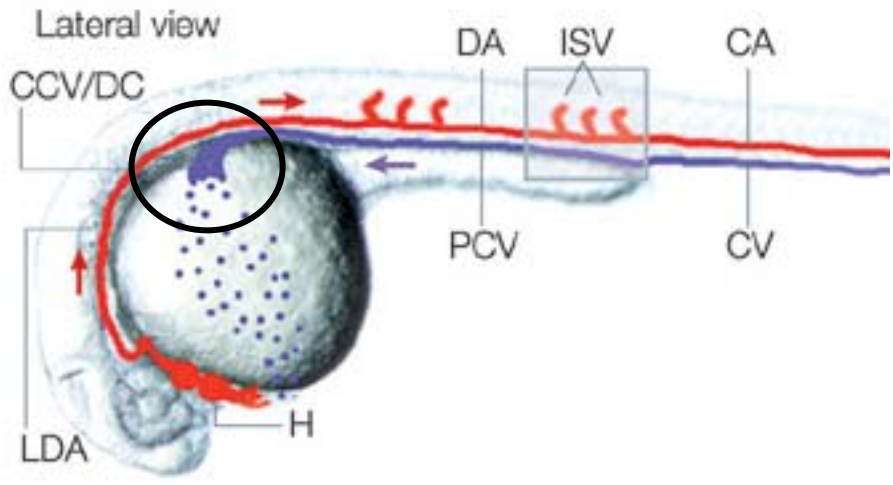

Figure 3.2.9: Vascular system of 24 hpf embryo (Lawson and Weinstein 2002)

common cardinal vein (**CCV**), Duct of Cuvier (**DC**), dorsal aorta (**DA**), intersegmental vessel (**ISV**), caudal artery (**CA**), caudal vein (**CV**), posterior cardinal vein (**PCV**), heart (**H**), lateral dorsal aortae (**LDA**)

Distribution of sulforhodamine b as measured via the ROI manager

Figure 3.2.10 shows the 24 hpf embryo exposed to sulforhodamine b (100 mg/L) with the selected ROIs: yolk, brain, chorion and background. In a total of 10 images of 24 hpf embryos and 4 images of 48 hpf embryos were investigated.

Figure 3.2.11 illustrates that the signal in 24 hpf embryos is equally distributed. The yolk showed the highest signal, whereas chorion and brain presented lower and almost identical signal strength. After 48 hours, the signal strength decreased and the distribution changed. It was then the chorion that showed the highest fluorescence signal; whereas the signals of yolk and brain were almost the same, but two times smaller than in the chorion. However, the difference in distribution after 24 hours is significant, whereas after 48 hours the change in distribution is not significant.

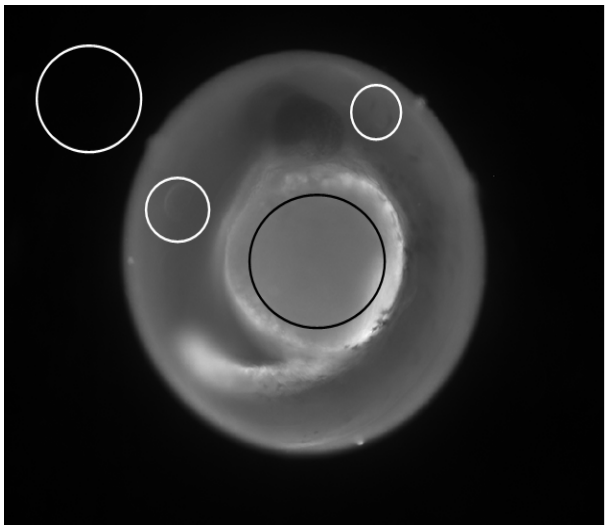

Figure 3.2.10: 24 hpf embryo with selected regions of interest: chorion, brain, yolk and background fluorescence; shutter speed of: 80 ms

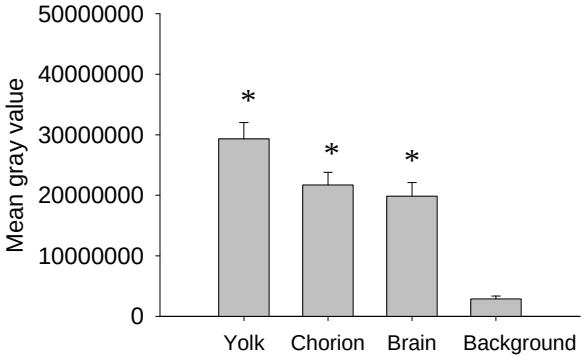

Figure 3.2.11: Distribution of fluorescence in 24 hpf embryos exposed to sulforhodamine b (100 mg/L), (significant (*), Dunn's test, $p<0,05$)

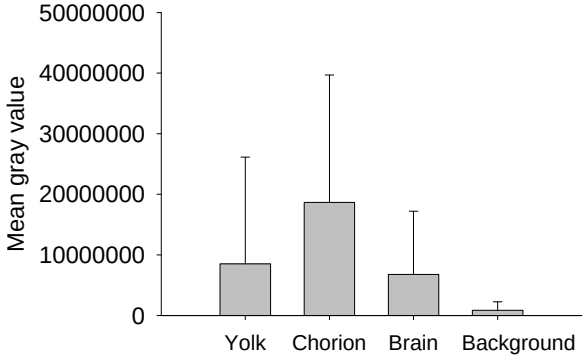

Figure 3.1.12: Distribution of fluorescence in 48 hpf embryos exposed to sulforhodamine b (100 mg/L)

3.2.3 Confocal laser scanning microscopy (CLSM) – Sulforhodamine b

Figure 3.2.13 highlights the attachment of sulforhodamine b at the chorion; in addition; an accumulation in the embryo was detectable. The signal was strong therefore, the images (Fig. 3.2.13-18) were taken with laser power of 15 and the photomultiplier worked with a high voltage of 27.

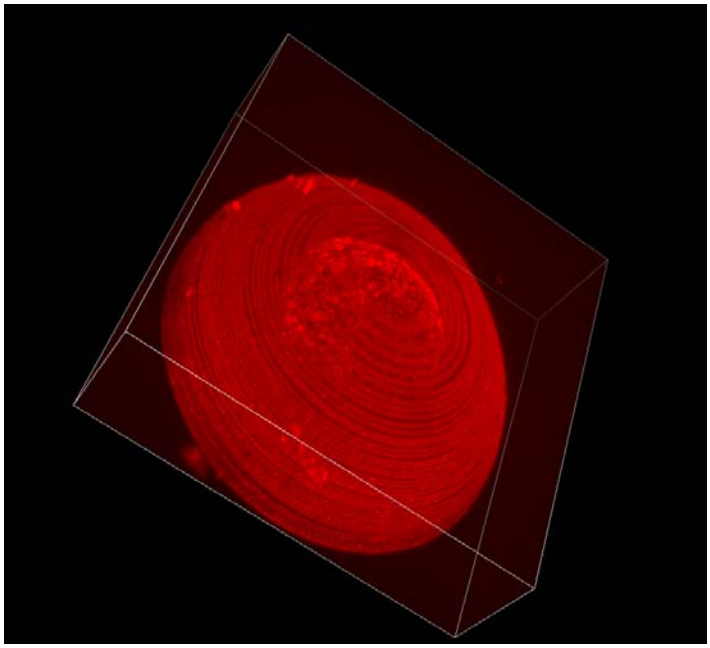

Figure 3.2.13: 24 hpf embryo exposed to sulforhodamine b (200 mg/L), attachment of sulforhodamine b at the chorion; laser power: 15; high voltage: 27

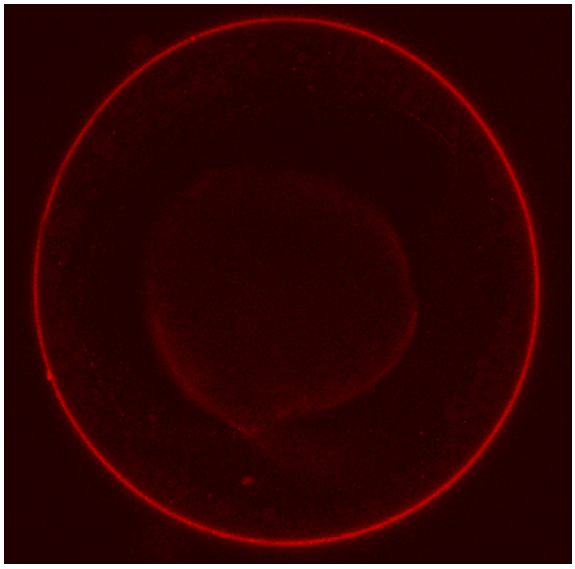

Figure 3.2.14: Presents one section plane out of 40 slices across the center; laser power: 15; high voltage: 27

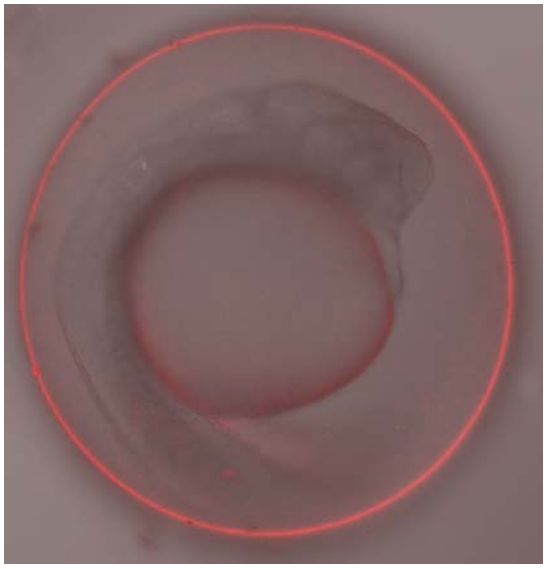

Figure 3.2.15: Same Section plane across the center of the egg with transmitted light; laser power: 15; high voltage: 27

The slightly decreased signal in the chorion after 48 hours is shown in Figure 3.2.16. The fluorescence dye had the same distribution as after 24 hours.

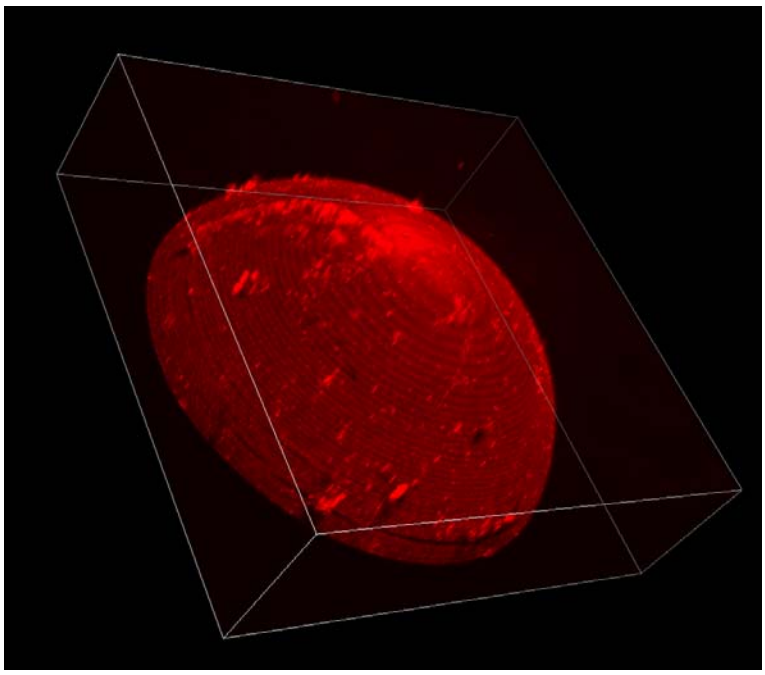

Figure 3.2.16: 48 hpf embryo exposed to sulforhodamine b (200 mg/L), slightly decreased signal in the chorion, laser power: 15; high voltage: 27

The selected section plane after 48 hours exposure (Fig. 3.2.17) shows no differences in distribution of sulforhodamine b. The lack of signal in the yolk was a result of the different positions of embryo in the egg (Fig. 3.2.18).

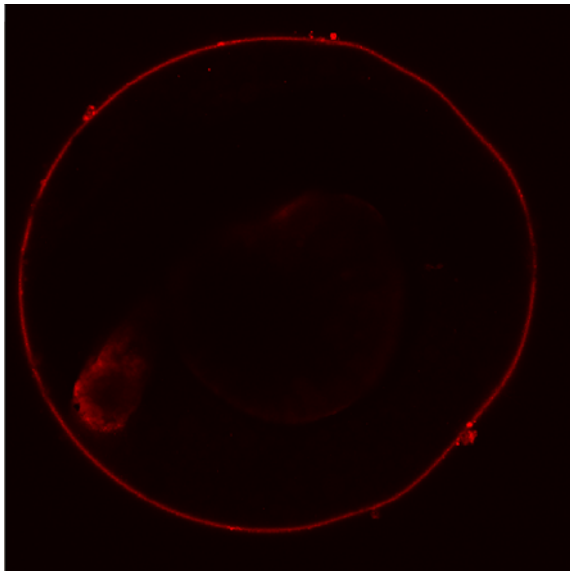

Figure 3.2.17: Section plane across the center of the egg; laser power: 15; high voltage: 27

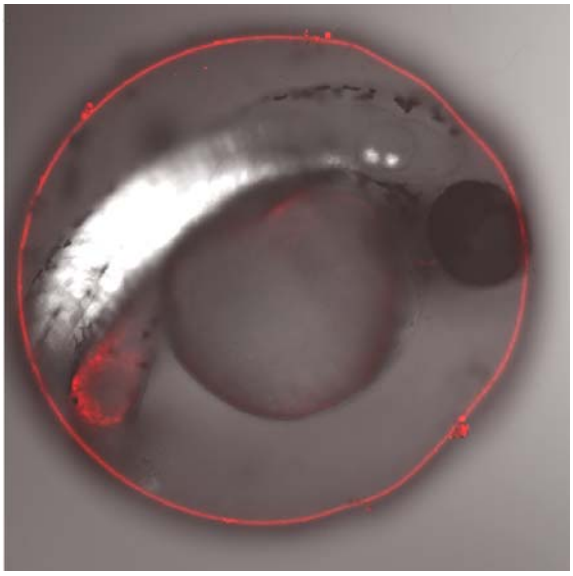

Figure 3.2.18: Section plane across the center of the egg with transmitted light; laser power: 15; high voltage: 27

Dechorionation

The investigation of 24 hpf dechorionated embryos confirmed an accumulation of sulforhodamine b in the yolk. The signal detected in the embryo was as powerful as in the intact egg. The images were taken with laser power of 12, and the photomultiplier worked with a high voltage of 18. The portion of sulforhodamine b which passed through the chorion accumulated in the yolk only (Fig. 3.2.19 and Fig. 3.2.20). When comparing 24 hpf (Fig. 3.2.19) with 48 hpf embryos (Fig. 3.2.20), no differences in distribution could be seen.

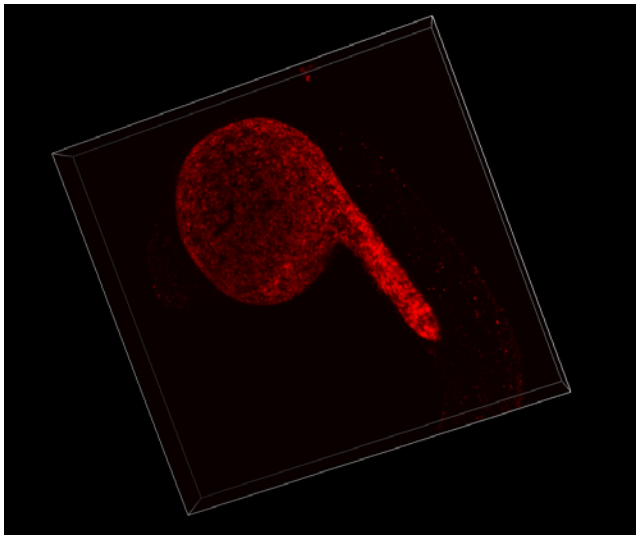

Figure 3.2.19: 24 hpf dechorionated embryo exposed to sulforhodamine b (200 mg/L), laser power: 12, high voltage: 18

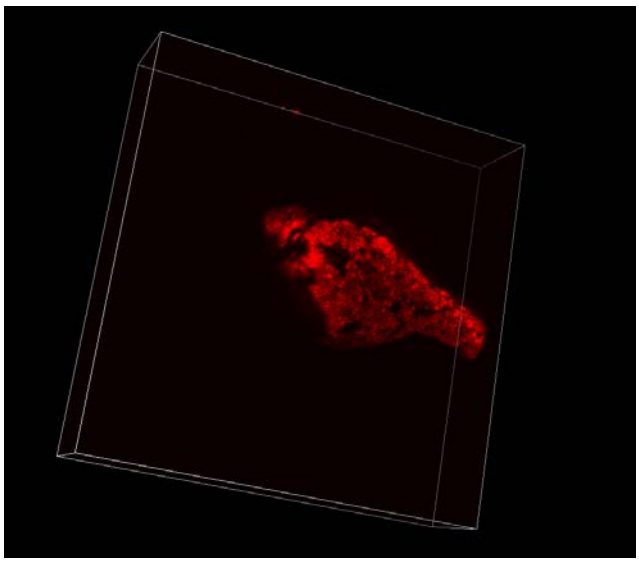

Figure 3.2.20: 48 hpf dechorionated embryo exposed to sulforhodamine b (200 mg/L), laser power: 12, high voltage: 18

3.3 Fluorescein

3.3.1 Pre-test

The outcomes of two range finding-tests show that fluorescein was not as toxic as rhodamine b or sulforhodamine b. Even a concentration of 1 g/L showed no effects; however, the solubility was a limiting factor. At concentrations of ≥ 200 mg/L, fluorescein started to precipitate. To increase solubility, fluorescein can be solved in DMSO. The influence of different DMSO-concentrations on the distribution in the embryo is described in a separate chapter 3.6. Fluorescein has a good brightness, but the photobleaching phenomenon is very prominent (see chapter 2.1.2). Based on the results of the pre-test, concentrations of 100-200 mg/L were chosen for the measurement of fluorescence.

Even with the light microscope, the accumulation of fluorescein could clearly be visualized, especially in the stomach and the brain (Fig. 3.3.1).

Figure 3.3.1: Larva showing accumulation of fluorescein in stomach and brain after 72 hpf exposure to 500 mg/L fluorescein

3.3.2 Epi-fluorescence microscopy - Fluorescein

Fluorescein passed the chorion and accumulated in the area around heart and brain (Fig. 3.3.2). The colored pictures use the option to replace the different gray values with colors of higher contrast (created with the software ImageJ). This results in a better delineation of the fluorescence signal. Red stands for a higher and green for a lower gray value. This illustration highlights the accumulation in heart (see Fig. 3.2.9, page 13) and brain.

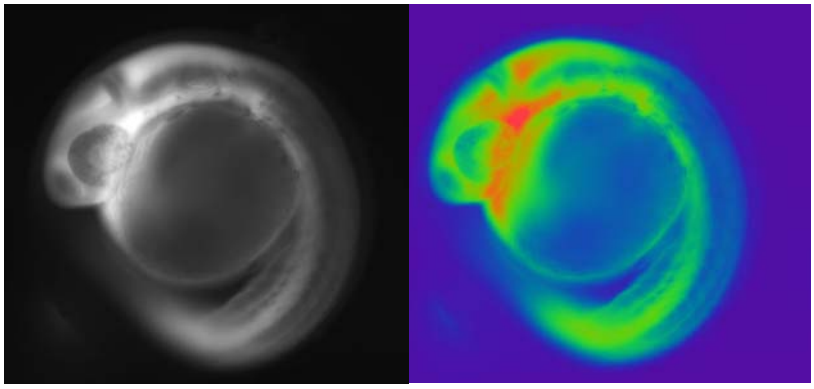

Figure 3.3.2: 24 hpf embryo exposed to fluorescein (200 mg/L); shutter speed: 2 ms

After 48 hours, (Fig. 3.3.3) there was no difference in distribution detectable. After a while, fluorescein spread throughout the body and accumulated increasingly in the brain.

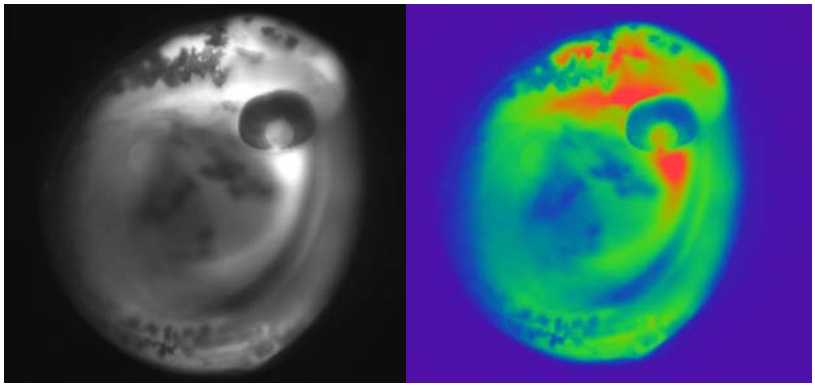

Figure 3.3.3: 48 hpf embryo exposed to fluorescein (200 mg/L); shutter speed: 2 ms

After depuration of the 48 hpf embryos in artificial water for 24 hours, the distribution changed: the whole fluorescein was located in the stomach (Fig. 3.3.4). After 120 hours, fluorescein was completely accumulated in the intestinal lumen and even the bile was visible (Fig. 3.3.5).

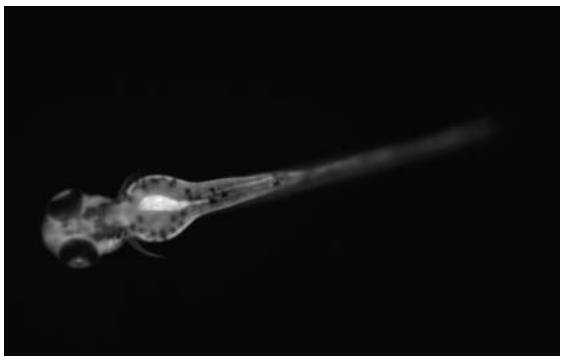

Figure 3.3.4: 72 hpf larva showing accumulation in stomach after 24 h exposure to fluorescein (100 mg/L) and 24 h washing in artificial water; shutter speed: 7 ms

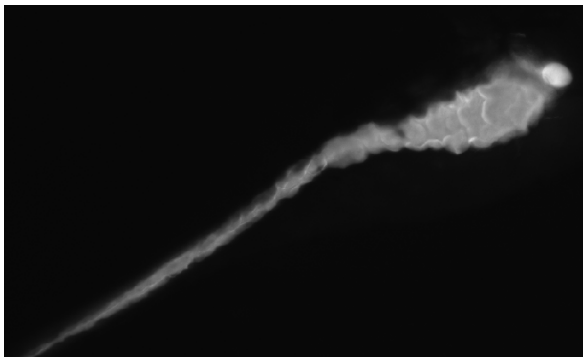

Figure 3.3.5: 120 hpf larva showing accumulation in stomach and bile (right) after 24 h exposure to fluorescein (100 mg/L) and 48 h washing in artificial water; shutter speed: 2 ms

In total, 48 eggs exposed to different concentrations (50 mg/L; 100 mg/L; 200 mg/L; 300 mg/L; 500 mg/L) were photographed. Except that the signal was weaker at the lower concentration, there were no differences observable; the distribution was the same.

Distribution of fluorescein inside the embryo

Plot profile

Figure 3.3.6 shows the plot profile of a 24 hpf embryo exposed to 200 mg/L fluorescein. Fluorescein accumulated in the vascular systems like the heart (left circle in the plot profile) and supposedly in the lateral dorsal aorta (middle circle, cp. Fig. 3.2.9) and also in the brain, more precisely in the hindbrain (right circle in the plot profile).

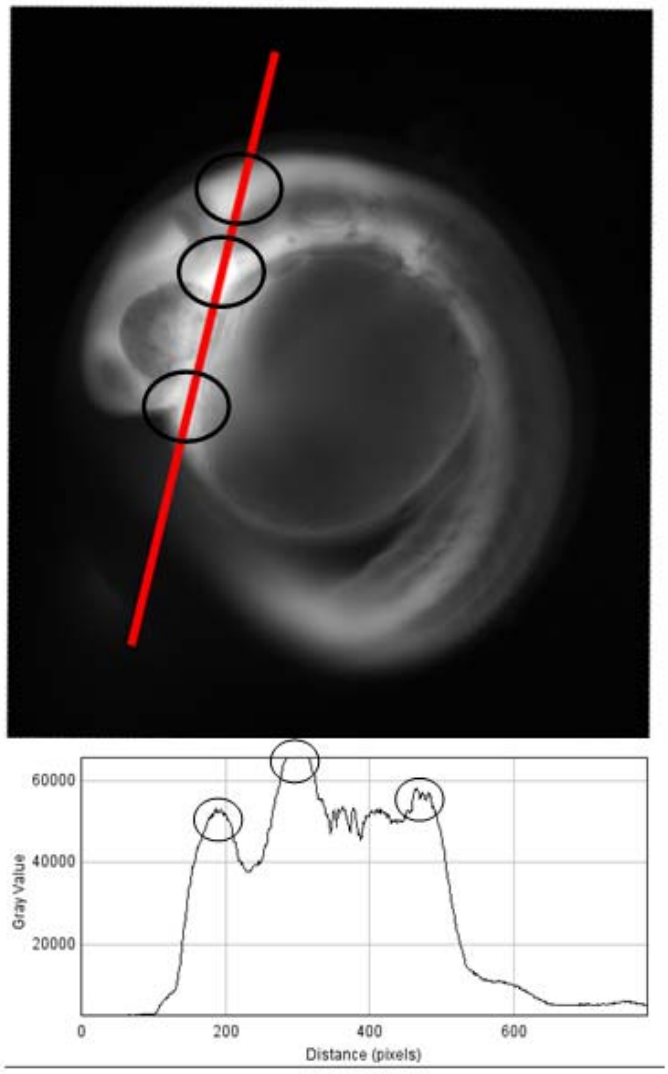

Figure 3.3.6: Plot profile of 24 hpf embryo exposed to fluorescein (200 mg/L); peaks present strong signal in: the heart (**left circle**); the lateral dorsal aorta (**middle circle**); hindbrain (**right circle**); shutter speed: 2 ms

Distribution of fluorescein as measured *via* the ROI manager

Figure 3.3.7 shows the selected regions of interest: yolk, midbrain, aorta and background. In total, 8 images for 24 hpf and 14 images for 48 hpf were investigated.

After 24 hours as well as after 48 hours, the general distribution does not change (Fig. 3.3.8 and Fig. 3.3.9). The highest signal is in the blood, in the area of the aorta. After 48 hours, the signal was increased by about 25 %. After 48 hours, the signal in the brain was almost twice as high as after 24 hours. The signal in the yolk remains constantly weak, even after 48 hours. All differences in distribution of fluorescein are significant (Dunn´s test $p<0.05$).

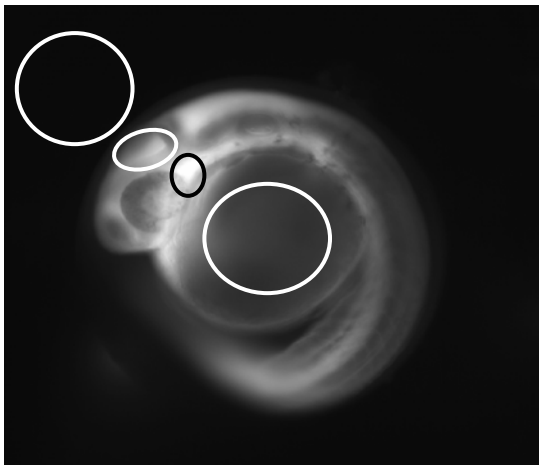

Figure 3.3.7: 24 hpf embryo**,** region of interest: yolk, aorta, midbrain and background (**from right**)

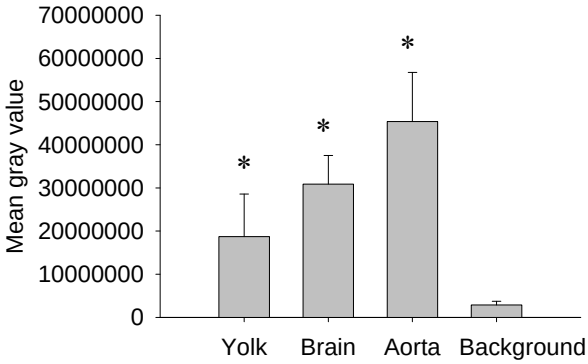

Figure 3.3.8: Distribution of fluorescence in 24 hpf embryos exposed to fluorescein (200 mg/L), differences in distribution are significant (*), Dunn´s test $p<0.05$

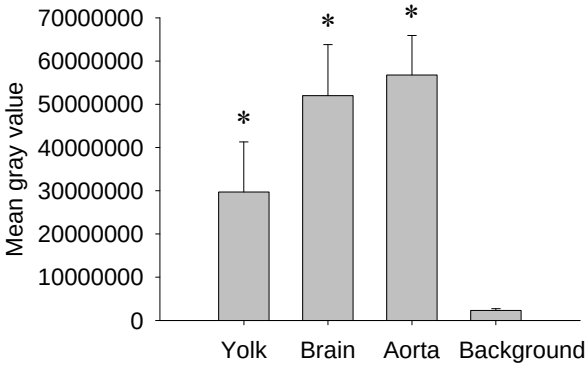

Figure 3.3.9: Distribution of fluorescence in 48 hpf embryos exposed to fluorescein (200 mg/L) differences in distribution are significant (*), Dunn´s test $p<0.05$

3.3.3 Confocal laser scanning microscopy (CLSM) - Fluorescein

In contrast to epi-fluorescence microscopy, after 24 hours exposure in confocal microscopy the signal of the chorion is higher than in the embryo. Embryos were exposed to fluorescein (100 mg/L) with a DMSO concentration of 0.1 %. The chorion gave a strong signal. The image was taken with laser power of 100 and high voltage of 20. The position of the embryo inside the egg and the fluorescence signal can be seen in Figure 3.3.11, which was taken with transmitted light.

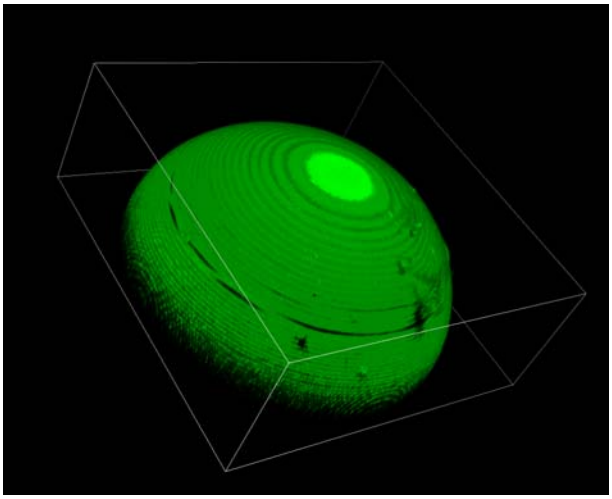

Figure 3.3.10: 24 hpf embryo exposed to fluorescein (100 mg/L) with a DMSO concentration of 0.1 %; the signal of the chorion outshine the signal of the embryo; laser power: 100; high voltage: 20

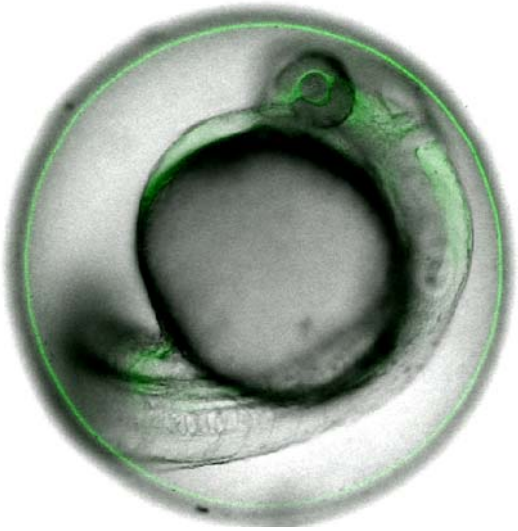

Figure 3.3.11: 24 hpf embryo exposed to fluorescein (100 mg/L) with a DMSO concentration of 0.1 %; laser power: 8; high voltage: 100; bright field microscopy

Dechorionation of embryos exposed to fluorescein

In dechorionated embryos after exposure ensured an accumulation in the embryo. The distribution of fluorescein was even. The bright spot in the yolk reflects the contact surface; this is an interference signal. It is assumed that the missing fluorescence signal of the embryo in Fig. 3.3.10 is not detectable, because the signal of the chorion is brighter and denser.

The signal in the chorion got weaker with time and fluorescein accumulated gradually in the

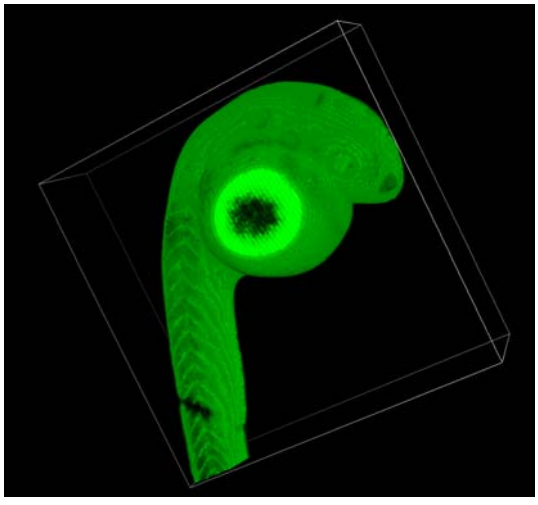

Figure 3.3.12: 24 hpf dechorionated embryo exposed to fluorescein (100 mg/L); laser power: 100; high voltage: 20

embryo (Fig. 3.3.13). A precise distinction in several areas of the embryo, however, is not possible because the signal is supersaturated with a laser power of 100. The laser power of 100 was chosen for a better comparison with the 24 hpf embryos, because it is important to compare images only at the same laser power and, when possible, even at same high voltage. The picture taken with transmitted light (Fig. 3.3.14) confirmed that the signal in the chorion decreases, whereas the signal in the embryo increases.

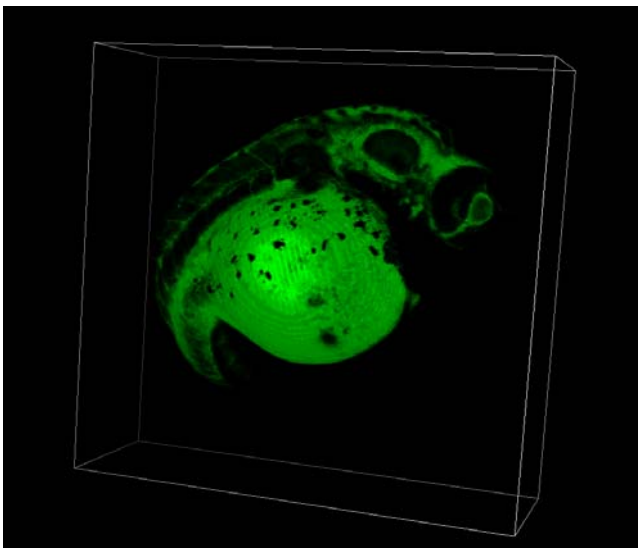

Figure 3.3.13: 48 hpf embryo exposed to fluorescein (100 mg/L) with a DMSO concentration of 0.1 %; the signal in the chorion decreases and the signal in the embryo increases; laser power: 100; high voltage: 1

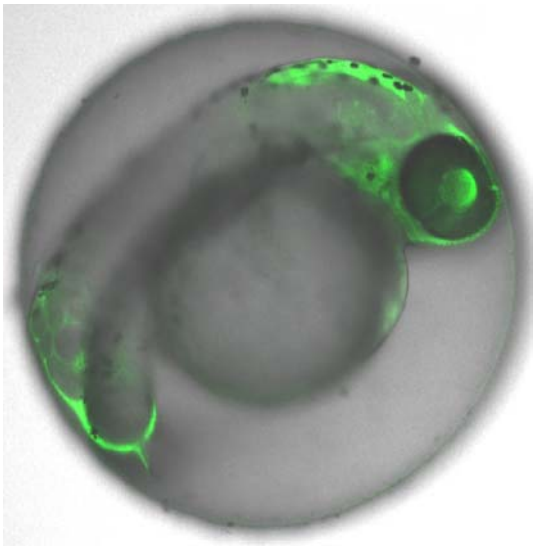

Figure 3.3.14: 48 hpf embryo exposed to fluorescein (100 mg/L) with a DMSO concentration of 0.1 %; laser power: 5, high voltage: 30, imaged with transmitted light

Dechorionation of embryos exposed to fluorescein

The embryos were dechorionated after 48 hours exposure and showed the same distribution of fluorescein as the 24 hpf embryos. In general, the dechorionated embryos (Fig. 3.3.15) show stronger signals than the chorionated ones (Fig. 3.3.13), since the chorion weakens the signal. As already mentioned, a precise distinction within the embryos is rather difficult. The different black spots on the body surface are pigments. The pigmentation pattern becomes more and more distinct after 48 hours.

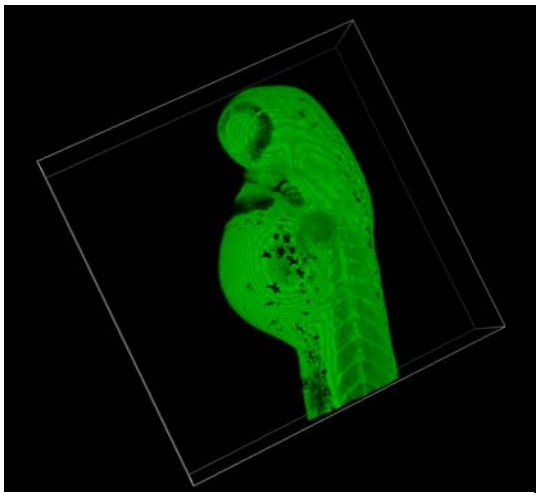

Figure 3.3.15: 48 hpf dechorionated embryo exposed to fluorescein (100 mg/L); shows a strong signal in the embryo, laser power: 100; high voltage: 1

3.4 2,7-Dichlorofluorescein (DCF)

3.4.1 Pre-test

2,7-Dichlorofluorescein (DCF) is much more toxic than fluorescein. It was difficult to find a suitable concentration range, because the difference between NOEC and LOEC was very small. The NOEC was found to be 50 mg/L dichlorofluorescein, whereas 65 mg/L already showed a mortality of 100 % (see appendix p. IV). Due to this small range, the concentration of 50 mg/L was chosen for the measurement of fluorescence, although the signal was weak. The brightness of DCF is not as high as that of fluorescein, but its molecular structure is more stable. Therefore photobleaching was not prominent.

Notably, the chorion appeared to turn red when exposed to DCF (Fig. 3.4.1 **A**). On the other hand the embryo did not show a simultaneous discoloration (Fig. 3.4.1 **B**).

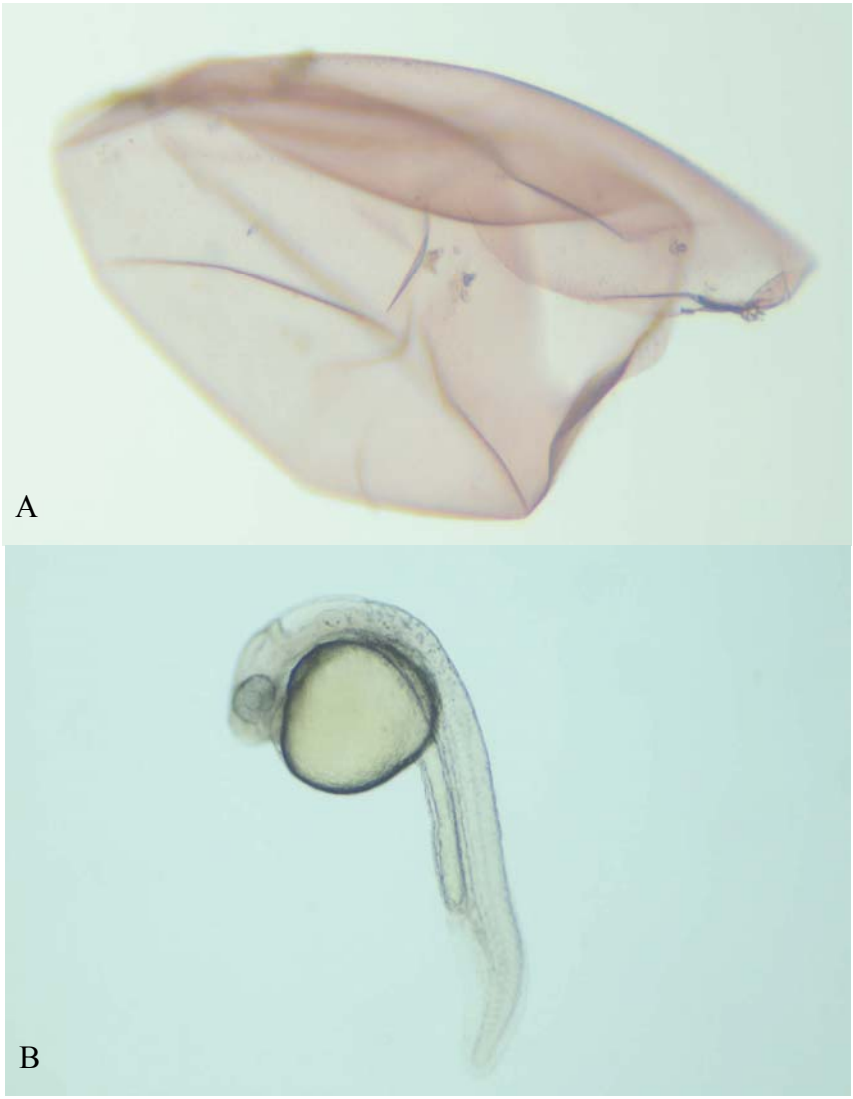

Figure 3.4.1: Colored chorion **(A),** 24 hpf dechorionated embryo exposed to 50 mg/L 2,7-dichlorofluorescein does not show a red coloration (**B**)

3.4.2 Epi-fluorescence microscopy – 2,7-Dichlorofluorescein

DCF shows a weaker signal, but the distribution is the same as with fluorescein (Fig. 3.4.2-3). The colored pictures illustrate an accumulation in blood, especially in the aorta (Fig. 3.4.2) and in the heart (Fig. 3.4.3); the brain also shows an increased signal. The micrographs appear to be a bit blurry, probably due to DCF adsorption to the surface of the chorion.

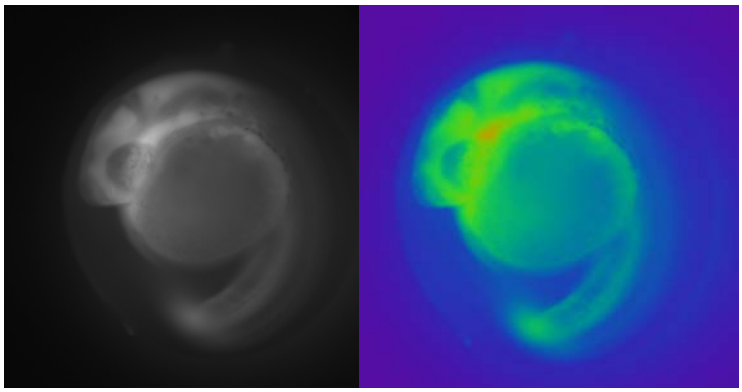

Figure 3.4.2: 24 hpf embryo exposed to DCF 50 mg/L; shutter speed: 40 ms

Dechorionation of embryos exposed to DCF

Dechorionated embryos gave a weaker signal in the embryo than in the chorion (Figure 3.4.4). Both images had an exposure time of 40 ms. Although a direct comparision of the embryo and the chorion is not possible due to differences in structure and volume, the high signal in the chorion suggests that DCF accumulates in the chorion.

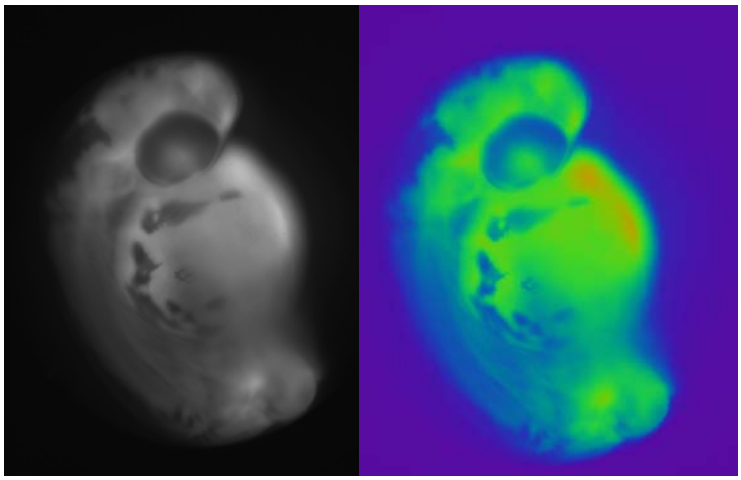

Figure 3.4.3: 48 hpf embryo exposed to 2,7-dichlorofluorescein 50 mg/L; shutter speed: 10 ms

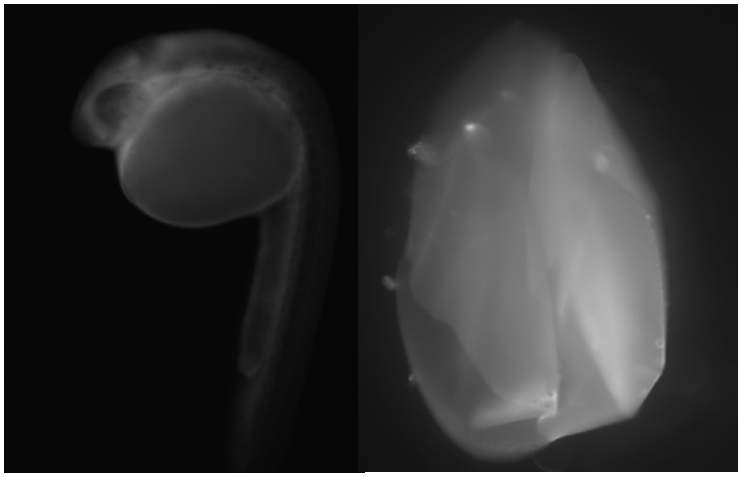

Figure 3.4.4: left: (24 hpf) dechorionated embryo exposed to 2,7-dichlorofluorescein 50 mg/L;
right: chorion of the embryo, both shutter speed: 40 ms

Distribution of DCF inside the embryo

Plot profile

In the plot profile of DCF (Fig. 3.4.5) four different areas of fluorescence were analyzed inside the egg. The accumulation in the blood, more precisely in the aorta, is represented by the first peak, whereas the plateau (arrow) stands for the low accumulation in the yolk. The even lower fluorescence signal in the chorion is illustrated by a minimum, which is followed by a second peak resembling the tail.

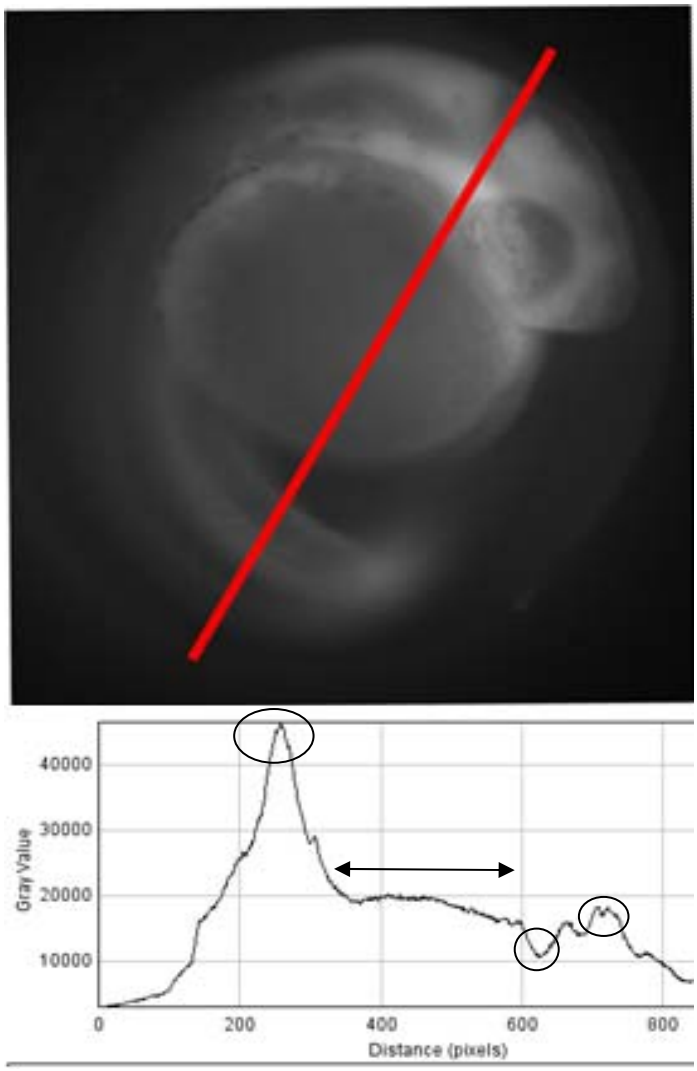

Figure 3.4.5: Plot profile of 24hpf embryo exposed to 2,7-dichlorofluorescein 50 mg/L; peaks present strong signal in: aorta (**left circle**), low signal in the yolk (**plateau, arrow**), even lower signal in the chorion (**second circle**), higher signal in the tail (**third circle**); shutter time 40 ms

Distribution of DCF as measured *via* the ROI manager

Figure 3.4.6 shows the 24 hpf embryo exposed to DCF (50 mg/L) with the selected regions of interests: brain, chorion, aorta, yolk and background fluorescence. The 48 hpf embryos have different ROIs: yolk, heart, brain and background fluorescence (not shown). In total 15 images of 24 hpf embryos and 9 images of 48 hpf embryos were investigated.

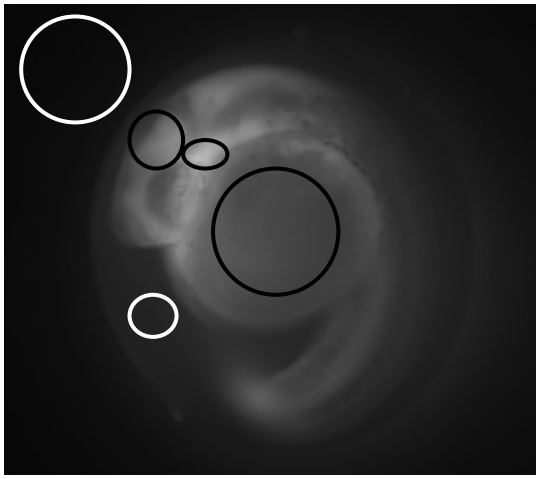

Figure 3.4.6: Regions of interest: **big white circle**: background fluorescence, **right to left black circles**: brain, aorta and yolk, **small white circle**: chorion of 24 hpf embryo exposed to DCF 50 mg/L, 50 mg/L, shutter speed: 40 ms,

The small differences in signal intensity between the selected areas are shown in Figure 3.4.7: The highest signal was found in blood; brain and yolk had similar, rather weak signals, and the lowest signal was detected in the chorion.

After 48 hours (Fig. 3.4.8), there were no conspicuous changes in distribution detectable except for the yolk, which accumulated more DCF with time. The chorion was not analyzable because, as mentioned earlier, the differentiation in general was difficult. The high standard deviation shows big differences in gray value within one selected area; especially blood was subject to fluctuations. Nevertheless, the differences in distribution after 48 hours are significant (Dunn´s test, $p<0.05$).

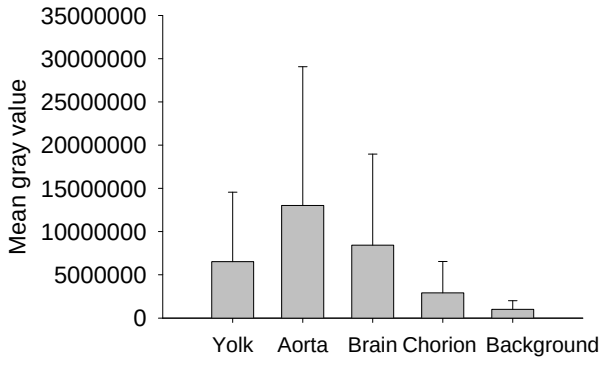

Figure 3.4.7: Distribution of fluorescence in 24 hpf embryos exposed to DCF (50 mg/L)

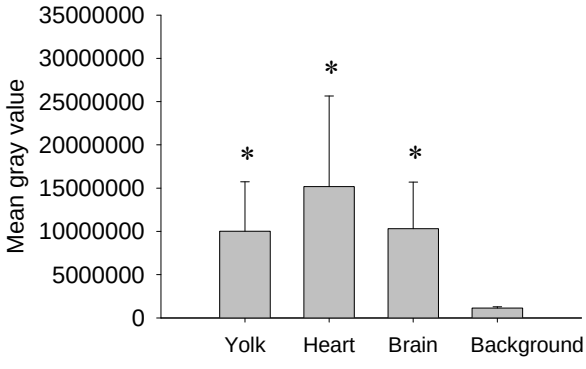

Figure 3.4.8: Distribution of fluorescence in 48 hpf embryos exposed to DCF (50 mg/L), differences in distribution of DCF are significant, Dunns test $p<0.05$ (*)

3.4.3 Confocal laser scanning microscopy (CLSM) – 2,7-Dichlorofluorescein

Figure 3.4.9 confirms the assumption that DCF attaches to the chorion during the first 24 hours, since the embryo is not visible. The image was taken with laser power of 100 and a high voltage of 30. After 48 hours, DCF passed the chorion, but there was still a weak signal visible in the chorion. Figure 3.4.9 and Figure 3.4.10 were imaged with transmitted light and show the positions of the embryos and demonstrate an accumulation in the embryo, even after 24 hours.

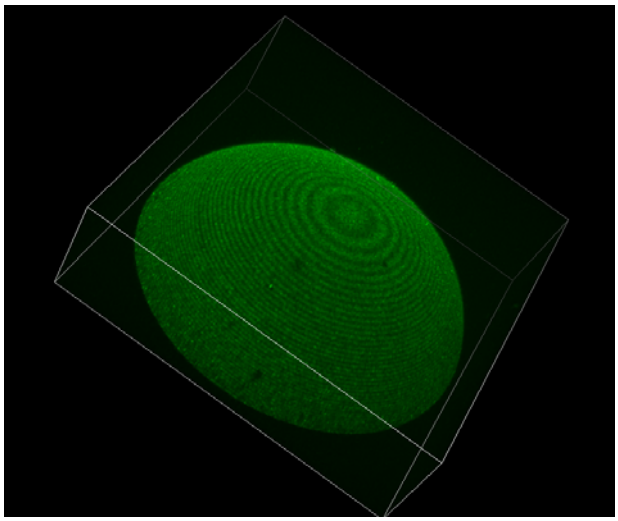

Figure 3.4.9: 24 hpf embryo exposed to DCF with DMSO concentration of 0.1 %; strong signal in the chorion; laser power: 100; HV: 30

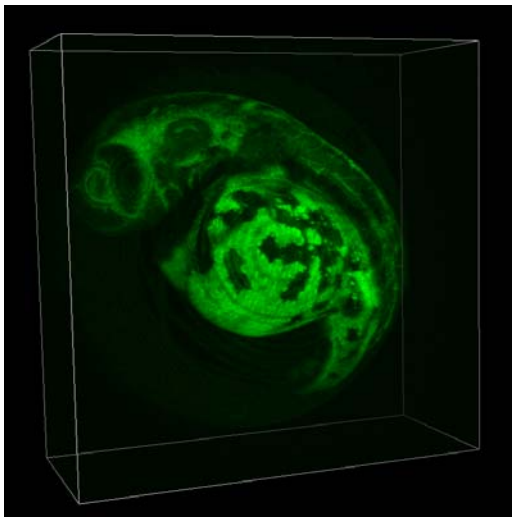

Figure 3.4.10: 48 hpf embryo exposed to DCF with DMSO concentration of 0.1 %; strong signal in the embryo; laser power: 100; HV: 10

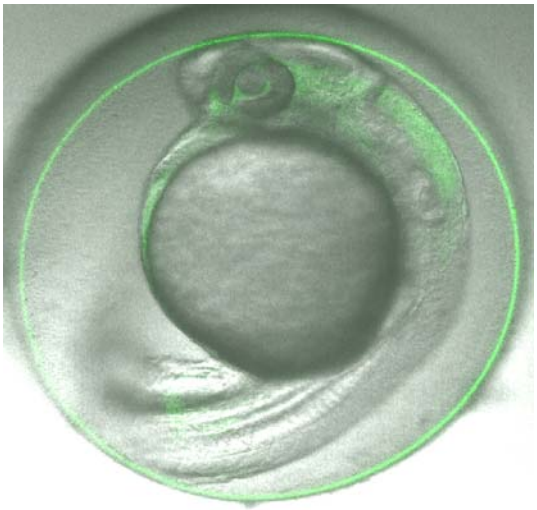

Figure 3.4.11: 24 hpf embryo exposed to DCF (DMSO concentration 0.1 %); strong signal in the chorion and a weaker signal in the embryo; laser power: 100; HV: 30; imaged with transmitted light

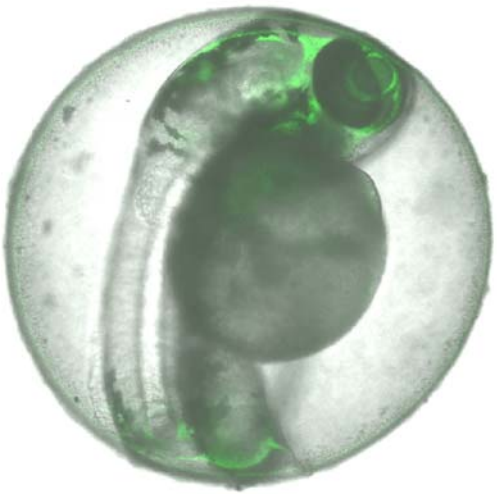

Figure 3.4.12: 48 hpf embryo exposed to DCF (DMSO concentration 0.1 %); no signal in the chorion and a stronger signal in the embryo; laser power: 40; HV: 30; imaged with transmitted light

Dechorionation of embryos exposed to DCF

After exposure dechorionated embryos (Fig. 3.4.13) show that DCF did not pass the chorion during the first 24 hours. The signal of the embryo was very low; the images were taken with laser power of 100 and a high voltage of 50.

In contrast, the 48 hpf embryos showed a strong signal (Fig. 3.4.14). The images were taken with laser power of 100 and a high voltage (HV) of 5. The low HV indicates the strong signal. A special illustration mode was used in Figure 3.4.14 to highlight the overexposure in color. The yellow regions represent a low overexposure, whereas the red regions demonstrate a very high overexposure. This illustration mode allows a better differentiation inside the embryo. The strongest accumulation was in the brain and blood; especially the venous vessels in the yolk sac were prominent. The arrow in Figure 3.4.14 shows the intestinal lumen with a high accumulation of fluorescein. This indicates that DCF has the same distribution as fluorescein after passing the chorion.

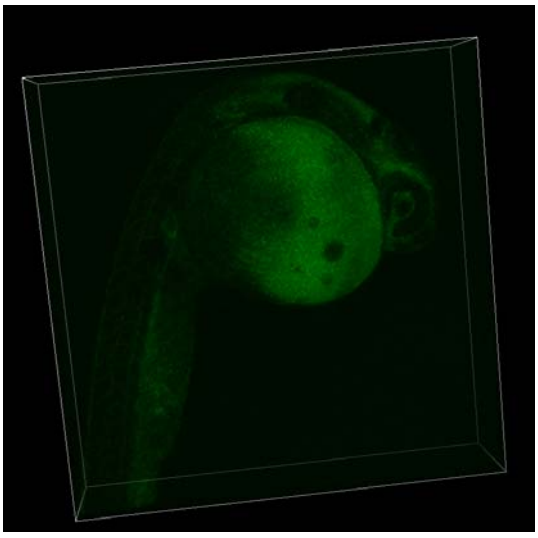

Figure 3.4.13: 24 hpf dechorionated embryo exposed to DCF (DMSO 0.1 %); laser power: 100; HV: 50

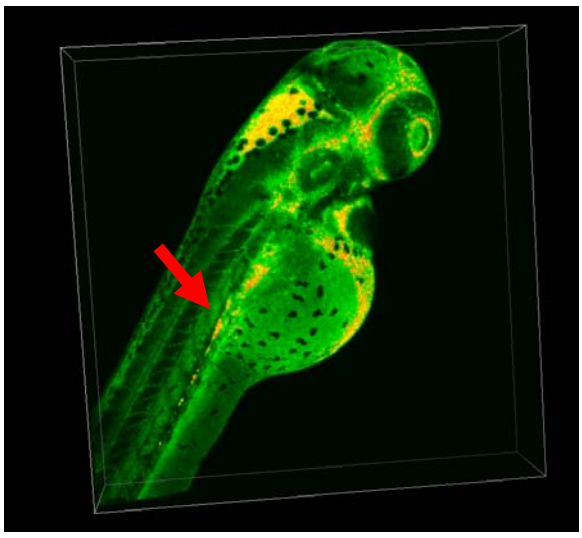

Figure 3.4.14: 48 hpf dechorionated embryo exposed to DCF (DMSO 0.1 %); laser power: 100; HV: 5; **red arrow**: strong signal in the intestinal lumen

3.5 5-(and-6)-Carboxy-2,7-dichlorofluorescein

3.5.1 Pre-test

5-Carboxy-2,7-dichlorofluorescein (carboxy-DCF) is the most complex molecule tested in this study, and the carboxy group makes it more soluble in water. Because of the assumption of lower toxicity than DCF, only one pre-test was done (see appendix, p. IV) with concentrations of 10, 25, 50 and 80 mg/L. Each concentration was tested with 20 eggs. The results of the toxicity tests did not show linear dose dependency. Based on this test, the highest concentration with 80 mg/L (0 % mortality) was chosen for the measurement of fluorescence, since this concentration guaranteed a good brightness.

Carboxy-DCF colored the chorion red as did DCF (Fig. 3.5.1). Figure 3.5.2 shows the control group with normally colored chorion.

Figure 3.5.1: 24 hpf embryo exposed to carboxy-DCF (80 mg/L), red coloration of the chorion

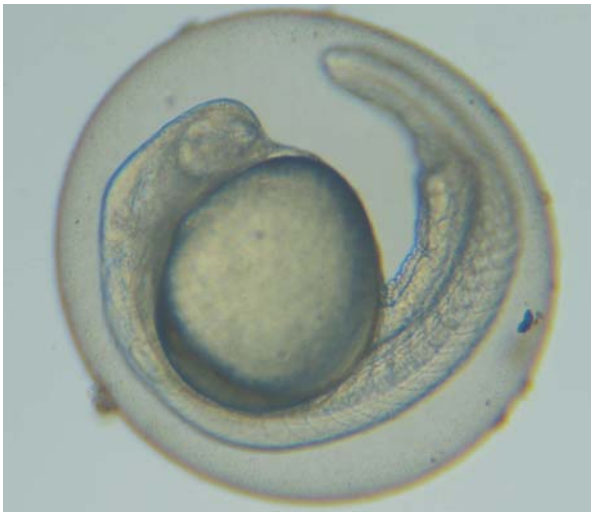

Figure 3.5.2: 24 hpf embryo control group

3.5.2 Epi-fluorescence microscopy - 5-(and-6)-carboxy-2, 7-dichlorofluorescein

The adsorption of carboxy-DCF to the outside of the chorion is shown in the picture of Figure 3.5.3. Due to this attachment, the embryos appeared to be blurred and the chorion showed an intense fluorescence.

Even after 48 hours, a low concentration in the embryos was still detectable, but the signal in chorion was getting weaker.

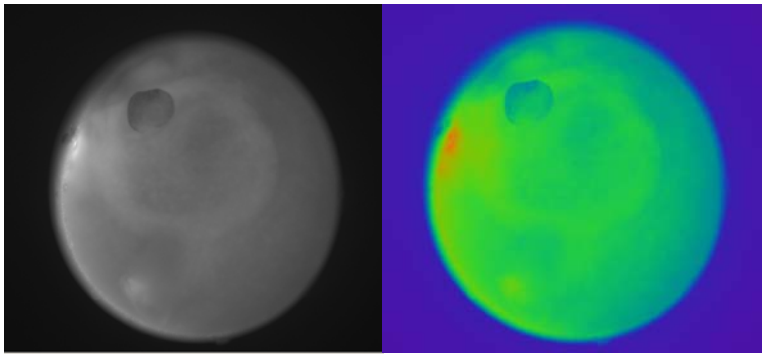

Figure 3.5.3: 24 hpf embryo exposed to 5-Carboxy-2,7-dichlorofluorescein (80 mg/L); shutter speed: 75 ms

Dechorionation

The distribution of carboxy-DCF differs from those of fluorescein and DCF. Figure 3.5.5 presents the embryos dechorionated after 24 and 48 hours of exposure and demonstrates that the substance rather accumulated in the yolk than in the brain. However, this distribution was not equal; since there was a higher signal in the area near to the heart (Fig. 3.5.5; left), and another one in the intestinal lumen, more precisely in the stomach (Fig. 3.5.5; right).

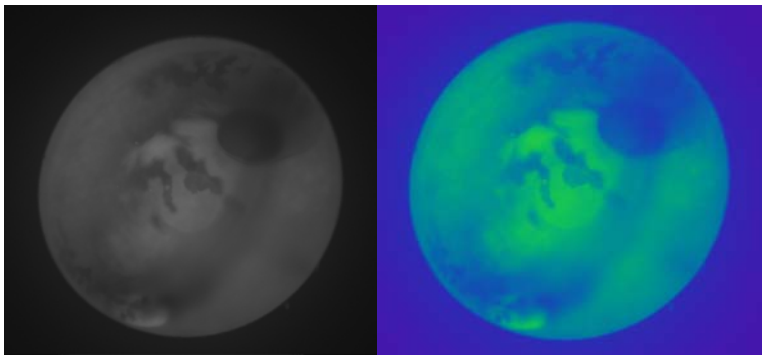

Figure 3.5.4: 48 hpf embryo exposed to 5-Carboxy-2,7-dichlorofluorescein (80 mg/L); shutter speed: 75 ms

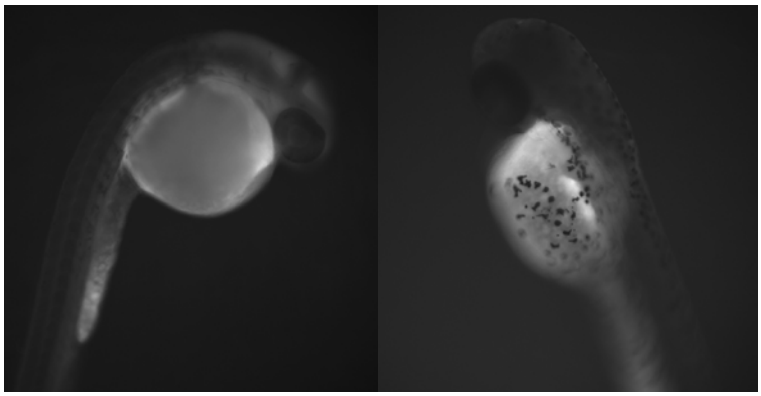

Figure 3.5.5: right: 24 hpf dechorionated embryo, **left:** 48 hpf dechorionated embryo, both exposed to 5-Carboxy-2,7-dichlorofluorescein (80 mg/L); shutter speed: 214 ms

Distribution of 5-Carboxy-2,7-dichlorofluorescein inside the embryo

Plot Profile

In the plot profile of carboxy-DCF (Fig. 3.5.6), the high accumulation in the chorion is reflected by the fact that the gray value is quite equal along the entire profile. The peak is regarded as an interference signal, supposedly from some dirt particles. The plateau reflects a constant mean gray value of the whole egg.

The high accumulation of carboxy-DCF in the chorion becomes even more evident when taking a look at the plot profile of the control group (Fig. 3.5.7). Here, the chorion reflects the light of the microscope at the edge of the egg, which is represented by the first and last high peak. The embryo itself is depicted by the plateau in the middle, with two smaller peaks labeling the margins of yolk sac.

By comparing the two plot profiles, it becomes evident that the dye covers the exposed eggs.

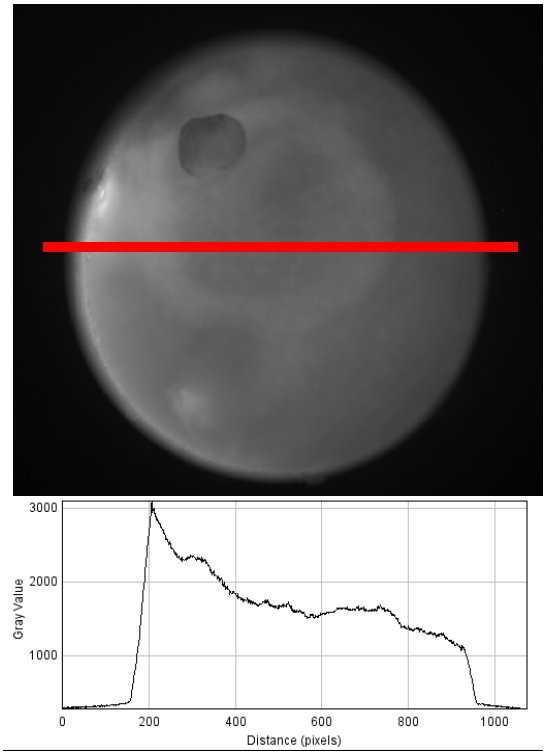

Figure 3.5.6: Plot profile of 24 hpf embryo exposed to 5-Carboxy-2,7-dichlorofluorescein (80 mg/L); shutter speed: 75 ms

Distribution of carboxy-DCF as measured *via* the ROI manager

An analysis with the ROI manager was not possible, because the differences in gray values were too low for differentiation.

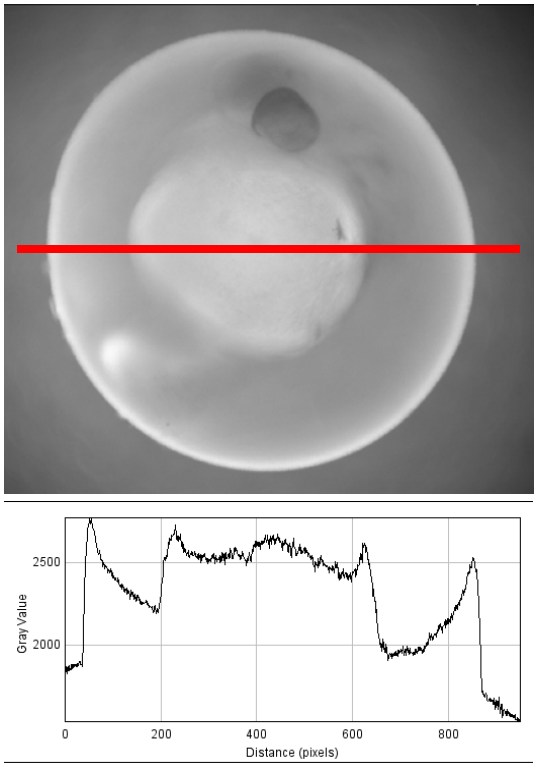

Figure 3.5.7: Plot profile of auto fluorescence (control group); shutter speed: 1.26 s

Additional measurement

To answer the question if carboxy-DCF is really held back by the chorion and if an increased uptake of carboxy-DCF (80 mg/L) in dechorionated embryos is possible, 24 hpf dechorionated embryos were transferred directly into carboxy-DCF (80 mg/L), whereas the embryos of the comparison group were dechorionated after 48 hours exposure.

The analysis was made with the ROI manger, and the observed area was the yolk sac. Figure 3.5.8 shows that there is hardly an increased uptake detectable in the dechorionated specimens. The signal of the dechorionated embryos, which were directly exposed to carboxy-DCF, increased about 10 %.

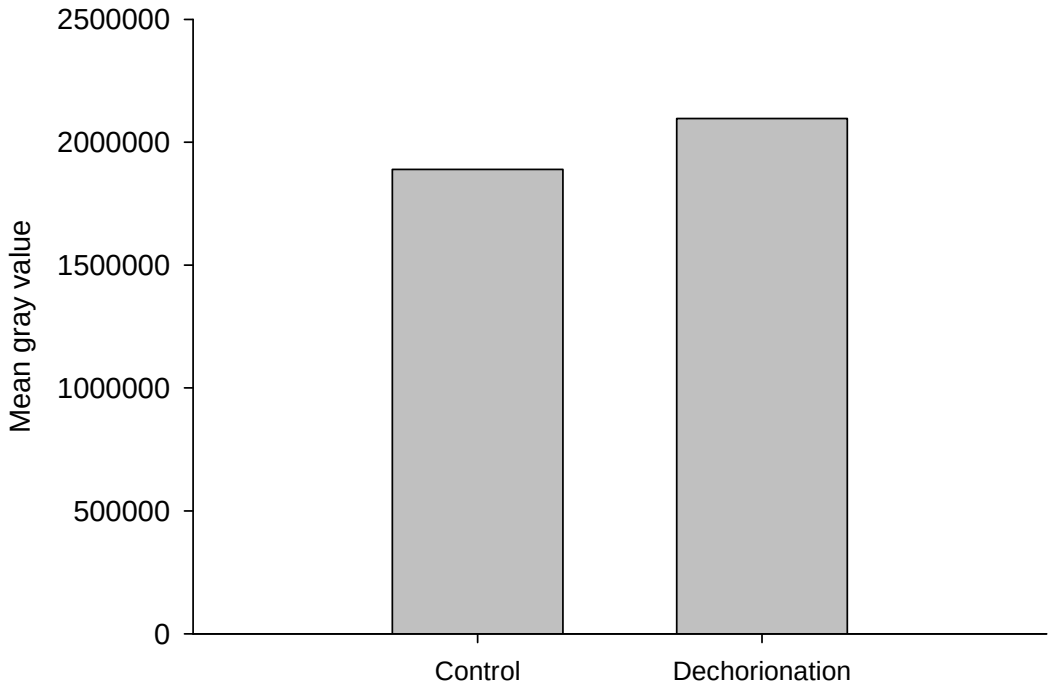

Figure 3.5.8: Comparison of mean gray values in the yolk sac of 48 hpf dechorionated embryos exposed after 24 hours directly to 5-carboxy-2,7-dichlorofluorescein (80 mg/L) (**right)** and embryos dechorionated after 48 hours exposure to CX-DCF (80 mg/L) (**left)**

3.5.3 Confocal laser scanning microscopy (CLSM) – Carboxy-DCF

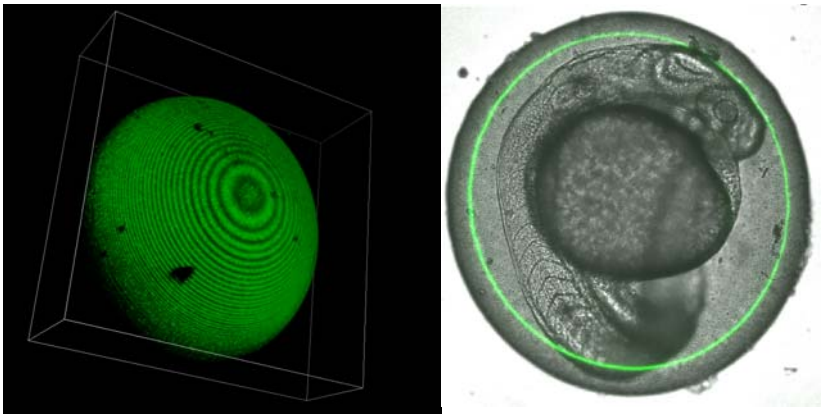

Figure 3.5.9: 24 hpf embryo exposed to 5-carboxy-2,7-dichlorofluorescein (80 mg/L); strong fluorescence signal in the chorion and no signal in the embryo; laser power: 100; HV: 10

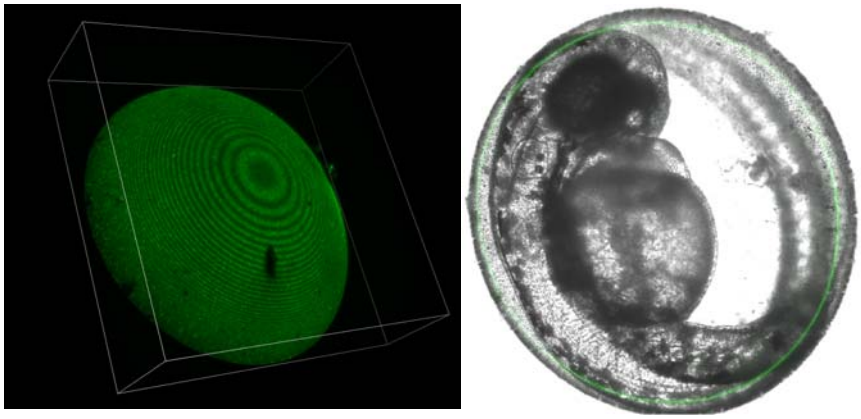

Figure 3.5.10: 48 hpf embryo exposed to 5-Carboxy-2,7-dichlorofluorescein (80 mg/L); strong fluorescence signal in the chorion and no signal in the embryo; laser power: 100; high voltage: 10

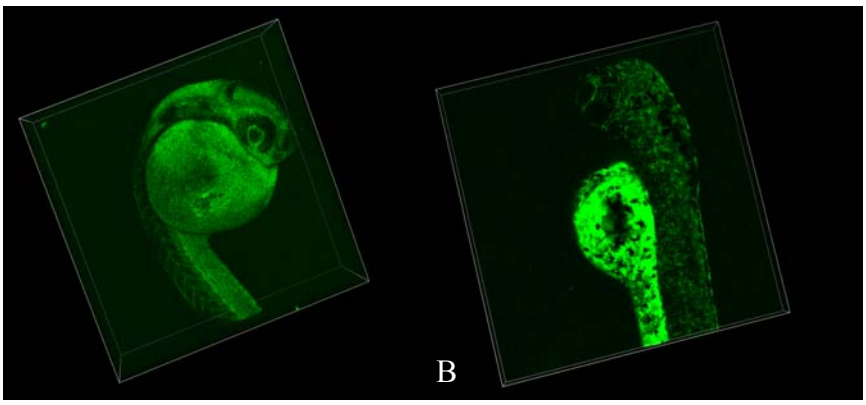

Figure 3.5.11: left: 24 hpf dechorionated embryo; **right**: 48 hpf dechorionated embryo exposed to 5-Carboxy-2,7-dichlorofluorescein (80 mg/L); dechorionated embryos show a weak signal in the yolk; laser power: 100; high voltage: 100

Figures 3.5.9-10 confirm the assumption that carboxy-DCF attached to the surface of the chorion. The signal of the chorion outshines the signal of the embryo. Even after 48 hours, there is no signal in the embryo detectable. The images taken with transmitted light show the position of the embryo inside the egg and confirm the lack of signal in the embryo. All images were taken with laser power of 100 and high voltage (HV) of 10.

Dechorionation of embryos exposed to carboxy-DCF

Figure 3.5.11 presents the dechorionated embryos with their weak signal. This becomes evident by comparing the high voltage, which is ten times higher than in Figures 3.5.9-10. When carboxy-DCF passed the chorion; it accumulated especially in yolk.

24 hpf chorion in detail

Figure 3.5.12 shows the chorion of a 24 hpf embryo in detail. The red square demonstrates the area of the picture detail. The 3d image is taken with 50 slices; each slice has a thickness of 0.26 µm therefore, the image of the chorion represents 13 µm in total.

The bright spots are likely to represent the pores of the chorion. Carboxy-DCF has a high molecular complexity; hence, it does not pass the chorion and possibly attach to the pore channel. However, to make a statement, there needs to be more in-depth research into the chorion.

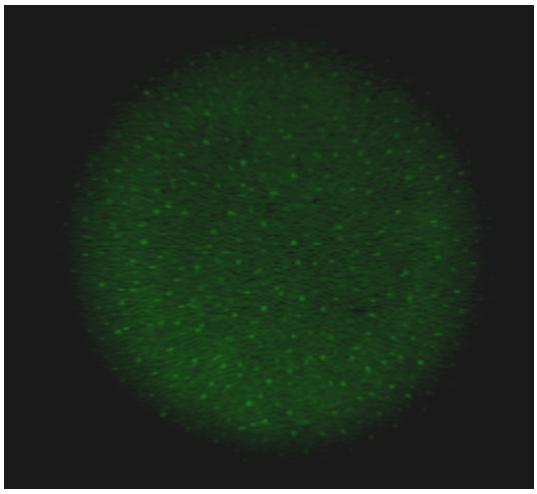

Figure 3.5.12: above: selected area of the chorion**; below:** frontal view: detail of 24 hpf chorion, 3d image of chorion, thickness 13 µm (50 slices, each 0.26)

3.6 Dimethyl sulfoxide (DMSO) as a solvent

3.6.1 Autofluorescence of DMSO

An important aspect for evaluating the results of tests with different DMSO concentrations was to measure the autofluorescence of the solvent used. Therefore, a test with eggs exposed to 1 % (Figure 3.6.1 **A, D**) and 0.01 % (Figure 3.6.1 **B, E**) DMSO plus one control group, which had been exposed to artificial water, was performed (**C, F**). All images were taken with laser power of 100 and high voltage of 200 after 24 hours (**A-C**) and a lower HV of 100 after 48 hours (**D-F**). The comparison to the control group demonstrated an autofluorescence of DMSO: The higher the DMSO concentration, the higher the autofluorescence of the chorion. However, it is important to note that the images of 24 hours were taken with a high voltage of 200. Nevertheless, an increased signal was visible. After 48 hours the autofluorescence of DMSO did not change, the fluorescence signal in Figure 3.6.1 seemed to be weaker due to the smaller HV of 100. The lesion in the chorion of Figure 3.6.1 **D** did not affect the prior statement. Furthermore, all dechorionated embryos showed no signal at all, even at a high voltage of 200. The phenomenon of autofluorescence was only detected in the chorion.

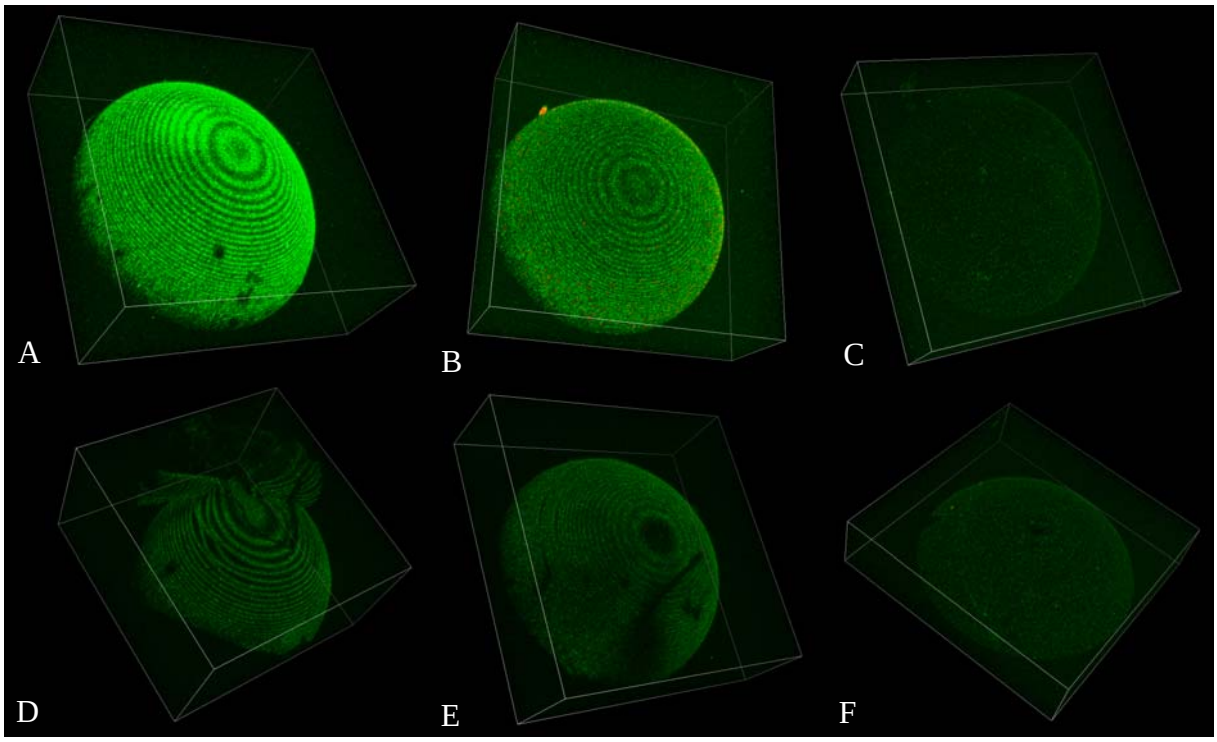

Figure 3.6.1: 24 hpf (**A-C**) and 48 hpf (**D-F**) embryos were exposed to 1 % (**A, D**), 0.01 % (**B, E**) DMSO and the control group (**C, F**); DMSO 1 % (**A,D**) show the highest and DMSO 0.01 % (**B, E**) the lowest autofluorescence in the chorion, even the control group show a weak autofluorescence in the chorion (**C, F**); all images were taken with a laser power of 100 and HV of 200 (24 hpf embryos) or 100 (48 hpf embryos)

3.6.2 Epi-fluorescence microscopy-Fluorescein

In order to check whether DMSO influences the distribution or signal strength of fluorescein, 100 mg/L of fluorescein were solved in 0.01 %, 0.1 % and 1 % DMSO. All images of 24 hpf embryos had an exposure time of 30 ms, whereas the 48 hpf embryos had one of 2 ms.

Comparing the images of Fig. 3.6.2 (**A-F**), it was notable that the signal strength in the embryos decreased with lower DMSO concentrations. However, not only the signal intensity changed with a lower DMSO concentration, but also the distribution of fluorescein. Figure (**E-F**) shows the distribution of fluorescein in the lowest solvent concentration of 0.01 %. The accumulation appears to be higher in the chorion, than in the embryo (**E**).

Even after 48 hours, a difference in signal strength could be detected (**B**, **D** and **F**). The distribution of fluorescein in the lowest DMSO concentration was similar with a decreased signal in the chorion and a stronger signal in blood, especially in the venous return of the yolk sac (**F**).

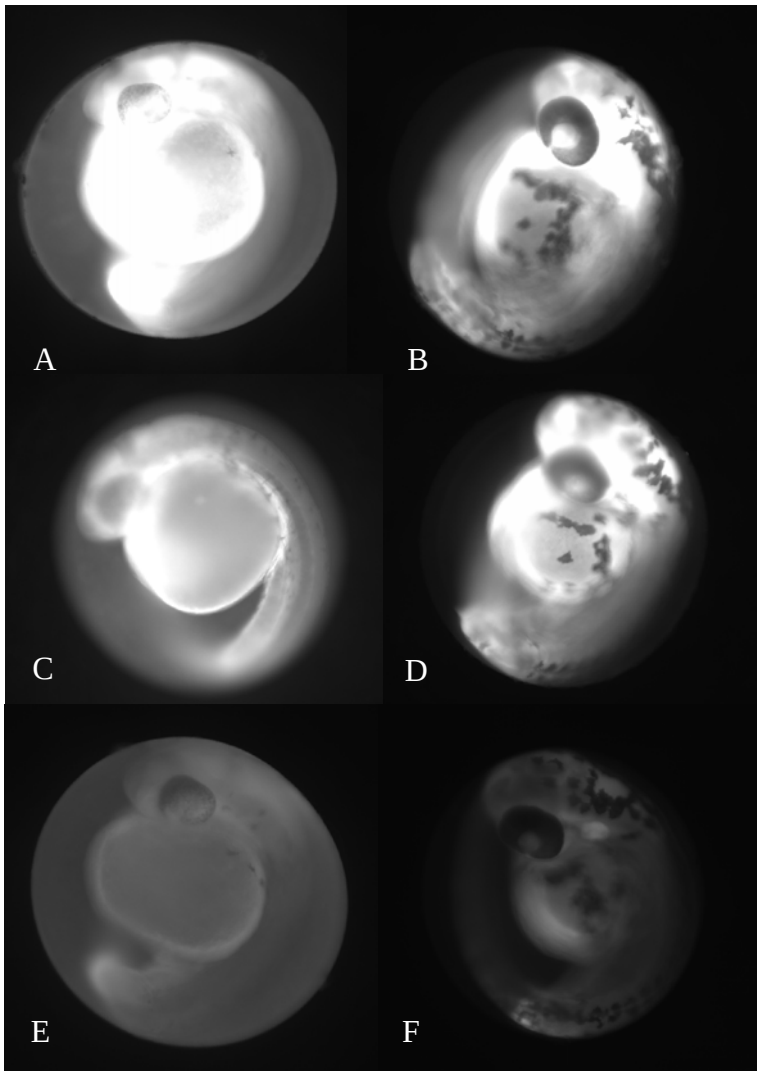

Figure 3.6.2: 24 hpf (**A, C, E**) and 48 hpf (**B, D, F**) embryos exposed to fluorescein (100 mg/L). **A-B** 100 mg/L fluorescein in 1 %, **C-D** in 0.1 % and **E-F** in 0.01 % DMSO; fluorescein in 1 % and 0.1 % show a strong signal in the embryo (**A-D**), 0.01 % DMSO show a weak signal in the embryo and a higher signal in the chorion (**E-F**), the signal strength increase with higher DMSO concentration (**A > C > E**); shutter speed: 30 ms (for 24 hpf embryos) and 2 ms (for 48 hpf embryos)

Permeability of chorion

This extended test determines the permeability of the chorion to fluorescein: One group of 24 hpf embryos was exposed directly without chorion to 100 mg/L fluorescein with a solvent concentration of 1% DMSO (Fig. 3.6.3 **A**). The other group was exposed with their chorion for 24 hours and dechorionated after 48 hours (**B**). This test was also done with 100 mg/L fluorescein in 0.01 % DMSO (dechorionated after 24 hours (**C**) and after 48 hours (**D**)).

The embryos which were directly exposed to fluorescein in 1 % DMSO (**A**), showed a higher accumulation of fluorescein compared to embryos which were protected by the chorion (**B**). Both pictures have an exposure time of 1 ms.

The embryos which were exposed to fluorescein (100 mg/L) in 0.01 % DMSO generally showed a lower signal (**C**, **D**). The accumulation in those embryos was smaller than in the embryos which had been exposed to fluorescein solved in 1 % DMSO. Furthermore, the difference between the exposure with and without chorion was also small. The signal of embryos which were exposed directly was slightly higher (**C**). Both pictures were taken with an exposure time of 103 ms.

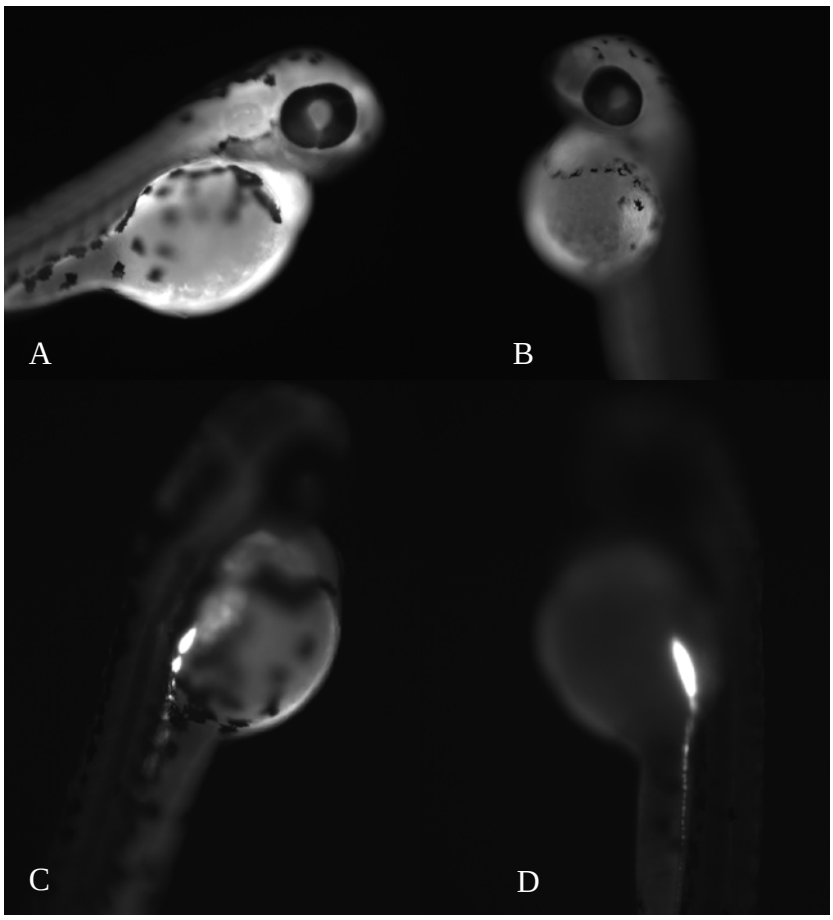

Figure 3.6.3: 48 hpf embryos exposed to 100 mg/L fluorescein in 1 % DMSO (**A, B**) and in 0.01% DMSO (**C, D**); dechorionation after 24 hours (**A, C**) and dechorionation after 48 hours (**B, D**); shutter speed: 1 ms (**A, B**) and 103 ms (**C, D**)

Does the structure of the chorion change during the embryonic development?

In order to check if the chorion changes its structure during the embryonic development, an additional test was done. One group of 3 hpf embryos (Figs. 3.6.4 **C, F, I**) was directly exposed to fluorescein (100 mg/L) and the other group was exposed to fluorescein (100 mg/L)

at an age of 24 hpf (**B, E, H)**. For a better comparison, Figs. 3.6.4 (**A, D, G)** show the distribution of fluorescein in the 24 hpf embryo which had a direct exposure.

Figure 3.6.4 (**B**) shows that fluorescein passed through the chorion of 48 hpf embryos, even though the exposure time was only 24 hours. The comparison with 24 hpf chorions (**A**) showed only a weak signal in the embryo (**D**). In contrast, the embryos which had the same time of exposure but in a different stage of development (**E**, 48 hpf), showed a stronger signal than the 24 hpf-group (**D**). Nevertheless, the accumulation in embryos exposed for 48 hours (**C, F**) is higher than after 24 hours exposure (**B, E**).

The test was also conducted with 100 mg/L fluorescein solved in 0.1 % DMSO. Except for an increased signal, there were no differences in the distribution detectable (**G, H, I**) to that with 0.01 % DMSO. All images were taken with laser power of 100 and high voltage of 10.

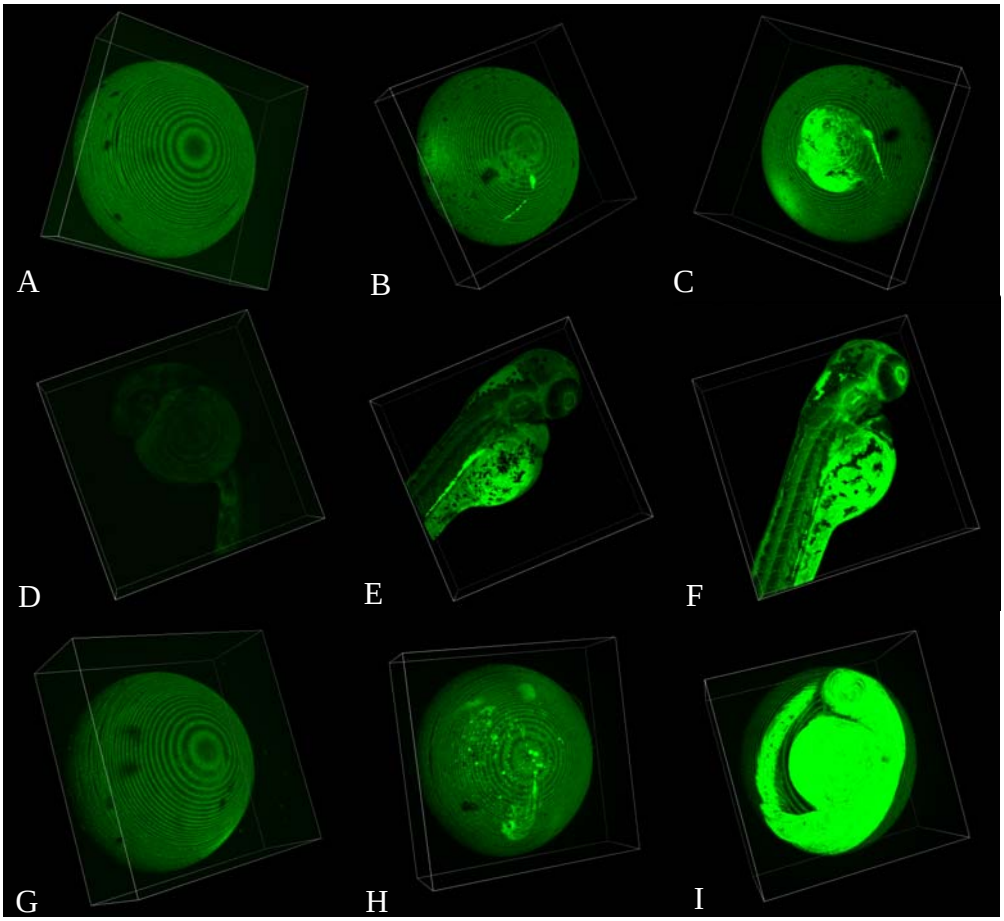

Figure 3.6.4: 24 hpf (**A, D, G**) and 48 hpf embryos (**B, C, E, F, H, I**) exposed to fluorescein (100 mg/L) in 0.01 % DMSO (**A-F**) and 0.1 % DMSO (**G-I**), exposure not before 24 hpf (**B, E, H**), all others had a direct exposure (**A, C, D, F, G, H**); all images were taken with laser power: 100 and HV: 10

Uptake of the dye from the chorion?

To check if there is an uptake of the dye from the chorion to the embryo, dechorionated and non-dechorionated embryos were investigated. The observation took place within the period from 24 hpf to 48 hpf, because in this time the structure of the chorion changes and becomes thinner (Hermann 1993; Hagedorn et al. 1997).

In general, the signal of fluorescein solved in 1 % DMSO (Figs. 3.6.5 **A, B**) was higher than in 0.01 % DMSO (**C, D**). If there had been an uptake from the chorion into the embryo, the signal of the non-dechorionated embryo (**B, D**) would have had to be higher than in the dechorionated embryo (**A, C**), given that the additional dye could have only come from the egg water or chorion. Neither fluorescein solved in 1 % DMSO, nor fluorescein solved in 0.01 % showed a definitely increased signal. The brighter signal in the embryo with chorion (**A** and **C**), was more likely an interference signal caused by different focal planes.

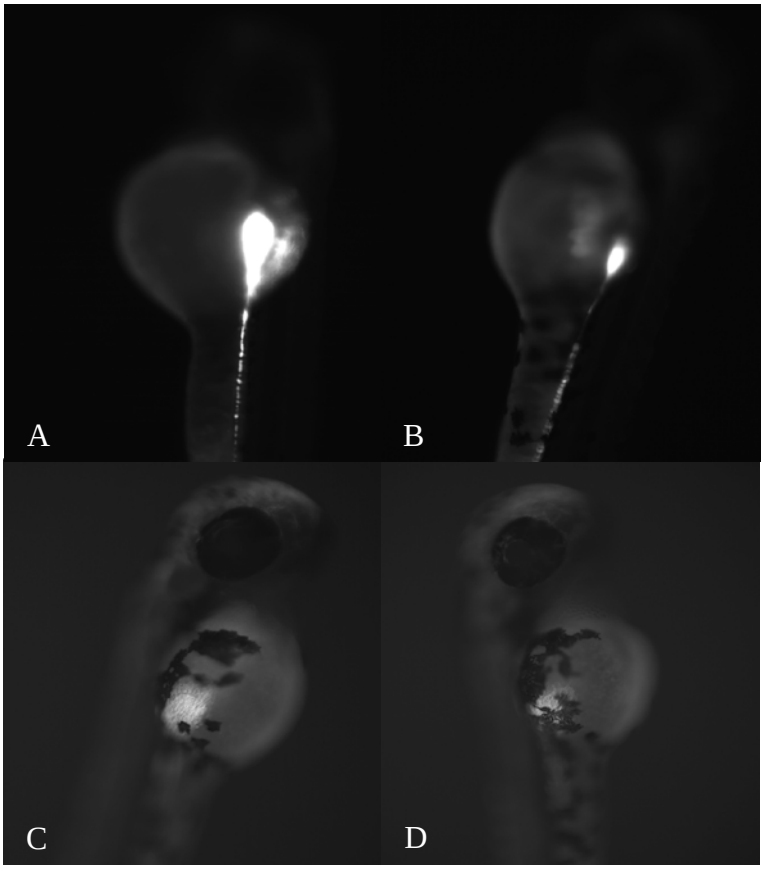

Figure 3.6.5: 48 hpf embryos washed for 24 hours in artificial water with chorion (**A, C**) and without chorion (**B, D**); exposure to fluorescein (100 mg/L) in 1 % DMSO (**A, B**), and in 0.01 % DMSO (**C, D**); shutter speed: 33 ms (**A, B**); 470 ms (**C, D**)

3.6.3 Confocal laser scanning microscopy (CLSM) DMSO-Fluorescein

All embryos were exposed to fluorescein (100 mg/L) in three different DMSO concentrations: 1 %, 0.1 %, and 0.01 %. All images were taken with a laser power of 100 and a high voltage of 20; therefore, a comparison of intensity was possible. Figs. 3.6.6 (**A** and **B**) show the highest concentration of DMSO and the strongest signal. The chorion outshines the signal of the embryo (**B**). However, the cross-section of the egg illustrates the accumulation in the embryo. A difference in distribution between 1 % and 0.1 % DMSO was not detectable. Fluorescein in 0.1 %DMSO attached at the chorion (**D**) and accumulated in the embryo (**C**). The signal intensity was also the same as with 1 % DMSO. The distribution inside the embryo did not differ from the results in chapter 3.3, where fluorescein accumulated in brain and blood.

In contrast to these results, the distribution of fluorescein in 0.01 % DMSO did not pass the chorion (**F**), and, likewise, the cross section gave no signal in the embryo after 24 hours (**E**). Furthermore, the signal strength also decreased with lower DMSO concentration.

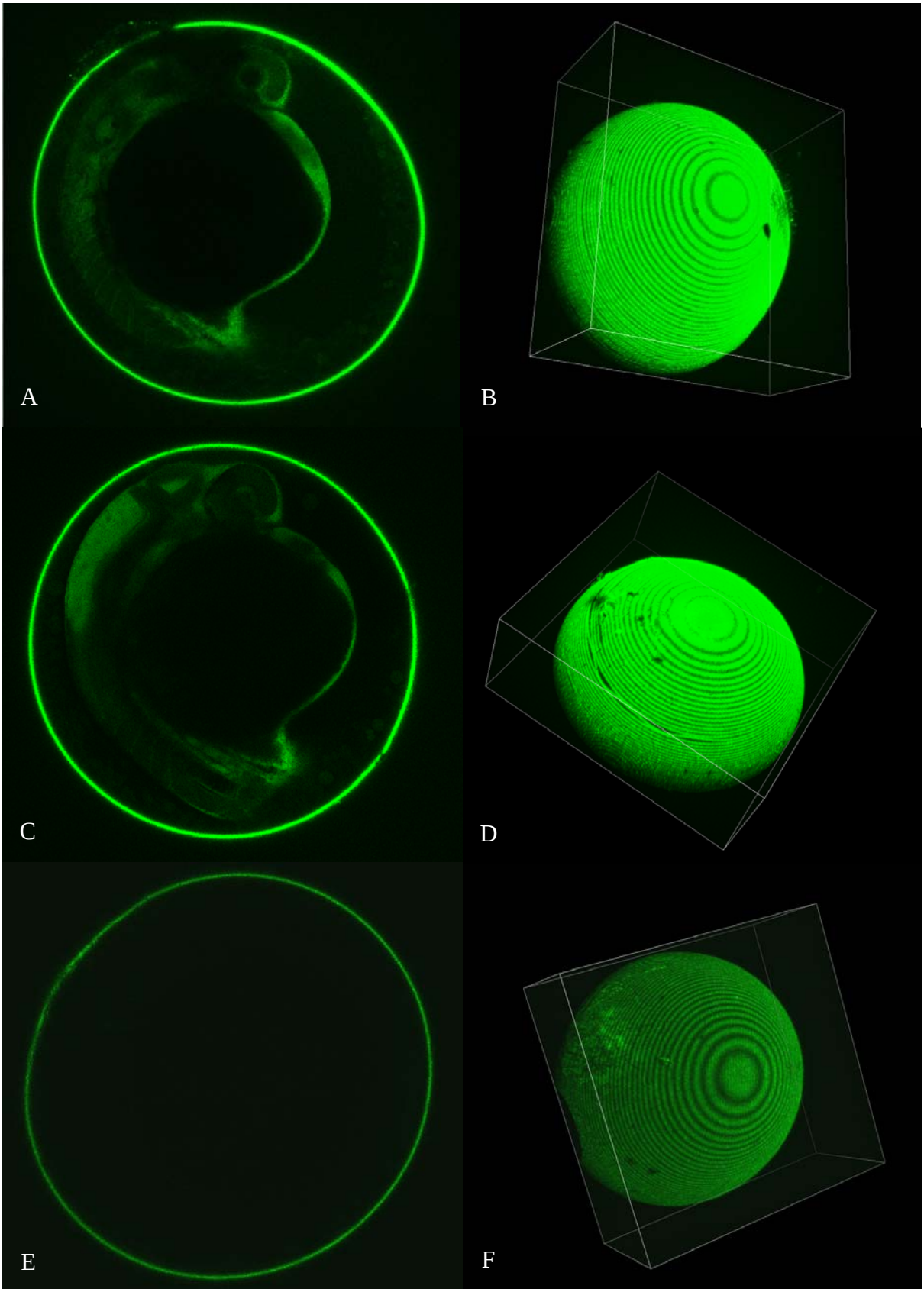

Figure 3.6.6: 24 hpf embryos exposed to fluorescein (100 mg/L) in 1 % (**A-B**), in 0.1 % (**C-D**) and in 0.01 % (**E-F**) DMSO, fluorescein in 1 and 0.1 % DMSO passes the chorion and accumulates in the embryo (**A, C**); fluorescein in 0.01 % DMSO does not pass the chorion and no signal in the embryo is detectable (**E**), the signal strength decreases with lower DMSO concentrations (**B, D, F**); all images were taken with laser power: 100 and high voltage: 20

After 48 hours of exposure, the distribution of fluorescein changed: fluorescein in 1 % and 0.1 % DMSO increasingly accumulated in the embryo (Figs. 3.6.7 **A-F**). The signal of the embryo outshined the one of the chorion (**C, F**). The fluorescence signal of 1 % and 0.1 % was so bright that the high voltage had to be reduced to 1. Even the images taken with transmitted light still showed the high intensity of the dye, although the laser power and high voltage had been reduced (**A, D**). The distribution of fluorescein solved in 0.01 % differs after 24 and 48 hours. A small portion of fluorescein diffused with time through the chorion and accumulated in the intestinal lumen (**H**) and showed the same distribution as described in chapter 3.3.2 (Figs.3.3.4 and - 5) after 24 hours washing and illustrates that there is no saturation of fluorescein inside the egg (cp. chapter 3.3.2). Nevertheless, the majority of the dye was still attached to the chorion (**I**).

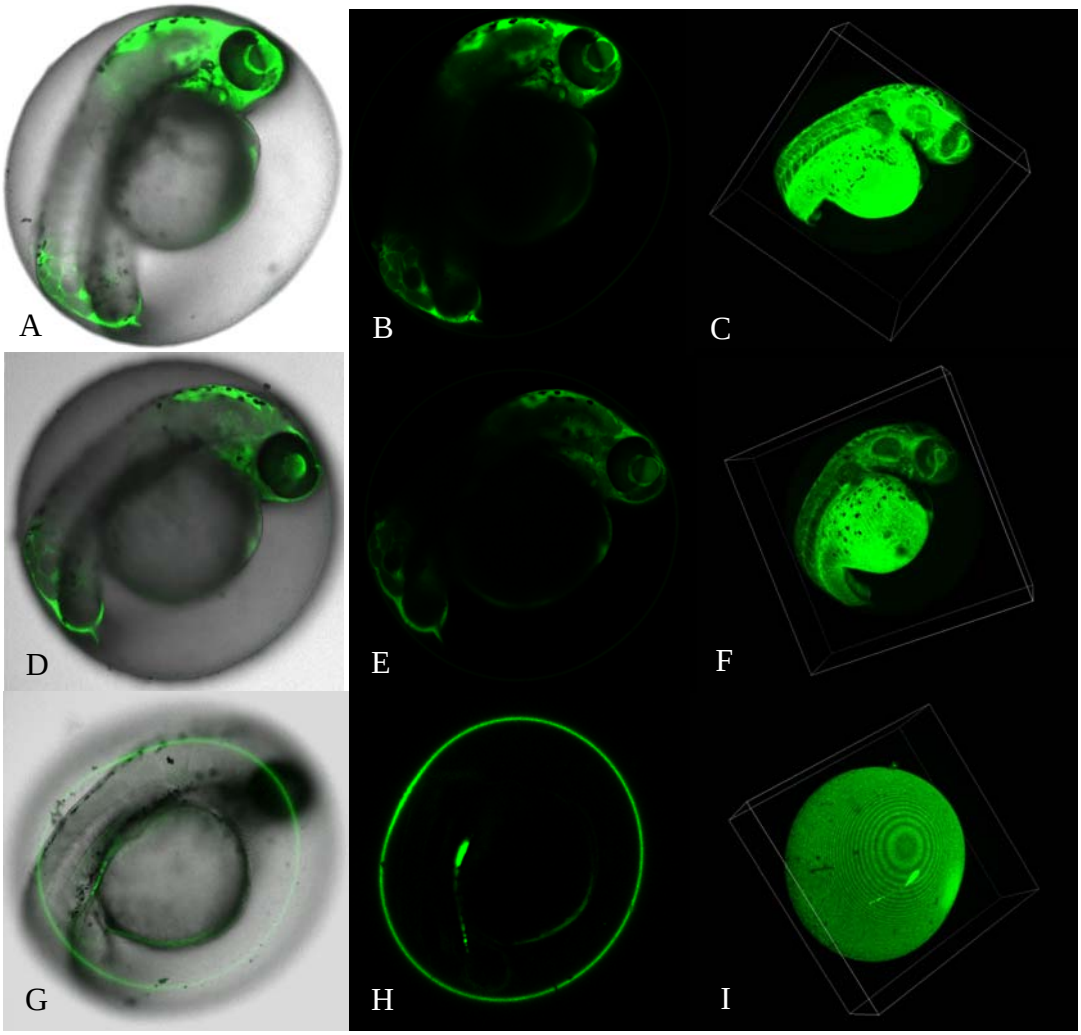

Figure 3.6.7: 48 hpf embryos exposed to fluorescein (100 mg/L) in 1 % (**A-C**), in 0.1 % (**D-F**) and in 0.01 % DMSO (**G-I**), 1 % and 0.1 % DMSO show a strong signal in the embryo and outshine the one of the chorion (**A-F**), 0.01 % DMSO shows a strong signal in the chorion and a small portion of fluorescein in the intestinal lumen (**G-I**); images with transmitted light were taken with L: 15, HV: 10 (**A**), L:5, HV: 30 (**D**), L: 6, HV: 100 (**G**); fluorescence images were taken with L: 100 HV: 1(**B, C, E, F**) and HV: 20 (**H, I**)

Dechorionation of embryos exposed to fluorescein in 1 % - 0.1 % – 0.01 % DMSO

The 24 hpf and 48 hpf dechorionated embryos exposed to 100 mg/L fluorescein in 1 % and 0.1 % DMSO (Fig. 3.6.8 **A**-**D**) showed the same effect of strong accumulation in their bodies like the ones with chorion (**C**, **F**). The distribution inside the embryo was difficult to assess, since the signal was oversaturated. In contrast, the 24 hpf dechorionated embryos exposed to fluorescein in 0.01 % DMSO showed a weak signal (**E**). After 48 hours, the signal increased gradually; especially the signal in the intestinal lumen saves a strong signal (**F**). Nevertheless, the signal was weak, which is demonstrated by the high HV of 150 (**E**) and 100 (**F**).

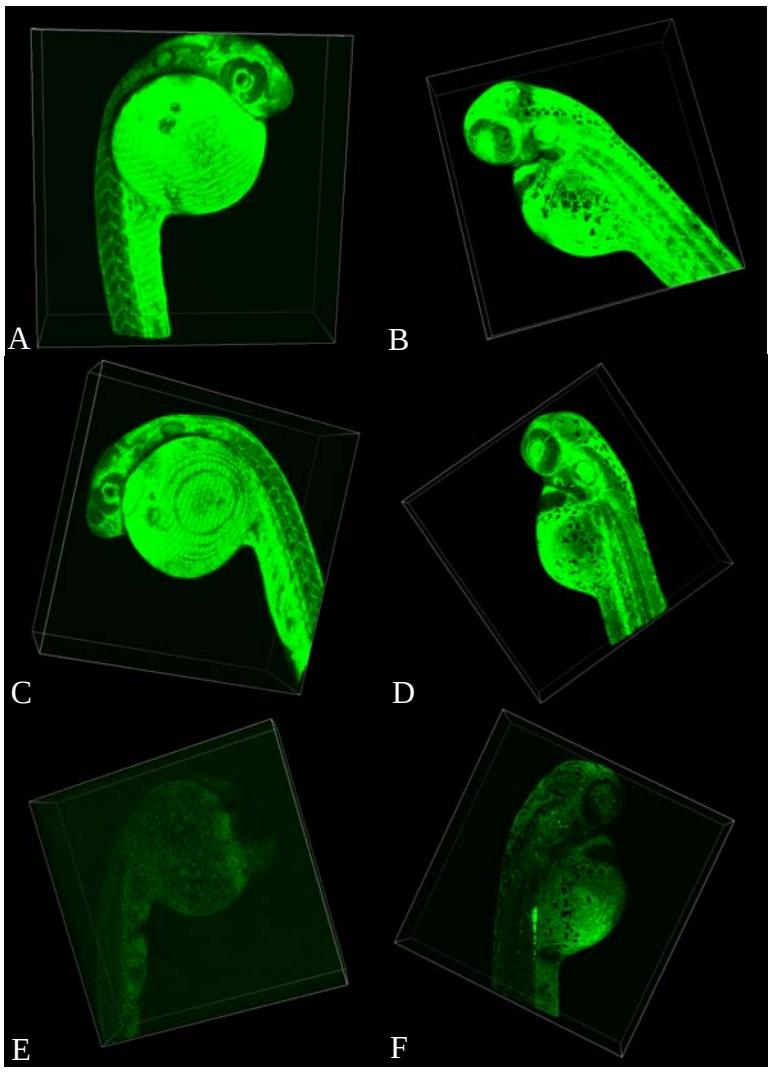

Figure 3.6.8: 24 hpf (**A, C, E**) and 48 hpf (**B, D, F**) dechorionated embryos exposed to fluorescein in 1 % (**A, B**); 0.1 % (**C, D**) and 0.01 % (**E, F**) DMSO; 1 and 0.1 % DMSO concentrations show a strong signal in the embryo (**A**-**D**); 0.01 % show a weak signal in the embryo (**E, F**) and a small part of fluorescein in the intestinal lumen (**F**); 24 hpf embryo laser power: 100, but different HV: 20 (**A**), 30 (**C**) and 150 (**E**), 48 hpf embryo laser power: 5 (**B**), 3 (**D**) and 100 (**F**) and HV: 15 (**B, D**) and 100 (**F**)

3.6.4 Epi-fluorescence microscopy DMSO-DCF

24 hpf (**A, C, E**) and 48 hpf (**B, D, F**) embryos had been exposed to 2,7- dichlorofluorescein (DCF) in 1 % (**A, B**), 0.1 % (**C, D**) and 0.01 % (**E, F**) DMSO (Figure 3.6.9). The effect of the distribution by using different concentrations of DMSO was not as prominent as with fluorescein. Especially the differences after 24 hours were small and there was no increased uptake visible. The brighter signal in **C** was an interference signal, because DCF was still diffusing out of the egg and, therefore, the washing time was most likely too short. All images of the 24 hpf embryos have the same exposure time of 40 ms.

After 48 hours, the differences in signal strength increased. The embryos which had been exposed to DCF in 1 % and 0.1 % DMSO showed a higher signal (**B, D**) than those in 0.01 % DMSO (**F**); otherwise, there was no difference in the distribution inside the embryo. It seems as if the uptake of DCF was not significantly increased by different DMSO concentrations.

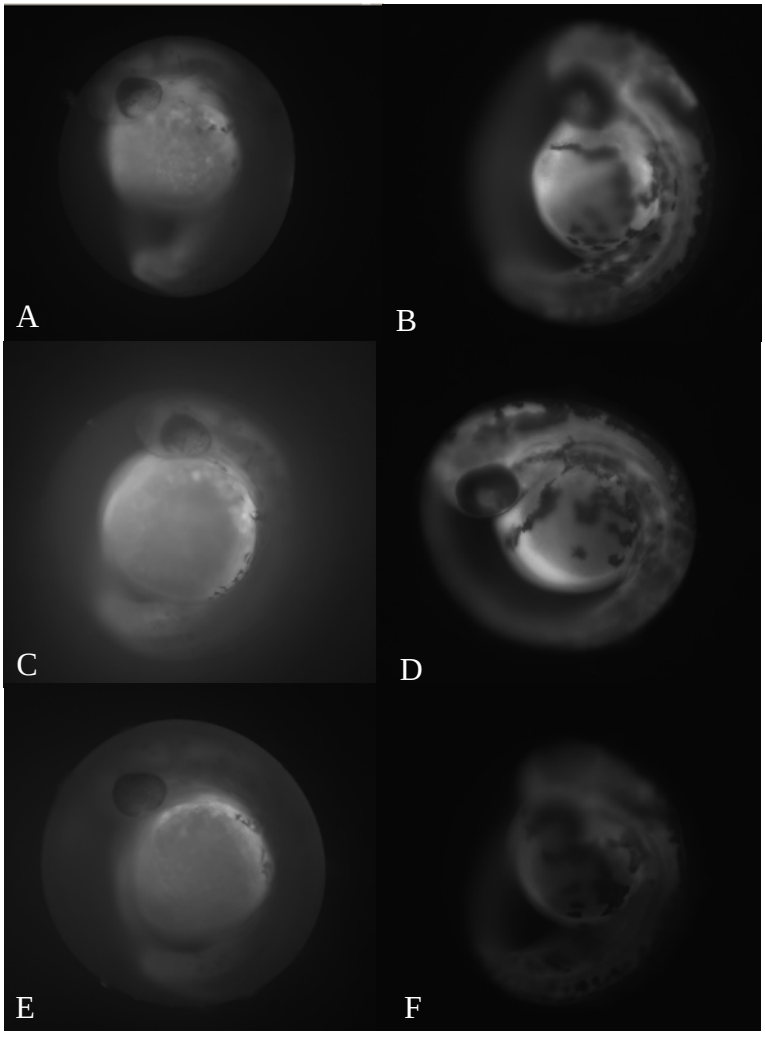

Figure 3.6.9: 24 hpf (**A, C, E**) and 48 hpf (**B, D, F**) embryos were exposed to DCF in 1 % (**A, B**), 0.1 % (**C, D**) and 0.01 % (**E, F**) DMSO; 24 hpf embryos show no prominent differences in signal strength in 1, 0.1, 0.01 % DMSO (**A, C, E**), 48 hpf embryos in 1, 0.1 % DMSO (**B, D**) show a stronger signal in the embryo than in 0.01 % DMSO (**F**); shutter speed for 24 hpf embryos: 40 ms and for 48 hpf embryos: 2 ms

3.6.5 Confocal laser scanning microscopy (CLSM) - DCF

24 hpf embryos (**A-I**) which had been exposed to DCF in 1 % (**A-C**), 0.1 % (**D-F**) and 0.01 % (**G-I**) DMSO (Fig. 3.6.10). All images were taken with a laser power of 100 and a high voltage of 30. It is demonstrated that there were no real difference between the different concentrations of DMSO. Only a weak signal was detectable in the embryos, which had been exposed to DCF in 1 % and 0.1 % (**A, B, D, E**) DMSO. The signal of the embryo exposed to 0.01 % DMSO was barely detectable (**H**). The images which were taken with transmitted light illustrate the same effect, a strong signal in the chorion and a weaker one in the embryo (**A, D, G**).

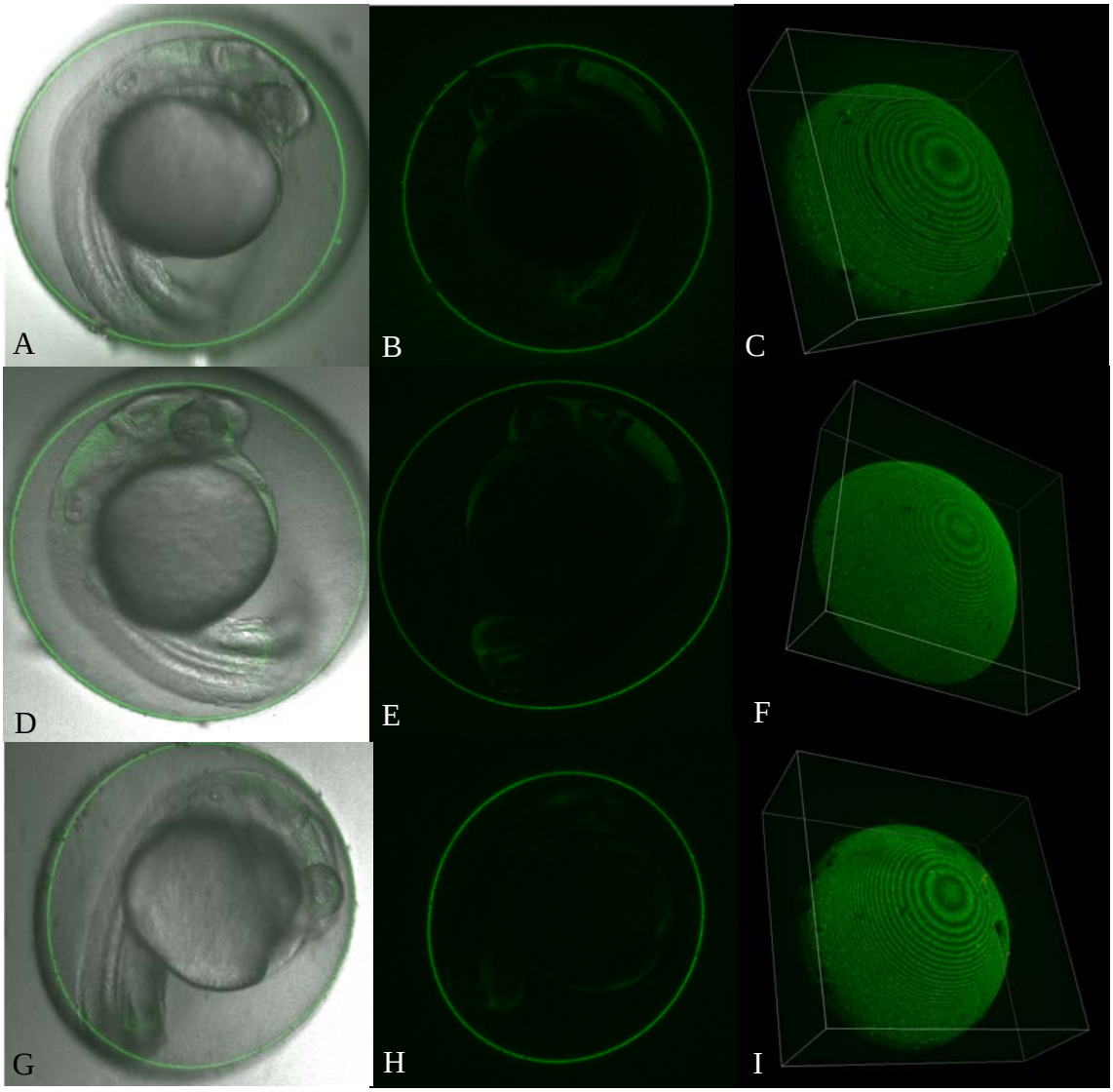

Figure 3.6.10: 24 hpf (**A-I**) embryos exposed to 2,7-dichlorofluorescein in 1 % (**A-C**), 0.1 % (**D-F**) and 0.01 % (**G-I**) DMSO; 1, 0.1 % DMSO show a weak signal in the embryo and a higher one in the chorion (**A-F**), in 0.01 % DMSO the signal of the embryo is barely detectable, but the chorion shows a strong signal (**G-I**); all images were taken with laser power: 100 and HV: 30

Apart from the fact that the signal of the embryos with a concentration of 1 % and 0.1 % DMSO increased (**B, D**), no differences in distribution were detectable after 48 hours. All images were taken with a laser power of 100 and an HV of 10 except Figure **E**, which was taken with an HV of 30 in order to point out the signal in the chorion.

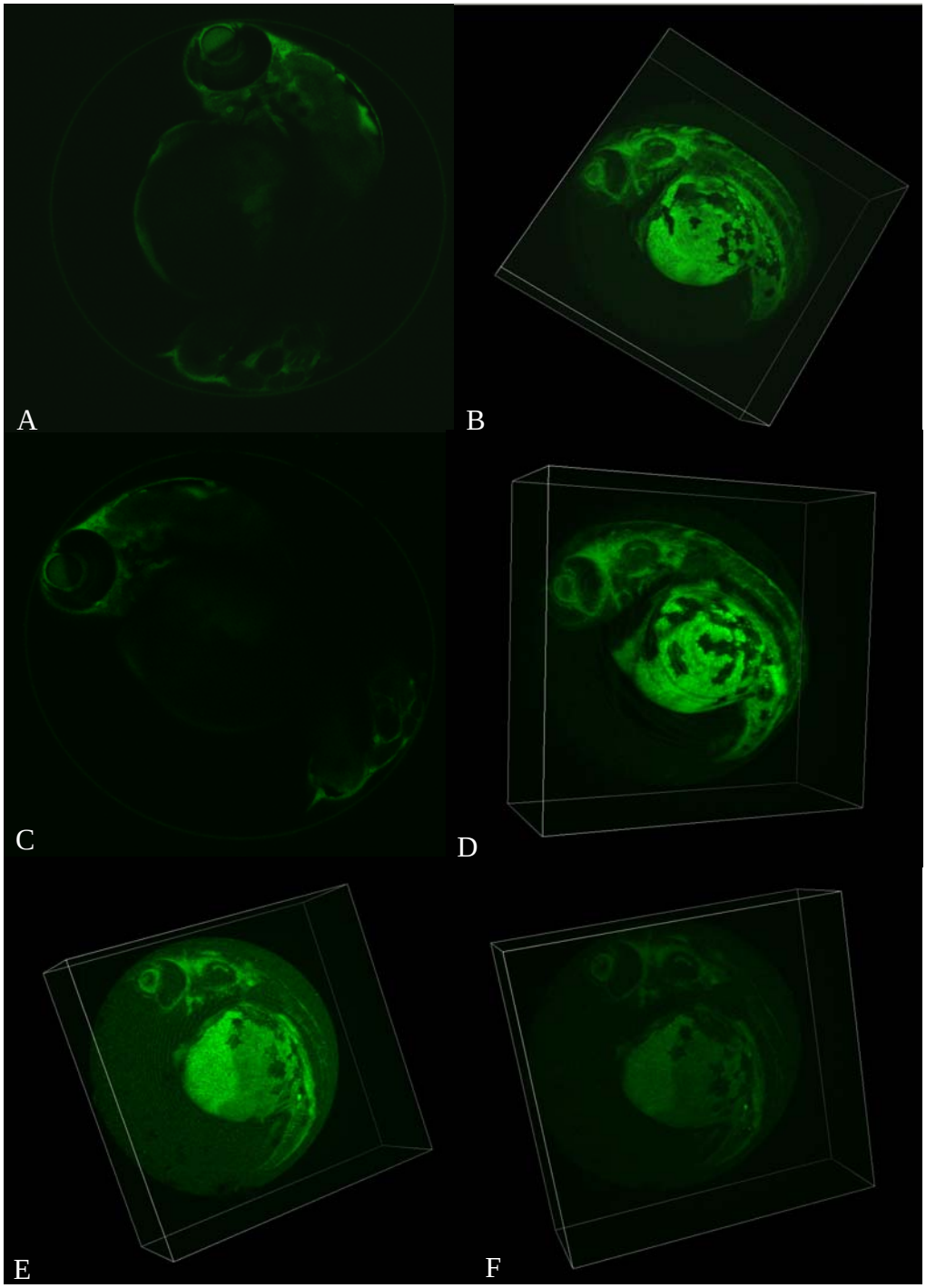

Figure 3.6.11: 48 hpf (**A-F**) embryos exposed to 2,7-dichlorofluorescein in 1 % (**A-B**), 0.1 % (**C-D**) and 0.01 % (**E-F**) DMSO, 1, 0.1 % DMSO show an increased signal in the embryo (**A-D**), 0.01 % DMSO does not show a change in the signal strength (**E-F**); all images were taken with laser power: 100 and HV: 10, except **E** was taken with HV: 30

Dechorionation of embryos exposed to DCF in 1 % - 0.1 % – 0.01 % DMSO

The dechorionated embryos demonstrate that there were no differences in distribution after 24 hours, nor after 48 hours. The 24 hpf embryos showed a weaker signal than the 48 hpf embryos as illustrated in Fig. 3.6.12 with the high voltage of 50. The distribution inside the embryo was the same as mentioned in chapter 3.4. After 48 hours, a higher accumulation of DCF was detectable, and the HV could be reduced to 5. Nevertheless, the signal of the embryos, which had been exposed to DCF in 0.01 % DMSO, was weaker. The accumulation was also the same as already described (chapter 3.4). Figure 3.6.12 **B** illustrates the strong accumulation in the intestinal lumen.

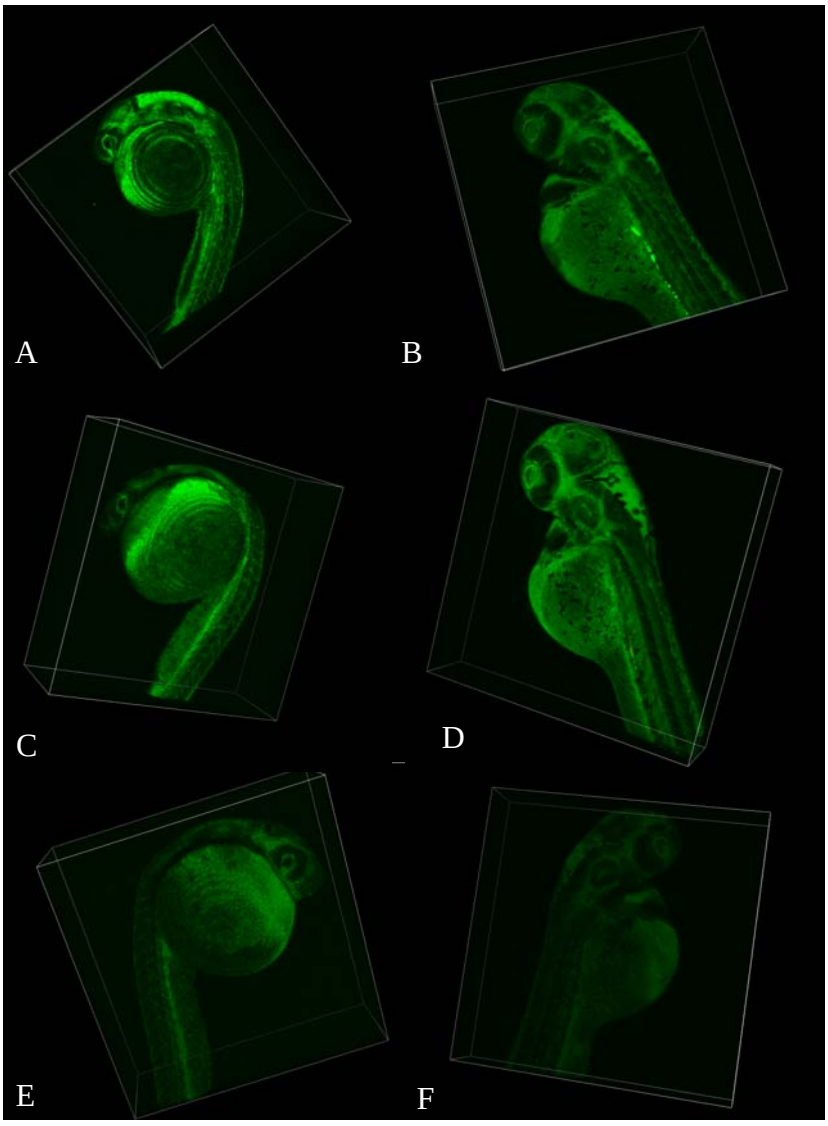

Figure 3.6.12: 24 hpf (**A, C, E**) and 48 hpf (**B, D, F**) dechorionated embryos were exposed to DCF in 1 % (**A, B**), 0.1 % (**C, D**) and 0.01 % (**E, F**) DMSO, 1, 0.1 % DMSO show a strong signal in the embryo (**A-D**), especially in the intestinal lumen (**B**), 0.01 % DMSO show a weaker signal in the embryo (**E-F**); all images were taken with laser power: 100, the 24 hpf embryos with HV: 50 and the 48 hpf embryos with HV: 5

Influence of DMSO concentration on toxicity

Based on the pre-test, DCF had a high toxicity (see appendix p. IV). The NOEC was determined to be 50 mg/L dichlorofluorescein, whereas 65 mg/L already showed a mortality of 100 % (see appendix p. IV). Therefore, it was interesting to see whether a change in toxicity would correlate with different DMSO concentrations. Consequently, the test was repeated with DCF 50 mg/L and DCF 65 mg/L solved in 1 % and 0.01 %.

The test failed, because there was no mortality observed at all. Figure 3.6.13 shows the 48 hpf embryos which have been exposed to DCF with a concentration of 65 mg/L (**B, D**) and 50 mg/L (**A, C**) solved in 0.01 % (**A, B**) and 1 % (**C, D**). The signal in the embryo in **A** is visible, but not in **B**, even though a higher accumulation was expected. Otherwise the difference between Figure **C** and **D** are barely detectable. These results suggest that the concentration of the dilution differs with the concentrations of DMSO.

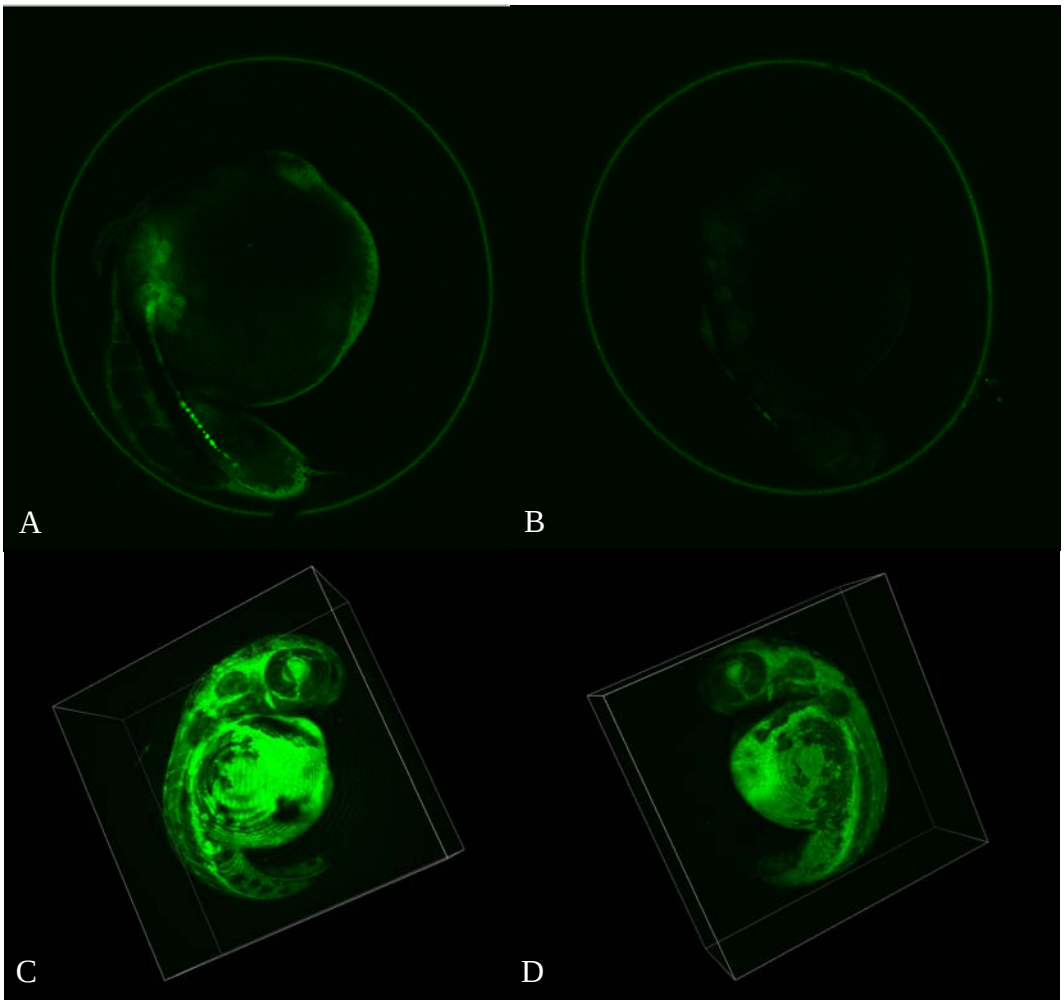

Figure 3.6.13: 48 hpf embryos exposed to 50 mg/L (**A, C**) and 65 mg/L DCF (**B, D**) in 0.01 % (**A, B**) and 1 % (**C, D**) DMSO; the signal strength of 50 mg/L in 1 % (**C**) and in 0.01 % (**A**) DMSO is stronger than the one of 65 mg/L in 1 % (**D**) and in 0.01 % (**B**); all images were taken with laser power: 100 and HV: 10 (**A, B**) and 1 (**C, D**)

Time-depending changes in concentration

To make sure that the difference in the distribution was not caused by concentration fluctuations of the dye because of its low solubility, the test was extended to determine the change of extinction with time. Therefore, four solutions of fluorescein (100 mg/L) solved in 10, 1, 0.1 and 0.01 % DMSO were tested over eight days. The solutions were continuously mixed and heated at 50°C. The changes in extinction versus time are shown in Figure 3.6.14 and demonstrate that the concentration of 100 mg/L was relatively constant at all DMSO concentrations. It must be pointed out that a change of 0.1 units in extinction is equivalent to 5 mg/L. The highest discrepancy between basic value and final value was shown with the highest concentration of DMSO (10 %) with a difference of about 3.3 %. The discrepancy decreased with increased concentration of DMSO; therefore, 1 % DMSO showed a discrepancy of 2.6 %, 0.1 % DMSO of 1.3 % and 0.01 % the lowest concentration of DMSO approx. 1 %. Assuming that after one day 100 mg/L of fluorescein was completely solved in 10 % DMSO and set this as a basic value, the highest discrepancy was in the 0.01 % DMSO solution and is about 1.8 %, which is equivalent to 1.8 mg/L. All dilutions which were used in this study were mixed over 24-48 hours, therefore a relatively constant concentration is guaranteed. The abrupt rise in the 1 % curve remains unexplained and was possibly a chemical reaction between DMSO and fluorescein which became brighter. Additionally, the extinction was measured in the well to detect a difference since the solution was not mixed and heated, but the discrepancy was less than 1.5 % (data not shown) and is therefore within the measurement uncertainty.

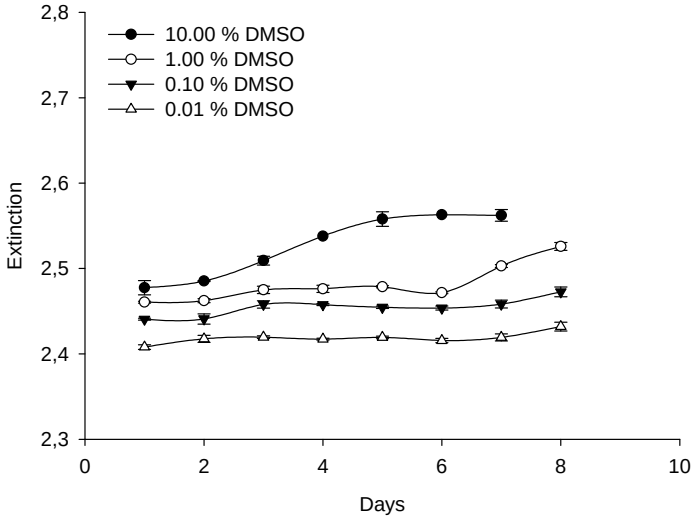

Figure 3.6.14: Extinction fluctuations over 8 days of fluorescein 100 mg/L solved in 10 %, 1 %, 0.1 %, and 0.01 % DMSO; the concentration of 100 mg/L fluorescein is relatively constant, 0.1 unit of extinction is equal with a concentration of 5 mg/L

3.7 Dextran fluorescein with 3 kDa

3.7.1 Test concentrations

Due to the low fish toxicity (Kane & Kishimoto 2001) and good brightness, no pre-test was conducted for dextran fluorescein with 3 kDa, since low concentrations produce a good signal. All tests were made with a concentration of 50 mg/L dextran fluorescein. At all times, 20 eggs were exposed and investigated at this concentration. The mortality was never higher than 10 % (see appendix, p. V).

3.7.2 Epi-fluorescence microscopy – 3 kDa Dextran fluorescein

3 kDa Dextran fluorescein is not able to pass the chorion (Fig. 3.7.1). Dextran fluorescein with 3 kDa is attached to the outside of the chorion, which can be seen in image (**A**) where the embryo is barely visible due to the high fluorescence of the chorion. Even after 48 hours, the highest signal is still found in the chorion (**B**). The embryos dechorionated after exposure corroborate this conclusion, because there was no signal at all (**C, D**). Comparing the dechorionated exposed embryos with the control group (**E, F**), no differences could be found. The images of the dechorionated embryos (**C, D**) as well as those of the control group (**E, F**) needed a very long exposure time to give any signal.

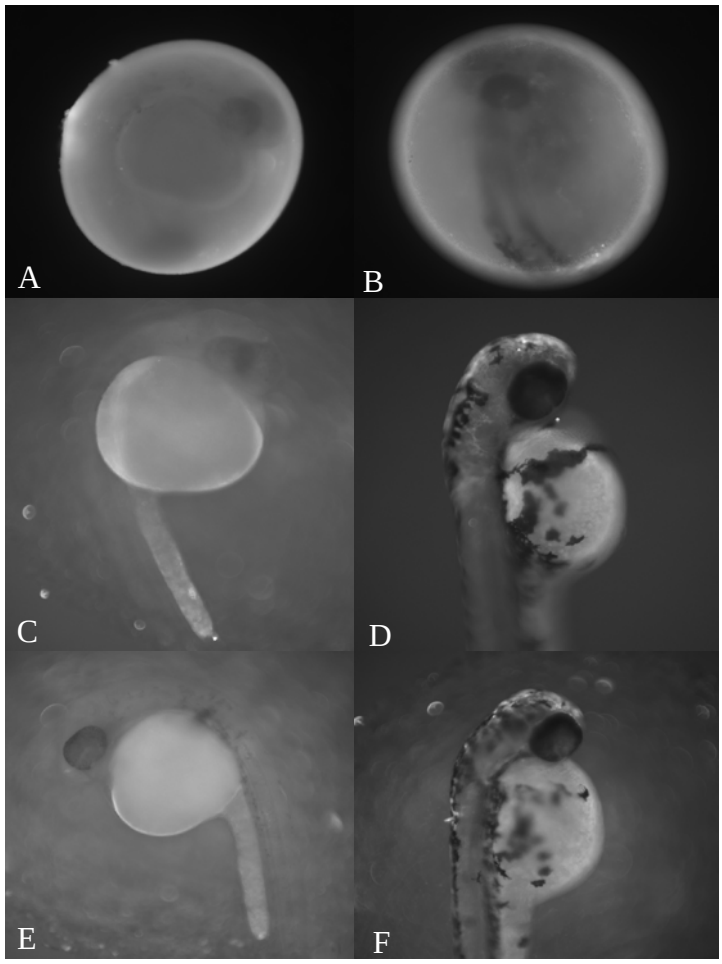

Figure 3.7.1 left: 24 hpf and **right:** 48 hpf embryos which were exposed to 3 kDa dextran fluorescein (50 mg/L) (**A-D**), 24 hpf dechorionated embryo (**C**), 48 hpf dechorionated embryo (**D**), dechorionated embryos of the control group (**E-F**); dextran fluorescein attached to the outside of the chorion (**A, B**), dechorionated embryos show no signal at all (**C, D**); shutter speed: 40 ms (**A-B**), 1.67 sec (**C**), 2.41 sec (**D**), 2.09 sec (**E**), 2.83 sec (**F**)

Figure 3.7.2 shows details of a part of the chorion after 24 hours of exposure to 50 mg/L 3 kDa dextran fluorescein. The picture was taken after dechorionation of the embryo. The white spots (**A**) are a result of a strong fluorescence signal and indicate that dextran fluorescein accumulates in the pores of the chorion. Converting the gray values to false coloration (software of NIS Viewer 3.00) enhances this impression (**B**).

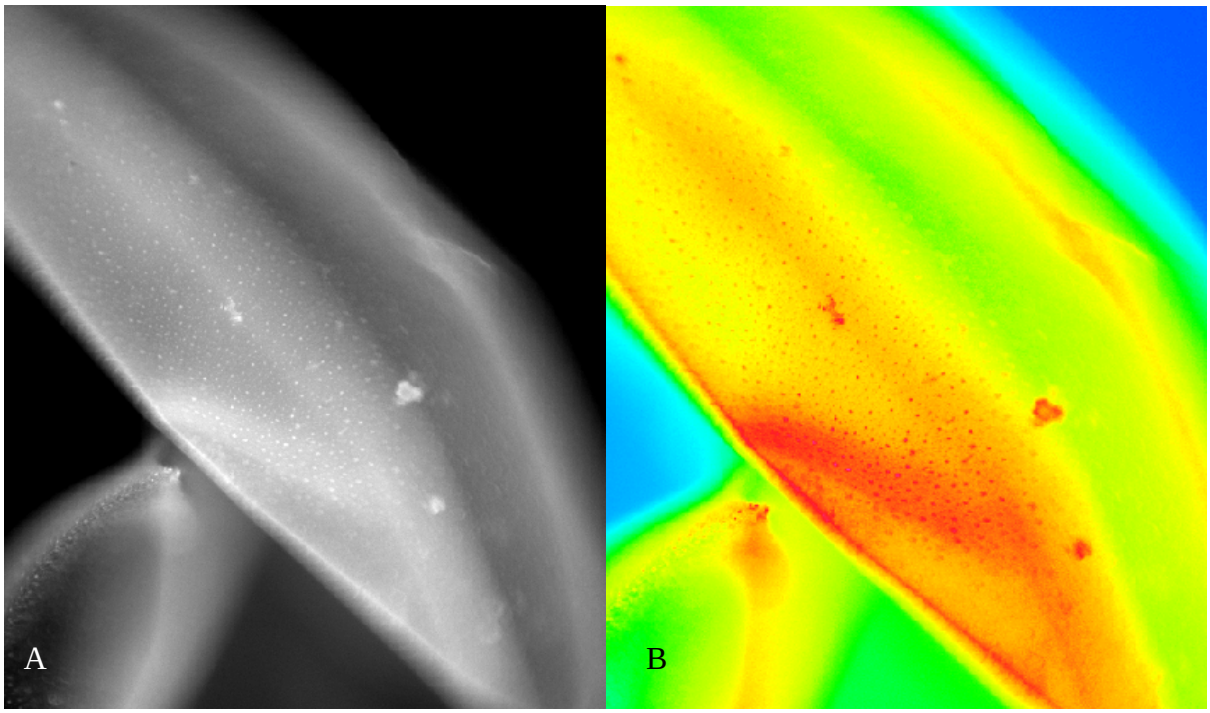

Figure 3.7.2: Part of the chorion of 24 hpf embryo exposed to dextran fluorescein (50 mg/L) in detail: The white spots illustrate the pores of the chorion (**A**); gray values are converted to colors with high contrast with the software of NIS Viewer 3.00 (**B**), shutter spedd: 48 ms

3.7.3 Confocal laser scanning microscopy (CLSM) 3 kDa Dextran fluorescein

Confocal laser scanning microscopy reveals that dextran fluorescein with 3 kDa is not able to pass the chorion (Fig. 3.7.3). The signal of the chorion was very strong after 24 hours as well as after 48 hours which is reflected in the low laser power of 29 and the low high voltage of 27. In contrast, the embryos dechorionated after exposure (**A, C**) did not show a signal higher than the embryos in the control group, even with laser power of 100 and high voltage of 200 (**E, F**).

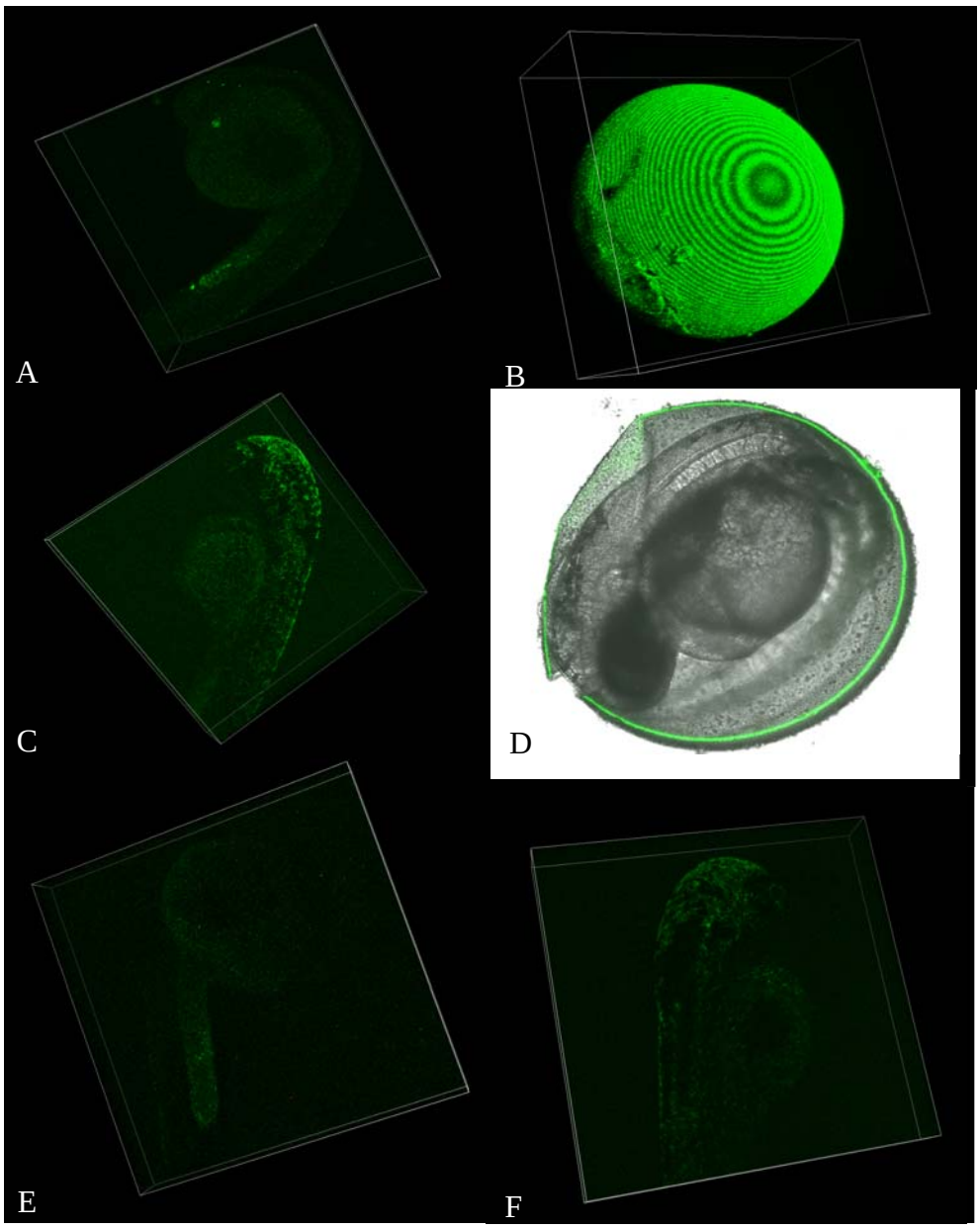

Figure 3.7.3 left: 24 hpf embryos, **right:** 48 hpf embryos exposed to 3 kDa dextran fluorescein; fluorescence signal in the chorion (**B, D**), embryos dechorionated after 24 hours (**A**) and 48 hours (**C**) show no fluorescence signal in comparison to the embryos of the control group dechorionated after 24 hours (**E**) and 48 hours (**F**); laser power of 100; HV 200 (**A, C, E, F**); laser power of 29 and HV 27 (**B, D**)

To get an overview of the position and number of the pores, an image of a 24 hpf egg was made with 373 slices (z-steps); the interspace is 1.16 µm. This high number of slices with such a small interspace allows to provide a precise illustration of the surface of the chorion. Figure 3.7.4 shows the pores in the chorion of a 24 hpf embryo. The dark patterns (red arrows) demonstrate defects in the chorion. This image was made with laser power of 100 and a very low HV of 1.

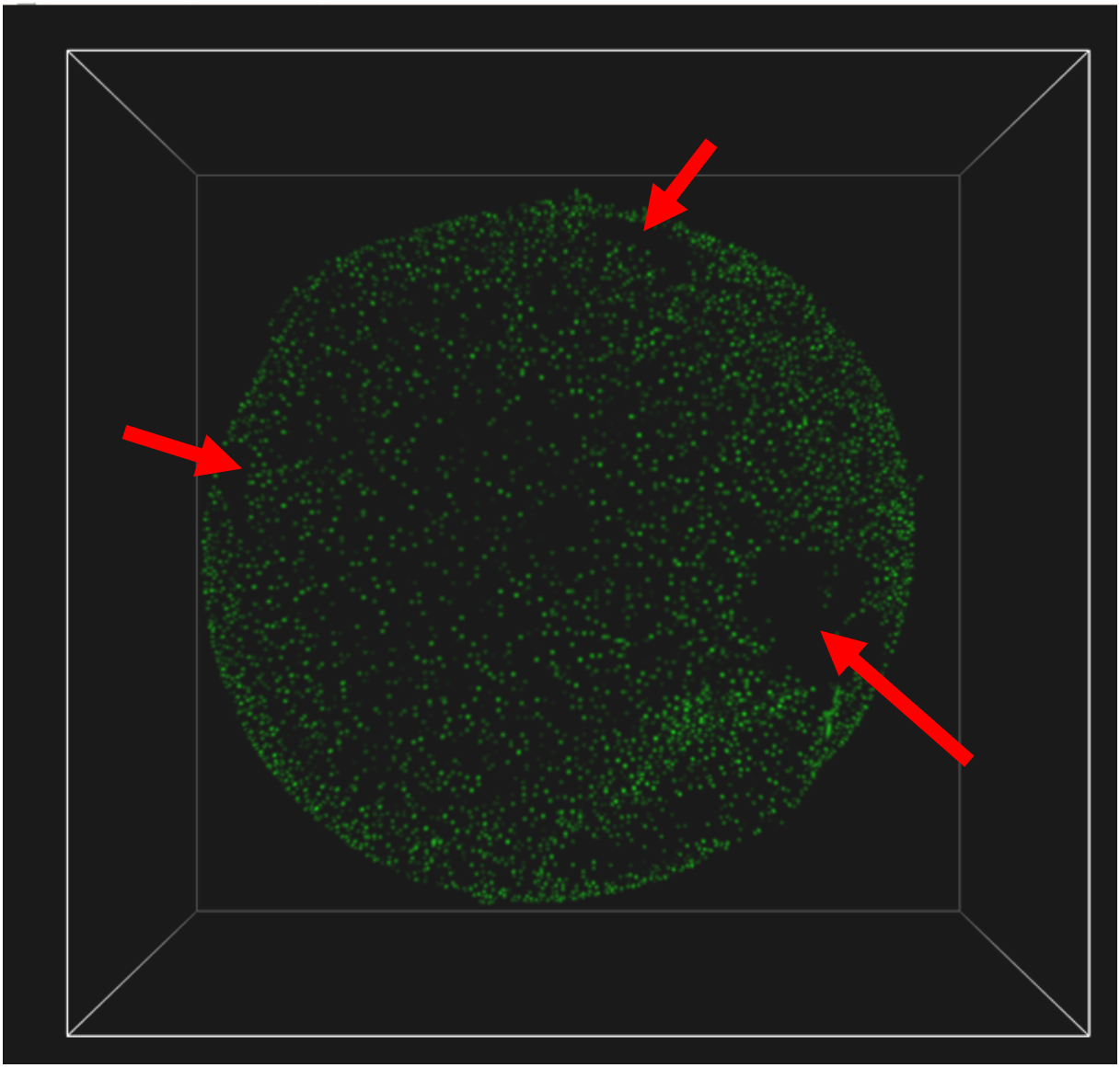

Figure 3.7.4: 24 hpf embryo exposed to dextran fluorescein with 3 kDa; overview of the position and number of the pores of the chorion**, red arrows**: lesion of the chorion; this image was made with 373 z-steps and an interspace of 1.16 µm, laser power: 100 and HV: 1

The lateral view of a part of the 24 hpf chorion (scan area see in Fig. 3.7.5) most likely shows the longitudinal orientation of the pore canals. The chorion in Fig 3.7.6 has a thickness of 15 µm. The image consists of 40 slices with an interspace of 0.39 µm and was taken with a laser power of 100 and HV 1, which allows a detailed reconstruction of this part of the chorion. It seems as if the pores were cone-shaped with a larger diameter at the inner surface of the pore canal.

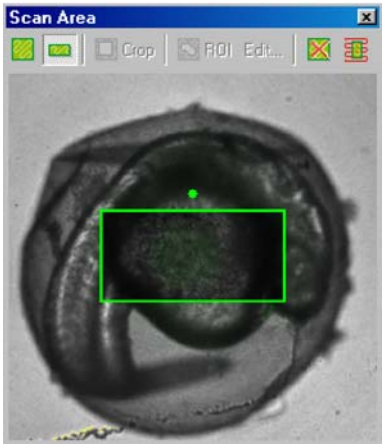

Figure 3.7.5: 24 hpf embryo, position of the scan area on the chorion

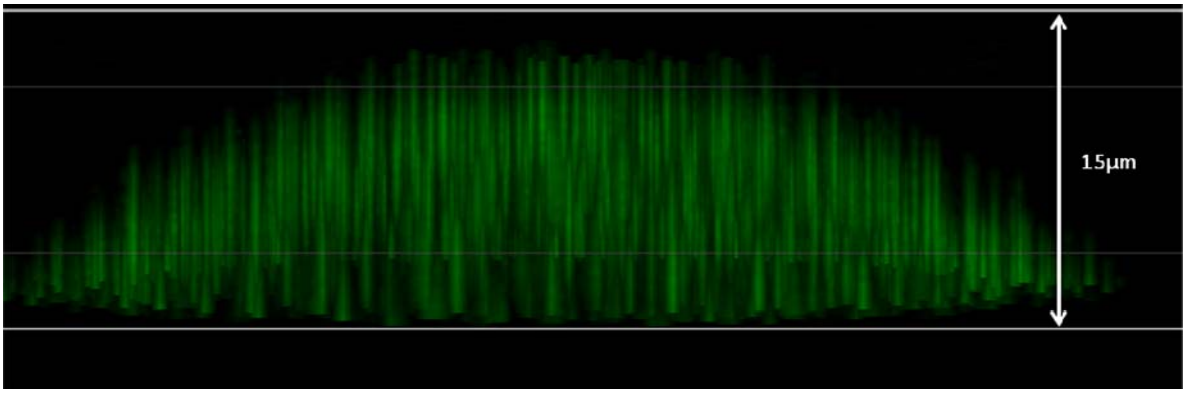

Figure 3.7.6: Lateral view of a part of a 24 hpf chorion in high resolution scan area 15 µm (40 slices) with an interspace of 0.39 µm; the illustration might show the cone shaped pores with their longitudinal orientation; the image was taken with a laser power of 100 and HV of 1.

3.8 Dextran fluorescein with a molecular weight of 40 kDa

3.8.1 Test concentrations

Due to the low fish toxicity (Kane & Kishimoto 2001) and a good brightness, no pretest was made with 40 kDa dextran fluorescein, since low concentrations give a good signal. All tests were conducted with a concentration of 50 mg/L 40 kDa dextran fluorescein. The procedure of testing was the same as previously described for 3 kDa dextran fluorescein. For each test, 20 eggs were investigated in parallel using the same concentration. The mortality was at no time higher than 10 % (see appendix, p. V).

3.8.2 Epi-fluorescence microscopy-Dextran fluorescein with 40 kDa

As was the case for dextran fluorescein with 3 kDa, dextran fluorescein with 40 kDa was not able to pass the chorion (Fig. 3.8.1). It attached to the outer face of the chorion, thus leading to an even more blurry image of the embryo. After 48 hours, no detectable differences in distribution (**A, B**) were found. No signal was seen for embryos dechorionated after exposure (**C, D**). Comparing them with the embryos of the control group Fig. 3.7.3 (**E, F**) there are also no differences to see. The images of the eggs were taken with a short shutter time of 24 ms, but the images of the dechorionated embryos needed a long shutter time of 2.21 sec (**C**) and 2 sec (**D**) , reflecting the weakness of the signal.

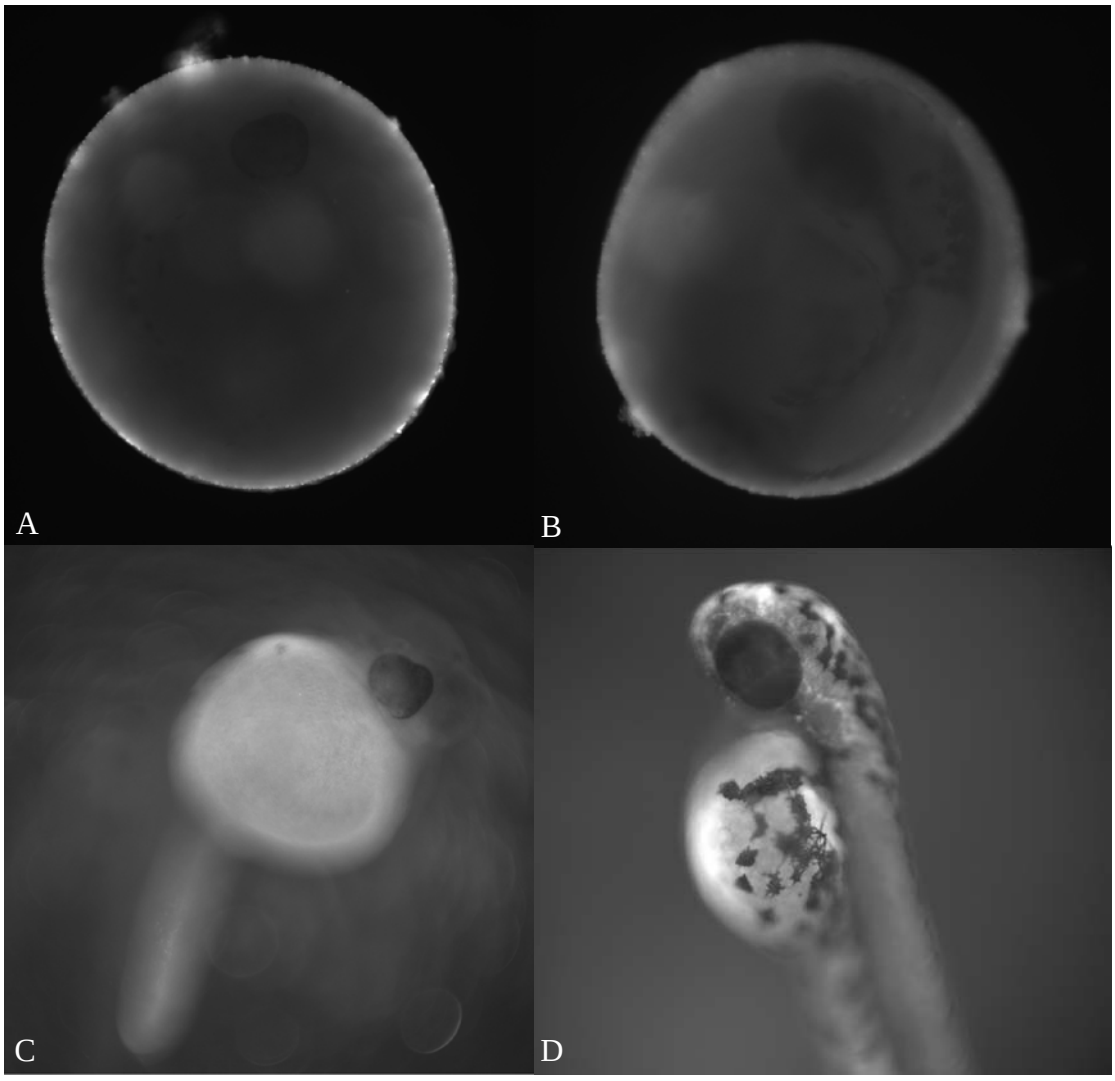

Figure 3.8.1 left: 24 hpf, **right:** 48 hpf embryos exposed to 40 kDa dextran fluorescein with (50 mg/L), 40 kDa fluorescein dextran attached to the chorion (**A, B**), the embryos dechorionated after 24 hours (**C**) and 48 hours (**D**) show no fluorescence signals; shutter time: 24 ms (**A**-**B**), 2.21 sec (**C**), 2 sec (**D**)

3.8.3 Confocal laser scanning microscopy (CLSM) - 40 kDa Dextran fluorescein

40 kDa Dextran fluorescein did not pass the chorion (Fig. 3.8.2 **A, B**). After 48 hours, no detectable differences in distribution (**A, B**) were found. Due to the lower laser power of 3, there seemed to be a weaker signal in the chorion after 48 hours. Furthermore, it is notable that the fluorescence dye looks more coarsely grained than with dextran fluorescein of 3 kDa. The embryos dechorionated after exposure (**C, D**) did not show a signal higher than that of the embryos of the control group Fig. 3.7.3 (**E, F**), even with a laser power of 100 and high voltage of 200 (24 hpf embryo) and 100 (48 hpf embryo).

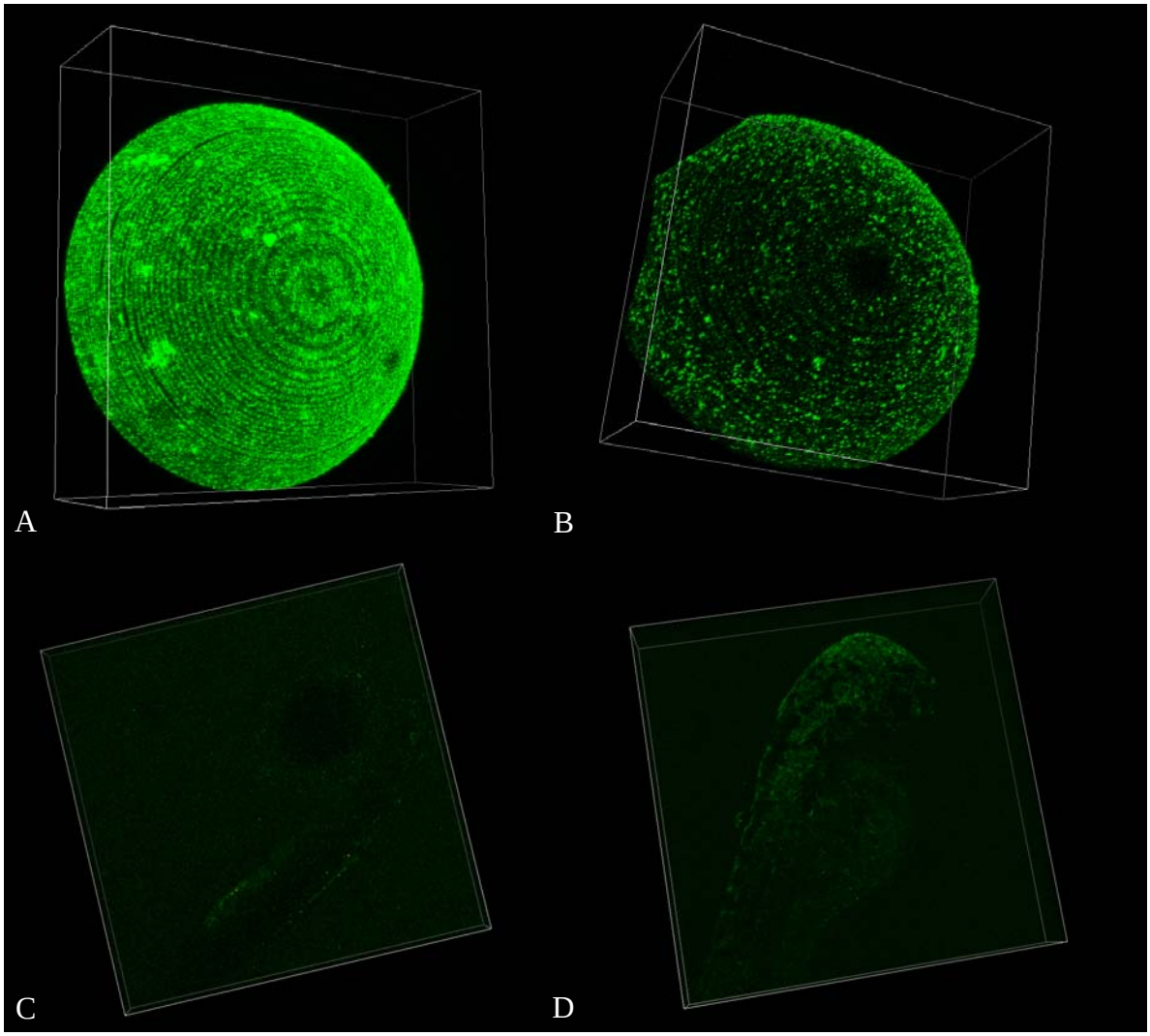

Figure 3.8.2 left: 24 hpf **right:** 48 hpf embryos exposed to dextran fluorescein of 40 kDa (50 mg/L), 40 kDa fluorescein dextran attached to the chorion (**A, B**), the embryos dechorionated after 24 hours (**C**) and 48 hours (**D**) show no fluorescence signals; laser power of 29, HV: 27 (A), laser power of 3, HV: 27 (B) and laser power: 100, HV: 200 (C), HV: 100 (D)

An image of a 24 hpf egg made with 197 z-steps with an interspace of 1.16 µm, demonstrates the surface of the chorion. Again the fluorescence dye looks more coarsely granular (Fig. 3.8.3) than with the dextran fluorescein 3 kDa if compared to Figure 3.7.4. Therefore, the pores do not appear as precise as these in Fig. 3.7.4. The red arrows demonstrate lesions in the chorion. The image was taken with laser power of 100 and a very low HV of 1.

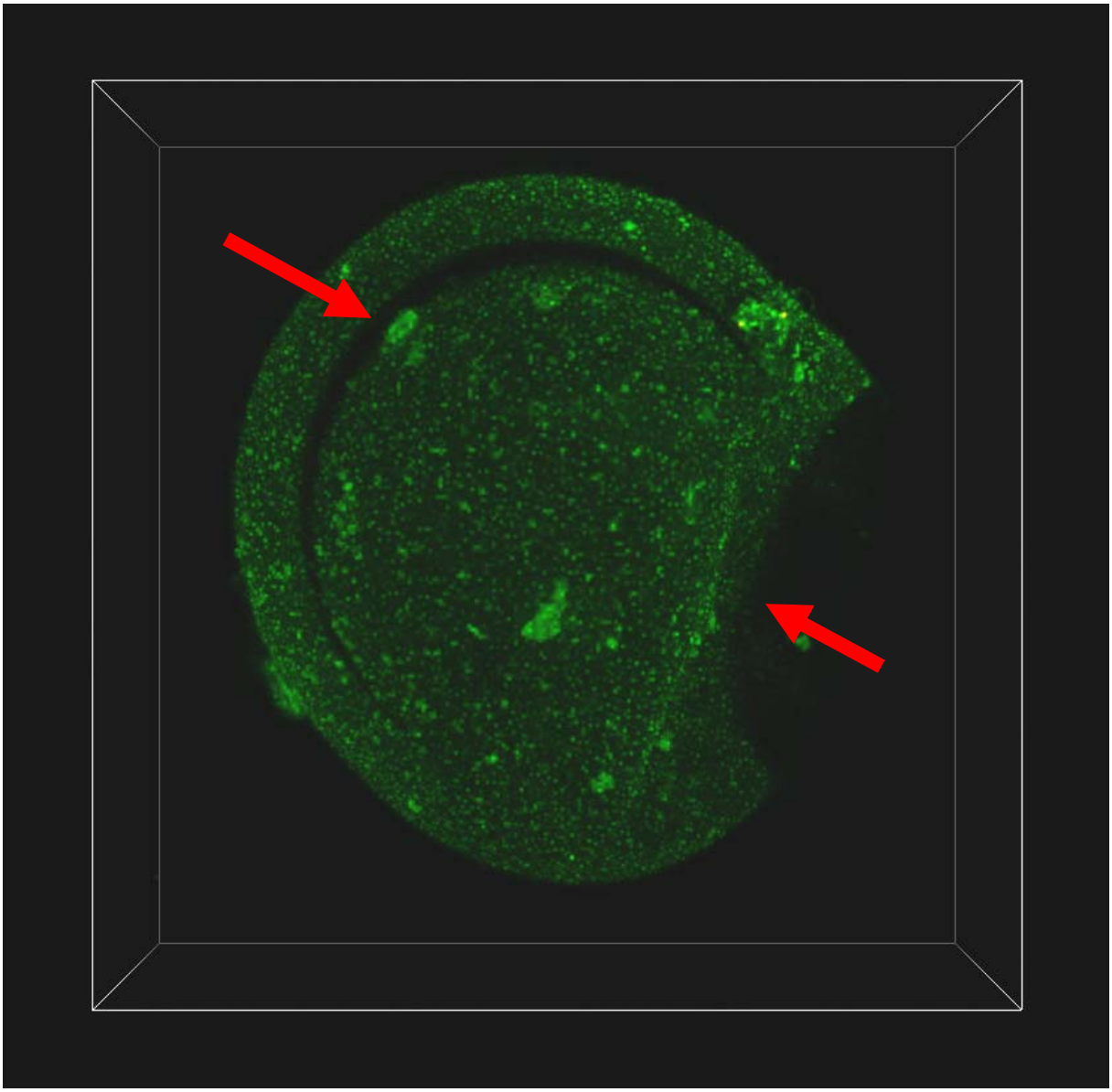

Figure 3.8.3: 24 hpf embryo exposed to 40 kDa dextran fluorescein of (50 mg/L); this image was taken with 197 z-steps and an interspace of 1.16 µm; 40 kDa dextran fluorescein attached to the chorion and looks coarsely granular, **red arrow**: lesion of the chorion, laser power: 100, HV: 1

4 Discussion

The primary aim of the pre-tests was to find suitable test concentrations that, on the one hand, cause strong fluorescence signals and, on the other hand, do not influence the physiology of the fish. Therefore, an effect level of 10 % was not exceeded (EC_{10}). Since no replicates were done, no statistic evaluation was possible to elucidate the exact toxicity of the dyes.

4.1 Fluorescence dyes with good water solubility and a low log P_{ow}

4.1.1 Rhodamine b

The water solubility of rhodamine b is good, and it has a relatively small polar surface area and average complexity. All tests showed that rhodamine b passes the chorion and accumulates in the yolk. In oviparous vertebrates such as fish, however, the yolk is critical for regular embryonic development providing a variety of nutrients (Wallace 1969). Beside minor amounts of vitamin-carrying proteins, riboflavin- and thiamine-binding proteins, albumin, transferrin, two classes of phosphoglycoproteins, phosvitins and lipovitellin are the major proteins found in the yolk (Wallace 1969). These two phosphoglycoproteins derive from a common precursor called vitellogenin. Vitellogenins generally constitute the major yolk proteins occurring in all oviparous animals (Byrne 1989), and they provide the embryo with essential nutrients, e.g. amino acids. Apart from being amino acid sources, vitellogenin-deriving proteins bind lipids, sugars, phosphates and metal ions and are, therefore, multidimensional nutrients sources for developing embryos. A potential mechanism of transport could be that rhodamine b with its small polar surface and a low log P_{OW} diffuses into the yolk. The 48 hpf embryo showed that rhodamine b spreads throughout the whole body (Fig. 3.1.3-5). Consequently, there must be a pathway between yolk and heart. As early as the blastula period, the yolk syncycial layer (YSL), a structure

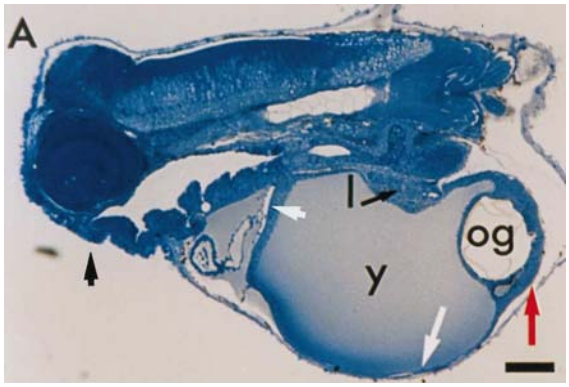

Figure 4.1.1: Yolk syncycial layer (YSL) and resorption of the endogenous reserves, 8 days after fertilization; **short black arrow**: the mouth was closed; **short white arrow**: indicates the extracellular space in contact with the YSL and visible in the anterior yolk cell; **long white arrow and long red arrow** indicate the YSL of the ventral side of the yolk (y) cell and around the oil globule (og), respectively; long black arrow: Liver (l); (Poupard 2000)

unique to teleosts, forms by collapse of open marginal blastomers into the immediately adjoining cytoplasm of the yolk (Kimmel & Law 1985; Trinkaus 1992, 1993). The YSL is in direct contact with the extracellular space (Fig. 4.1.1; short white arrow), in connection with the developing heart and surrounds the surface of the yolk. This perisyncytial space is filled with a clear fluid and scarce circulating cells. No vascular network and visible red blood cells are observed inside the yolk sac (Poupard 2000). After 26 hours, the heart tube is elongated and the blood cells begin to circulate. Henceforward, the distribution of the dye starts. A comparison of the ROIs after 24 hours (Fig. 3.1.17) and 48 hours (Fig. 3.1.18) demonstrates this effect. After 24 hours, the fluorescent signal in the brain was about five times smaller than in the yolk, whereas, after 48 hours, the difference between the yolk and the brain became smaller.

At the end of epiboly, the blastoderm has entirely engulfed the yolk and the YSL forms a boundary between the embryo and the yolk mass. Therefore, all nutrients from these endogenous reserves must pass through the YSL in order to reach the embryo and the larva (Poupard 2000). Furthermore, the formation of an YSL beneath the blastoderm and at the surface of the yolk cell enables resorption of the yolk reserves and development up to the larval stage. Gündel (2007) observed that post-hatch embryos show major alterations of the protein composition. These results indicate yolk exhausting and complete yolk protein utilization before starting of the feeding period (Kimmel 1995). Every developmental stage is characterized by its own specific composition of yolk proteins. Metabolic rates increase and most likely rhodamine b is then metabolized. Webb & Hansen (1961) showed that rhodamine b (tetraethyl-3,6-diamniofluoran) is de-ethylated in higher vertebrates to form N,N´-diethylaminofluoran, monoethyl-3,6-diamniofluoran, and the completely de-ethylated analog 3,6-diaminofluoran. There is evidence that the original dye and its metabolites occur in both the urine and feces and are excreted, to some extent, in the bile, to be subsequently absorbed by the gastrointestinal tract and recirculation in the bloodstream (Webb 1960; Webb & Hansen 1961). This means that the fluorescence signal, which spread throughout the body, demonstrates also the metabolites of rhodamine b, since all of them are also fluorescent.

4.1.2 Sulforhodamine b

Sulforhodamine b has two sulfo groups, which increase the polar surface area, whereas the log P_{ow} is decreased. Consequently, the water solubility is supposed to increase; however, literature data are contradictory. A better water solubility, even better than the one of rhodamine b, was also observed by preparing the test solution. These data resulted from calculation of the water solubility with high fluctuations, since several parameters influence the water solubility; therefore, the calculated values should rather be understood as rough guidance.

All images of the epi-fluorescence microscopy were rather blurry (Fig. 3.2.2-3). Most likely, this is caused by the attachment of sulforhodamine b to the chorion. Observations with the confocal microscope highlight the attachment to the chorion (Fig. 3.2.13 and Fig 3.2.16). Nevertheless, there was also a signal visible within the embryo. Single section planes (Fig. 3.2.14 and Fig. 3.2.17) demonstrate that the main distribution of sulforhodamine b was in the chorion and, therefore, reflects its function as a barrier. The chorion is an acellular envelope surrounding the embryo of teleost fish. The macromolecular composition of the zebrafish egg chorion, organized as a three-layered structure, has been analyzed by Bonsignorio (1996). The analysis of isolated and purified chorions reveals four major polypeptides (116, 97, 50, and 43 kDa). Lectin binding assays show that both 116 kDa and 50 kDa are N-linked glykoproteins such as collagen, gelantin, and fibronectin (Lee 2005). By contrast, neither the 97 kDa nor the 43 kDa polypeptides were stained by these lectins, indicating that these polypeptides are not glycosylated (Bonsignorio 1996). These results suggest that the main characteristic of the chorion trends to be lipophilic. This might indicate that the chorion limits the transport of the hydrophilic sulforhodamine b and works as a barrier. In an attempt to elucidate the effect of the chorion as a barrier, Braunbeck (2005) tested, among other substances, potassium chromate which is relatively hydrophilic. Whereas exposure of the chorionated embryos did not result in any change of the core endpoints, the prolonged exposure of dechorionated embryos over four days produced severe disturbances to swimming equilibrium in hatched larvae. This does indeed indicate that the chorion does act as a barrier at least for hydrophilic substances.

Another study (Marguerie 2007) was conducted to examine the influence of an intact chorion on the accessibility of test compounds to the embryo. Four compounds with a wide range of log P_{ow} values were tested for developmental toxicity in chorionated and dechorionated zebrafish embryos. The results show that hydrophilic compounds might be toxic at lower

concentrations in dechorionated embryos than in embryos with an intact chorion. This suggests that the chorion limits the transport of these substances. Furthermore, this study represents the hypothesis that the presence of the chorion did not appear to significantly influence the embryo toxicity of compounds with higher log P_{ow}.

The permeability of the chorion changes during development, which influences the chorion as a barrier as well. The observation with the CLSM shows a slightly decreased signal in the chorion (Fig. 3.2.16) and corroborates the assumption that the chorion permeability and its thickness changes during development (Herrmann 1993; Hagedorn et al. 1997). According to Kim (2004), the chorion envelope undergoes a thinning process called "chorion softening" before the basic body formation is complete and the embryo hatched (Schoots 1983). Upon hatching, the chorion is digested by hatching enzymes, which are proteolytic enzymes secreted from hatching gland cells of the embryo (Inohaya 1999). These hatching enzymes have been partially identified by Roberts & White (1992). Furthermore, Gellert et al. (2001) found a significant toxic response only for 1 hpf eggs and assumed that the process of swelling and hardening of the chorion making the egg more resistant and slows down intrusion of the toxicants.

Nevertheless, the dechorionated embryos in Figure 3.2.19-20 demonstrate that there is an accumulation of sulforhodamine b in the embryo after 24 hours as well as after 48 hours. The CLSM images show that if sulforhodamine b passes the chorion, it accumulates in the yolk and there are no differences in distribution after 24 or 48 hours. The observation with the epi-fluorescence microscope differs slightly and shows, especially after 48 hours, an increased signal inside the egg (Fig. 3.2.3). The plot profile demonstrates that if sulforhodamine b passes the chorion, it accumulates predominately in the vascular system in the area of the duct of cuvier (Fig. 3.2.8). As a consequence of the metabolism of rhodamine b, there is a high likelihood that the signal also demonstrates the metabolites of sulforhodamine b and rhodamine b, respectively. The analysis of the epi-fluorescence images with the ROI manger demonstrates a relatively equal distribution. After 24 hours, the yolk shows the highest accumulation, whereas after 48 hours the distribution changes and the chorion shows the highest signal. These results are in contrast to the observations with the CLSM, since Figure 3.2.13 demonstrates a high accumulation in the chorion after 24 hours and Figure 3.2.16 shows the decreased signal in the chorion after 48 hours. The method to measure the mean gray value with selected areas of interest are, therefore, only a rough estimate to get a tendency of the distribution. The failed Dunn´s test and the high standard division, especially

in Figure 3.2.12, demonstrate the high fluctuations of this method. The ROI-manager is only a useful tool, when there is a clear delineation of the fluorescence signal but no adsorption to the chorion. Due to interference signals caused by reflections of sulforhodamine b in the chorion, the results of its distribution in Figure 3.2.12 are not significant, and the differentiation inside the embryo is in general difficult.

The additional test to check if there is an uptake after 48 hours of sulforhodamine b in the embryo from the chorion shows no differences between the chorionated and dechorionated embryos. It is doubtful whether an increased signal would be visible, since the amount of the uptake is limited by the volume of the chorion. The volume of the chorion is about 0.025 µl (Goltz 2007) and would not increase the signal intensity. One way to measure such small amounts would be to use radio labeled substances.

4.2 Fluorescence dyes with low water solubility and high log P_{ow}

4.2.1 Fluorescein

Fluorescein is the smallest molecule tested in this study with a log P_{ow} of 3.4. The better part of fluorescein passes the chorion and accumulates in the area around the heart and brain. This distribution indicates that inside the embryo fluorescein is transported by blood. This effect is also used in the pharmacology more precisely in the pharmacodynamics. Norvatis provides fluorescein (500 mg/ 5 ml) as a sterile solution containing fluorescein sodium for intravenous injection for investigating pathological changes to the retinal blood circulation. Therefore, Therapeutic Goods Administration (2007) approves this pharmaceutical and monitors the absorption, distribution, metabolism and excretion of fluorescein in humans. After intravenous injection, fluorescein is rapidly distributed throughout the body and appears in the retinal tissues within a few seconds. The distribution in the retinal tissues can also be observed in the 24 hpf (Fig. 3.3.11) as well as in the 48 hpf old zebrafish embryo (Figs. 3.3.13-14). In humans, fluorescein binds to albumin and red blood cells in a reversible fashion and binding is moderate (~ 70-80 %) during the first hour. About 15-17 % is bound to erythrocytes. Within a few minutes of intravenous administration, a yellow discoloration of the skin occurs, which begins to fade after 6 to 12 hours of dosing. Various estimates of volume of distribution indicate that fluorescein spreads well into the interstitial space (Therapeutic Goods Administration 2007).

After 24 hpf, the heart tube of the zebrafish is elongated and the blood cells begin to circulate. In this time frame, fluorescein has already spread over the entire body and colored the embryo

(Figs. 3.3.2; 3.3.11-12). With proceeding development of the blood vessel system the amount of fluorescein increases within the embryo (Fig. 3.3.3; 3.3.13 and 3.3.15). Since no additional fluorescence dye diffuse the distribution changes: fluorescein disperses also into the intestinal lumen (Fig. 3.3.4 and Fig. 3.3.5).

In humans, fluorescein undergoes rapid metabolism to fluorescein monoglucuronide. After one hour, approximately 80 % of fluorescein in plasma is converted to glucuronide, indicating relatively rapid conjugation. Fluorescein monoglucuronide is about ⅓ to ¼ as fluorescent as fluorescein. The glucuronide contributes almost all the plasma fluorescence after four to five hours. Fluorescein glucuronide are less strongly bound to plasma than fluorescein. Fluorescein and its metabolites are mainly eliminated *via* renal excretion. After intravenous administration, the urine remains slightly fluorescent for 24 to 36 hours (Therapeutic Goods Administration 2007).

According to the results of this study, the distribution and metabolism of fluorescein in the zebrafish shows some similarities. Monoglucuronides are derivatives of the glucuronic acid, which conjugates, e.g., hydrophobic impurities and make them soluble in water; the glucuronidation is catalyzed in the liver by microsomal enzyme UDP-glucuronate glucuronosyltransferase (Jansen 1976). After washing the 48 hpf embryos in artificial water for 24 hours no additional fluorescein diffuses, all of the fluorescein and the monoglucuronide accumulate in the intestinal lumen (Fig. 3.3.4). A prolongation of the depuration time (48 hours) highlights this effect. The most of the fluorescein was transported into the bile and thus out into the small intestine (Fig. 3.3.5) and indicates a metabolism in the liver, which could be catalyzed by microsomal enzyme UDP-glucuronate glucuronosyltransferase. However, even though there was no elimination *via* renal excretion observable, it cannot be excluded that next to the degradation in the liver, a smaller part of the fluorescein glucuronide was also excreted with the urine, since the amount is probably too small to be detected. But to make a sound statement, there is a need for additional research into the kidney and the primordial of the kidney, respectively. Furthermore, the urogenital pore needs to be investigated with the confocal microscope in higher magnifications.

As previously mentioned, formation of a ramified vascular network cannot be observed on the surface of the yolk sac (Rieb 1973; Kimmel et al. 1995). Venous blood returns laterally on each side of the yolk sac through the ducts of Cuvier (Fig. 3.2.9 DC). These two vessels join and the embryonic venous blood stream enters the perisyncytial space of the yolk and returns to heart´s sinus venosus (Rieb 1973; Kimmel et al. 1995). Consequently, the embryonic

venous blood is in direct contact with the yolk syncytial layer (YSL; Rieb 1973) (see chapter 3.1.1) and is not enclosed by any vessel as it approaches the heart. The heart is in contact with the perisyncytial space at its venous end. Therefore, most of the fluorescent dye in Figures 3.3.2-3 was found in the perisyncytial space and thus in the blood plasma. According to humans, where 80 % of fluorescein in plasma is converted to glucuronide, it is most likely that the fluorescence signal in the blood plasma of the zebrafish is due to the metabolites of fluorescein, the monoglucuronides, which have a weaker signal.

In pelagic marine fish embryos, there is an enlargement of the perisyncytial space above the cephalic region, into which the heart opens directly (Poupard 2000). Supposedly, the increased signal in the brain of the zebrafish (Figs. 3.3.2-3) is caused by this direct connection and reflects the accumulation of fluorescein metabolites. The results of the plot profile after 24 hours document (Figs. 3.3.8 and -9) the accumulation in the region of the heart or rather in the aorta and (Fig. 3.3.9) the increased signal in the brain after 48 hours.

4.2.2 2,7-Dichlorofluorescein (DCF)

In contrast to fluorescein, 2,7-dichlorofluorescein (DCF) carries two chlorine residues, but its lipophilicity is 1.3 times higher than that of fluorescein. In other words, its water solubility is much lower than for fluorescein. Furthermore, the chemical structure of DCF contains two components of chlorophenols and the chlorine atoms were substituted at the ortho-position.

The mechanism of the toxicity of chlorophenols in fish was investigated by Kishino and Kobayshi (1996 a) through the relation between the *in vivo* toxicity and both P_{ow} and $\Delta\, pK_a$. The toxicity of chlorophenols increases with increasing number of chlorine atoms substituted at the ortho-position (Blackman et al. 1955; Kobayashi et al. 1979; Mc Leese et al. 1979; Liu et al. 1982; Ribo & Kaiser 1983; Devillers & Chambon 1986; Cohen et al. 1988; Kishino & Kobayashi 1996 b). Kobayashi et al. (1979) reported that an increase in the number of chlorine atoms in chlorophenols promotes an accumulation of the chemicals in fish, leading to the corresponding lethal levels, and consequently causes an abrupt increase in toxicity to fish. This abrupt increase in toxicity was also shown in the pre-test of DCF. The NOEC was found to be 50 mg/L DCF, whereas 65 mg/L already showed a mortality of 100 % (see appendix, p. IV), which reflects the enormous slope of the dose-response relationship. Due to these results, the following discussion is based on the assumption that DCF and ortho-chlorophenols have similarities in their toxicokinetics.

The ionizable moieties of DCF are another important aspect for the behavior in water and its ability to pass the chorion. Therefore, the pH is a crucial value which should be taken into consideration. The toxicity of chlorophenols to aquatic organisms steeply decreases with increasing pH of the media (Crandall & Goodnight 1959; Dalela et al. 1980; Holcombe et al. 1980; Saarikoski & Viluksela 1981). Kobayashi & Kishino (1980) demonstrate that the decreasing toxicity of pentachlorophenol (PCP) in fish can be related with an increase of pH inducing a decrease in PCP accumulation. Another paper of Kishino & Kobayashi (1995) also states that the transfer of chlorophenols from media to fish is mainly caused by passive diffusion of the undissociated molecule across gill membranes. The abrupt decrease of toxicity of chlorophenols in fish with increasing pH is primarily attributed to the conversion of the undissociated form to the dissociated form in media. These results suggest that the undissociated form plays a key role for the toxicity observed. The pH which was used in the study of Kishino & Kobayashi (1996 a) was 7.0 ± 0.1. However, in our present study, the pH was about 7.8 ± 0.1. Therefore, it is most likely that the small amount of DCF which passed the chorion by diffusion (Fig. 3.4.13) was undissociated, whereas most of it was dissociated and did not pass the chorion (Fig. 3.4.9). The uptake of DCF might not be across the gills, since their development is relatively late. The vital exchange processes take place presumably somewhere on the surface of the skin (Rombough 2002). Therefore it is most likely, that the uptake of undissociated DCF from egg water to the embryo might be through the skin and may support the idea of a pathway across various biological membranes to the site of toxic action in the fish. Finally, overtime, a significant uptake of DCF after 48 hours could be seen (Fig. 3.4.10), which is derived on the assumption of increased permeability of the chorion, as described above (chapter 4.1.2).

DCF has the highest log P_{ow} of the substances tested in this study. The P_{ow} value has been recognized as a good indicator for the transfer of chemicals to the site of action in the fish (Hansch & Dunn 1972; Rogers & Wong 1980). However, this study does not show a linear correlation between log P_{ow} and accumulation, since DCF would then have to show a higher accumulation in the embryo. Scherrer & Howard (1977) reported that the D_{ow} (distribution ratio in octanol-water system at pH 7) value is a better indicator than the P_{ow} value, since the pH is considered.

Thus the D_{ow} represents the concentration ratio of undissociated and dissociated DCF. P_{ow} and D_{ow} values are defined by following equations (quoted from Kishino & Kobayashi 1994):

$$P_{ow} = [HA]_{oct} / [HA]_w$$

$$D_{ow} = [HA]_{oct} / [HA]_w + [A^-]_w$$

$[HA]_{oct}$ (generic acid in octanol),

$[HA]_w$ (generic acid in water),

$[A^-]_w$ (conjugate base of the acid in water)

Kishino & Kobayashi (1995) set up a model for the absorption of chlorophenols into goldfish. The model consists of two compartments: surrounding water and fish body. It was based on the assumption that, on the one hand, an ionizable chemical agent such as chlorophenols partly ionizes in both compartments by diffusion and, on the other hand, that the concentration ratio of the undissociated form in the compartment fish to that in the compartment water is proportional to the P_{ow} value. From the above discussion, it can be concluded that the uptake of ionizable compounds such as DCF to aquatic organisms should not only be evaluated by the log P_{ow} but also by the log D_{ow}, because the concentration ratio of undissociated and dissociated DCF might be a crucial parameter for the occurrence of toxicity. Furthermore, the toxicity should be evaluated by the accumulation amounts in the fish instead of the concentrations in media, because the LC_{50} values of, e.g., chlorophenols vary significantly depending on pH of media. Their concentrations found in the dead fish during exposure, however, show relative small fluctuations (Kishino & Kobayashi 1996 a).

Once DCF has passed the chorion, it shows the same distribution as fluorescein, especially the same accumulation in the intestinal lumen was notable (Fig. 3.4.14). Kobayashi et al. (1977) showed that a part of the chlorophenols absorbed by aquatic organisms were potentially converted to non-toxic conjugates during exposure; e. g., PCP absorbed by goldfish was excreted into the gall bladder of fish as its non-toxic glucuronide after approx. 5 h of exposure to PCP-containing media. According to these results and the high accumulation in the intestinal lumen, the metabolism of DCF might be the same as for fluorescein (chapter 4.2.1) or rather it could be the same metabolism if the chlorine atoms were removed. The plot profile (Fig. 3.4.5) and the analysis with the ROI manager (Figs. 3.4.7-8) show the highest accumulation in the blood or rather in the heart, even after 48 hours. Furthermore, after 24 hours, accumulation in the brain and in the yolk is detectable (Fig. 3.4.7). After 48 hours,

the accumulation in the yolk increases, whereas the signal in the brain remains constant. However, all measurements show a high standard deviation; especially the measurements of blood or heart demonstrate high fluctuations which are due to the adsorption of DCF to the chorion, as also described for sulforhodamine b (chapter 4.1.2).

Nevertheless, the bulk of DCF did not pass the chorion after 24 hours. This is documented by observations with the confocal microscope on the one hand (Fig. 3.4.9) and with the comparison of the dechorionated embryos on the other hand (Fig. 3.4.13). When comparing the dechorionated 24 hpf embryos exposed to DCF with the dechorionated 24 hpf embryos exposed to fluorescein (Fig. 3.3.12), there is a clear difference in signal strength. Both images were taken with a laser power of 100, but the high voltage (HV) differs: fluorescein with its strong signal only needs a HV of 20, whereas DCF with its weak signal needs a higher multiplication; even with an HV of 50, the signal was still weak. This indicates that DCF does not pass the chorion after 24 hours. In contrast, in the 48 hpf old dechorionated embryos, the signal is stronger and needs only a HV of 5, which demonstrates that the permeability of the chorion changes with time and highlights its function as a barrier over the first 24 hours.

Finally, the red coloration of the chorion (Fig. 3.4.1) illustrates that there must be an interaction between DCF and the chorion. Since DCF is red in its crystalline form, it is most likely that there is a chemical precipitation at the chorion. Since fluorescein does not show this effect, this precipitation must be associated with the chlorine in the DCF.

4.2.3 5-(and-6)-Carboxy-2, 7-dichlorofluorescein

Compared to DCF, carboxy-DCF has a second carboxy group (Fig. 2.1.9). Therefore, its complexity and polar surface area are about three times higher. Consequently, the water solubility may be expected to be higher, whereas the log P_{ow} can be expected to be lower. However, the outcome of the calculated data was contradictory. Nevertheless, a better water solubility than DCF was observed by preparing the test dilution. Sigma Aldrich points out that the water solubility increases with increased pH (≥ 5) and allows the assumption of a better water solubility. As described for sulforhodamine b, the calculated values should be understood rather as a rough-guide, since several parameters influence the log P_{ow} and water solubility. Especially the pH is a crucial value which should be taken into consideration.

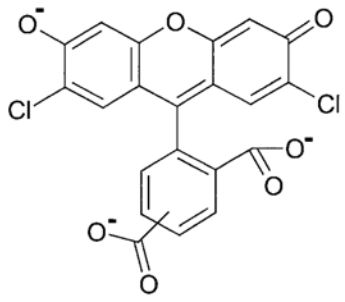

Figure 4.2.1: Chemical structure of CX-DCF at pH: 7.4

The fluorophore carboxy-DCF is a multivalent organic anion (Fig. 4.2.1) at physiological pH 7.4 (Zamek-Gliszczynski 2003). The plasma membrane of cells represents a diffusion barrier for carboxy-DCF, whereas carboxy-DCF diacetate carries only one negative charge (Leonhardt et al. 1971) and, therefore, permeates into cells. These results suggest that most carboxy-DCF is undissociated and did not pass the chorion, as already discussed in chapter 4.2.2. Observations under the epi-fluorescence microscope (Fig. 3.5.5) as well as with the confocal microscope (Fig. 3.5.11) of the dechorionated 24 and 48 hpf embryos corroborate this assumption. The high exposure time of 214 ms and the high voltage of 100 required emphasize the weakness of the signal. In contrast to DCF, carboxy-DCF does not pass the chorion after 48 hours. Its adsorption to the chorion is illustrated in Figures 3.5.4-10. Kishino & Kobayashi (1994) demonstrated that the Δ pK_a increases with increasing number of chlorine atoms, and also with the approach of the chlorine atom position to the OH group in chlorophenols, having the same number of chlorine atoms. Consequently, it is considered that the increase of the Δ pKa is mainly caused by the decreased electron density of the OH group. It is most likely that the additional carboxy group supports this effect and supports the dissociation of carboxy-DCF, which intern might inhibit the passage through the chorion.

On the one hand, there is the chorion as a barrier; on the other hand, the additional measurement (chapter 3.5.2) demonstrates that an increased uptake is hardly possible, even when the 24 hpf dechorionated embryos were transferred directly into carboxy-DCF (80 mg/L). The signal from dechorionated embryos which were directly exposed to carboxy-DCF increases only about 10 % (Fig. 3.5.8). Most likely, the additional carboxy group produces a steric effect and inhibits the uptake of carboxy-DCF into the embryo as well as its passage across the pores of the chorion. Figure 3.5.12 shows an increased accumulation of carboxy-DCF in the region of the pores and might thus illustrate an interaction with the chorionic pore canals. However, to make a sound statement, there is a need for additional research into the chorion. Due to the red coloration by carboxy-DCF, as has already been described for DCF, however, some kind of interaction seems likely, probably associated with the chlorine atoms. The distribution of carboxy-DCF inside the embryo differs from that of fluorescein and DCF, since the substance rather accumulates in the yolk than in the brain (Fig. 3.5.5 and Fig 3.5.11). The signal in the yolk is inhomogeneous: there was one stronger signal in the area near to the heart, and another one in the intestinal lumen, more precisely in the stomach (Fig. 3.5.5).

Zamek-Gliszczynski (2003) used carboxy-DCF in his study as a model compound to evaluate the biliary excretion of organic anions in sandwich-cultured rat hepatocytes. Carboxy-DCF is eliminated from hepatocytes primarily *via* biliary excretion and, hence, appears to be a promising probe to study biliary excretion of organic anions. However, the hepatic transport of carboxy-DCF has not been fully characterized (Zamek-Gliszczynski 2003). Therefore, the accumulation in the intestinal lumen suggests that metabolism of carboxy-DCF is similar to that of DCF and fluorescein, which is described in chapter 4.2.1 and 4.2.2.

The distribution inside the embryo is difficult to assess, since the high accumulation on the chorion disturbs the evaluation with the plot profile as well as with the ROI-manger. The homogenous signal along the profile is reflected in the plateau and highlights the adsorption of carboxy-DCF to the chorion (Fig. 3.5.6). The strong accumulation of carboxy-DCF on the chorion becomes even more evident by comparing the plot profile of carboxy-DCF with that of the control group (Fig. 3.5.7), since the two smaller peaks in the plot profile of the control group identify margins of the yolk sac.

4.3 Dimethyl sulfoxide (DMSO) as a solvent

The purpose of a chemical carrier is to provide the required physical and/or chemical environment needed to deliver a test substance to a test organism without induction of any extraneous variables, such as structural alteration of the test substance or adverse biological effects (Helmstetter 1996). Unlike other commonly used carriers such as methanol or acetone, DMSO has the ability to permeate biological membranes without significant damage to the structural integrity of these barriers (Rammler 1967).

4.3.1 Autofluorescence of DMSO

DMSO is used as a solubilising fluorescent dye with low water solubility, named fluorescein, DCF and Carboxy-DCF. Therefore, to avoid misleading results, it was a necessary to investigate whether there is an autofluorescence due to the solvent itself. After 24 hours, an autofluorescence signal could be seen in embryos exposed to 1 % DMSO (Fig. 3.6.1 A), but not in embryos exposed to 0.01 % DMSO (Fig. 3.6.1 B). The autofluorescence of DMSO is confirmed by the lack of signal in the control group (Fig 3.6.1 C). Autofluorescence is only observed in the chorion, which is why the dechorionated embryos do not show any fluorescence signal (at least not after 24 or 48 hours of exposure), not even with a high voltage of 200. These results suggest that the higher the DMSO concentration, the higher the autofluorescence in the chorion. After 48 hours, the autofluorescence of DMSO does not

change. The fluorescence signal in Figure 3.6.1 seems to be weaker due to the smaller HV of 100.

The broad solvent characteristics of DMSO are the result of its ability to form either stable solvates by dipole-dipole interactions or solvent-solute associations by hydrophobic interactions (Parker 1962). DMSO is extremely hygroscopic and miscible with water in all proportions. It has been suggested that the hydrogen bonds, which exist between water and DMSO, are stronger than the hydrogen bonds, which exist between water molecules (Cowie & Toporowski 1961). In medical research, DMSO has been shown to cross the dermal barriers rapidly and at high concentrations. This innocuous permeation of DMSO through a protein barrier, whose conformational integrity is dependent upon bound water, is the result of reversibly configurational changes of proteins because of water substitution by DMSO. Thus, DMSO appears to be effective in altering the configuration of proteins by water substitution and might, thus, also change the proteins of the chorion. With increased water content in the chorion, the chorion swells and is supposed to entail a different light reflection which causes the autofluorescence.

Furthermore, in protein topographical studies by difference spectra (Herskovits & Laskowiski 1962), solvent-induced shifts in the absorption maxima e.g. of tyrosine and tryptophan have been attributed to changes of the special environment that surrounds these groups in the native protein. However, it is unlikely that the fluorescence signal in Figure 3.6.1 A comes from any amino acids since the emission spectrum is too low for these filters. Additionally, the effectiveness of DMSO as a spectral pertubant is related not only to its special chemical characteristics, but also to its size. The comparatively small size of DMSO allows the molecule to penetrate regions of the protein subunits interfaces more readily than the other bulkier solvents and might cause the observed autofluorescence in Figure 3.6.1 A. Otherwise, there is also a weak autofluorescence without DMSO detectable, especially the autofluorescence after 24 hours must be considered (Fig. 3.6.1 C), whereas the autofluorescence after 48 hours is not as prominent (Fig. 3.6.1 F). Due to the thicker structure of the chorion after 24 hours, the higher autofluorescence might cause by a stronger reflection.

None the less, however, the high voltages of 100 and 200 documented that the autofluorescence of DMSO is very weak and does not interfere with of the results in the present study.

4.3.2 Fluorescein in 1 %- 0.1 % and 0.01 % DMSO

Comparing Figs. 3.6.2 (A-F), 3.6.6 (A-F) and 3.6.7, it is notable that the signal strength in the embryos decreases with lower DMSO concentration. Furthermore, the distribution of fluorescein changes with lower DMSO concentration, since it then accumulates rather in the chorion than in the embryo. These results suggest that with lower DMSO concentration, the chorion seems to be a stronger barrier. In other words, DMSO apparently supports the pathway across the chorion.

Helmstetter (1996) used dimethyl sulfoxide (DMSO) as a carrier solvent to deliver test chemicals across the egg chorion to the developing embryo. The effect of facilitated uptake in the embryo is already used as a non-invasive alternative to direct injection of chemicals through the chorion. During the development of the injection method of Black et al. (1985), it was observed that a drop of the solvent carrier, DMSO placed on the egg surface elicited a vigorous motor response from the embryo (Colwell & Grimes 1986). Based on this observation and the widely recognized membrane penetration properties of DMSO, it is hypothesized that chemicals could be carried across the chorion by DMSO resulting in increased exposure of the developing embryo to the corresponding chemical. In addition, Rammler (1967) suggests that if part of DMSO´s medicinal attributes are associated with its solvent action; these effects would be accepted to be most prominent in areas where it occurs at high concentrations and allows rapid and accurate exposure in peripherally areas of the body.

As mentioned earlier, DMSO is hygroscopic and it is possible that a 2:1 association complex is formed with water (Cowie & Toporowski 1961). Therefore, the DMSO hydrate contains 2 M of water and is formed exothermally. Rammler (1967) points out that the most effective concentration of this substance for topical applications, barring water evaporation after application, is greater than 67 volume per cent and that, with increasing concentrations, the heat of hydration would assist increasing the rate of diffusion across the epidermis. According to Boost (1965 a), the most effective concentration for topically applied DMSO is 90 volume per cent. In regard to the present study, the concentration of DMSO is more than 100 times less, but even in such low concentrations of 1 % and 0.1 % DMSO, the effect of facilitated uptake of the dyes into the embryo is demonstrated (Figs. 3.6.2; 3.6.4; 3.6.6-3.6.8).

As described in chapter 4.3.1, a crucial effect of DMSO is the alteration of the configuration of proteins by water substitution. Apart from the change of proteins in the chorion in form of water retention, a steric change e.g. in the pore canal of the chorion or the effect on lipid

membranes might increase the permeability. With regard to the stereometric structure of DMSO, and to the known special bond between S and O in the sulphoxides, Puig-Muset et al. (1965) studied the change of the isomeric conformation of linoleic and oleic acids in the cell membrane and tested the possibility that DMSO might produce this change. In linoleic acid, for instance, the cis-cis structure of the hydrocarbon chain is changed by peroxidation to the cis-trans form. Their experimental results demonstrate that DMSO probably indicates the destruction of the hydroperoxide and changes the structures of linoleic acid by fixation of peroxide, with an appearance of a space in the cell membrane wide enough to allow the passage of potassium and sodium ions in hydrated forms. Consequently, the permeability of the cell membranes increases. Although speculative, since there is no data about the ratio of saturated to non-saturated fatty acids in the chorion, this type of scheme is useful because it indicates the principal reaction of the special bond between S and O in the sulphoxides with its lipid peroxidations. Allison (1965) described an increased permeability of lipoprotein membranes of cells and cell organelles as a consequence of lipid peroxidation. These results suggest that DMSO might increase the permeability of the chorion by lipid peroxidation. Observation with epi-fluorescence microscopy (Fig. 3.6.2) and with the confocal microscope (Figs. 3.6.6-8) might demonstrate that even low concentrations of 1 % and 0.1 % DMSO are sufficient for lipid peroxidation since fluorescein could pass the chorion. In contrast, the concentration of 0.01 % DMSO might have been too low to induce sufficient lipid peroxidation, since fluorescein could not pass the chorion. However, to make a definite statement, there has to be more in-depth research on the components of the chorion and how exactly DMSO influences the chorion.

As already described in chapter 4.1.2, the permeability of the chorion changes during development. Depeche and Billard (1994) investigated turbots and suggested that the increased permeability might be due to an increase in the diameter of the chorionic canals during development, which may also favour DMSO penetration through this structure. Moreover, Cabrita (2003) tested permeability of the chorion to DMSO by high performance liquid chromatography (HPLC) in three different developmental stages of turbot embryos. The results show that the permeability is stage-dependent (stages defined by Jones 1972). The concentrations of DMSO at the tail-bud-free stages (G-stage) were significantly higher than those in embryos at the closed blastopore (E-stage) and tail bud stages (F-stage). DMSO concentrations inside the chorion also increased with the concentration of DMSO in the medium, with internal DMSO concentrations of 6.9 mM for the E-stage, 38 mM for the

F-stage and 113 mM for the G-stage in the embryos, which had been exposed to a 2 M solution (Cabrita 2003).

Comparing these developmental stages with the ones of the zebrafish, than the E-stage is equivalent to the 16- cell stage (1.5 hpf), the F-stage to the bud-stage (10 hpf) and the G-stage to the prim-5 stage (24 hpf) (defined by Westerfield 2007). Therefore, the same effect is shown after 48 hours exposure of 100 mg/L fluorescein in 1 % and 0.1 % DMSO: the signal in the chorion decreases, whereas the signal in the embryo increases (Figs. 3.6.2; -7). In contrast, with 100 mg/L fluorescein in 0.01 % DMSO, the signal in the chorion does not change, whereas the signal in the embryo shows a small increase (Fig. 3.6.7-Fig. 3.6.8). Furthermore, the extended test to determine the permeability of the chorion (chapter 3.6.2) supports the view that the uptake into the embryo increases with higher concentrations of DMSO (Fig. 3.6.3). Extended exposure also shows that, with higher concentrations of DMSO, the function of the chorion as a barrier becomes less significant, since the differences between the exposure with or without chorion become smaller. Nevertheless, the direct exposure of the embryo shows an increased uptake in 1 and 0.01 % DMSO, whereas the uptake in 1 % DMSO is definitely higher than in 0.01 % DMSO (Fig 3.6.3).

The test in order to check if the chorion changes its structure during the embryonic development (described in chapter 3.6.2) highlights that the structure of the chorion changes after 24 hours. The group exposed to 100 mg/L fluorescein in 0.01 % DMSO between 24 hpf and 48 hpf only demonstrated that, despite the short exposure time of 24 hours, fluorescein was able to pass the 48 h old chorion (Fig. 3.6.4 B, E). Compared to 24 hpf embryos, which were normally exposed for the same duration, but during a different stage of development (Fig. 3.6.4 A), these embryos showed a weaker signal in the embryo (Fig. 3.6.4 D). Consequently, the increased uptake in the embryo after 48 hours of exposure is due not only to an equilibrium reaction between several compartments, but also to an increased permeability of the chorion most likely caused by structural changes. Nevertheless, the equilibrium reactions are also involved, since the accumulation in embryos exposed for 48 hours (Fig. 3.6.4 C, D) is higher than after 24 hours exposure (Figs. 3.6.4 B, E). The same results were found with 100 mg/L fluorescein in 0.1 % DMSO (Figs. 3.6.4 G, H, I).

As already discussed in chapter 4.1.2, the test to see if there is an uptake of 100 mg/L fluorescein in 1 % or in 0.01 % DMSO in the embryo from the chorion after 48 hours (described in chapter 3.6.2) failed since the amount of the additional dye was too low to be detected (Fig. 3.6.5).

The distribution inside the embryo does not seem to be influenced by different concentrations of DMSO. However, Hagedorn (1996), working with zebrafish, observed that DMSO penetrates the perivitelline space, but not the yolk compartment. The experiments identified the yolk syncycial layer (YSL) (see chapter 4.2.1) as a barrier to the movement of DMSO into the yolk. These results imply that fluorescein accumulates in the yolk, whereas the solvent DMSO does not pass the YSL. Therefore, DMSO seems to be only a vehicle to pass the chorion, but not for further transport into the embryo. Harvey (1983) indicated a weak barrier function of the zebrafish chorion for labeled DMSO, since the embryo did not show any radioactivity. It rather reacts directly with the chorion (see above) or somewhere in the perivitelline space. Consequently, fluorescein seems to diffuse into the yolk on its own. In other words, DMSO affects the amount of fluorescein inside the egg, but not the direct uptake into the embryo.

4.3.3 2,7-Dichlorofluorescein in 1% - 0.1 % and 0.01 % DMSO

Figs. 3.6.9-12 demonstrate that the distribution of 2,7-dichlorofluorescein (DCF) in different concentrations of DMSO did not change as was the case for fluorescein. Especially the differences after 24 hours were minor and increased uptake could not be seen (Fig. 3.6.10). Nevertheless, after 48 hours, an increased uptake of DCF in 1 % and 0.1 % DMSO was seen in the embryo (Fig. 3.6.11). No difference in the distribution inside the embryo could be seen after 24 hours nor after 48 hours (Fig. 3.6.12). In contrast to fluorescein, it seems that the uptake of DCF was not significantly increased with different DMSO concentrations.

As discussed in chapter 4.2.2, the chlorine atoms produce many effects and factors such as compound polarity, steric factors, functional groups and structural configurations are crucial values for the distribution of DCF. However, these effects do not seem to be influenced by different concentrations of DMSO. In other words, the observed increased permeability of the chorion by the treatment with DMSO seems not to be sufficient for DCF to pass the chorion; rather, characteristics such as bulkiness of DCF seem predominant.

One important characteristic of DCF is its high log P_{ow}. Even though the uptake should not be evaluated by the log P_{ow} alone (see chapter 4.2.2), it is still a crucial parameter which influences uptake, accumulation and bioavailability of DCF. Helmstetter (1995) points out that even in the presence of a pure solubilizer such as DMSO; a passive transport takes place. Helmstetter (1995) suggests that the amount of toxicant penetrating the egg will depend on the lipid solubility of the chemical, which is established by various properties of the chemical

itself, and not by the solubility in, or penetrability of the DMSO carrier. The ratio of DCF permeating the egg is not changing significantly with DMSO carriers. Given that DMSO was unable to pass the YSL, the main transport of DCF across the chorion and especially in the embryo is supposed to be *via* passive diffusion (cp. chapter 4.2.2).

The test to check whether a change in toxicity would correlate with different DMSO concentrations failed, since there was no mortality observed at all. There are several possibilities why toxicity tests may deviate from each other, but one reason is obvious to see in Figs. 3.6.13 A, B. Figure 3.6.13 A present the 48 hpf embryo exposed to 50 mg/L DCF in 0.01 % DMSO with a stronger signal than the 48 hpf embryo exposed to 65 mg/L DCF in 0.01 % in Figure 3.6.13 B. These results suggest that the concentration of the dilution was less than 50 mg/L. The lack of mortality by 65 mg/L DCF in 1 % and the weaker signal Fig. 3.6.13 D than by 50 mg/L DCF (Fig. 3.6.13 C) also suggests that the concentration of the dilution is less than 50 mg/L. These small fluctuations in test dilutions are supposed to show significant effects in toxicity, since DCF has such a steep slope of toxicity.

4.3.4 Correlation between extinction and different DMSO concentrations

To make sure that the difference in the distribution was not caused by concentration fluctuations of the dye due to its low solubility, the test was extended to determine the change of extinction with time (chapter 3.6.5). Figure 3.6.14 illustrates that the concentration of fluorescein 100 mg/L in all DMSO concentrations is relatively constant, considering that 0.1 units in extinction as equivalent to 5 mg/L. The discrepancy between start and final values decreased with increased concentration of DMSO; therefore, DMSO 0.01 % presented the lowest fluctuations with time. Assuming that after one day 100 mg/L of fluorescein was completely solved in 10 % DMSO and set this as reference (100 %); the highest discrepancy was in the 0.01 % DMSO solution and is approx. 1.8 %, which is equivalent to 1.8 mg/L. Such a small amount is not significant for toxicity nor for distribution statements; therefore, the results of this study are not influenced by concentration fluctuations.

4.4 Fluorescence dye with different molecular weights

4.4.1 Dextran fluorescein with 3 kDa

After 24 hours as well as after 48 hours, dextran fluorescein attaches to the outer face of the chorion, which is illustrated by the images that show a high fluorescence of the chorion, which is why the embryos are barely visible (Figs. 3.7.1 A, B and Figs. 3.7.3 B, D). The lack of a signal in embryos dechorionated after 24 and 48 hours confirms this assumption since neither there is a signal detectable in the embryos at all (Figs. 3.7.1 C, D and Figs. 3.7.3 A, C). These results suggest that molecules of 3 kDa are not able to pass the chorion. This conclusion is in contradiction to Creton (2004), who investigated the inhibition of the endoplasmic reticulum Ca^{2+} pump in zebrafish embryos and claims that the chorion is still permeable to fluorescent dextrans of 3 kDa, but not to dextrans of 10 kDa. Furthermore, the spots on the chorion (Figs. 3.7.2 A, B) indicate that dextran fluorescein accumulates in the pores of the chorion. The observation with the confocal microscope corroborates this impression (Fig. 3.7.4) and highlights the distribution of the pore canals over the entire surface of the chorion.

Hart & Donovan (1983) studied the chorion using Nomarski differential interface optics as well as and scanning and transmission electron microscopy. The chorion consists of three distinct zones: an outer, electron-dense zone containing pore canal plugs (zona radiate externa), a middle fibrillar zone (superficial zona radiate interna), and an inner zone of 16 horizontal electron-dense lamellae alternating with 15 interlamellae of lower electron density (deep zona radiate interna). The zona radiate interna is penetrated by open pore canals. The pores across the chorion are necessary for oxygen and nutrient transportation from the aquatic environment to the embryo and for the elimination of wastes (Cheng 2007). The pore canals show a regular distribution with a center-to-center spacing about 1.5 - 2.0 µm (Rawson 2000). An estimate of the number of pore results in 45.6 pores/100 μm^2 therefore, the total number of pores was supposed to be 7.2×10^5 (calculated by Hart & Donovan 1983). The pores are cone-shaped with a larger diameter at the inner surface and display a corkscrew-like ridged wall with lamellae ringing the inner surface of the pore canal. Figure 3.7.6 might show the cone-shaped structure. It is more likely; however, that it presents an interference signal, since the signal strength is getting weaker with increasing distance; consequently the light cone gets smaller and looks cone-shaped.

According to Hart & Donovan (1983) the diameter of the outer opening of the chorion pore canal is about 0.2 µm just below its plug, whereas Rawson (2000) established one of 0.5 - 0.7 µm. In zebrafish, the better part of each pore canal remains open after oogenesis and oviposition. It is only the outer portion of each canal that becomes plugged. The material forming the plugs and its origin however, are still to be identified. Nevertheless, it is certain that, at the time of fertilization, the egg is completely "sealed off" from direct exposure to the external environment except in the area of the micropylar apparatus (Hart & Donovan 1983). The high number of pores suggests a high permeability of the chorion, but the relatively small opening, the cone-shaped structure, the corkscrew-like ridged wall of the pore canal and the canal plugs in the zona radiate externa are factors which increase the diffusion resistance and account for the function of the chorion as a barrier.

Dalton (Da) is a measuring unit used to express atomic and molecular masses. 1 Da is the approximate mass of a hydrogen atom, a proton, or a neutron (equivalent to g/mol). Although it is not conventional to convert daltons into µm, the comparison with the pore size of artificial membranes intended for separation purposes in the laboratory could be a useful tool to get an impression of the according molecule size. Howe & Clark (2002) investigated samples of water by sequential filtration process and characterized each fraction of dissolved organic matter (DOM) by size exclusion chromatography. They fractionated the water samples through regenerated cellulose (RC) membranes with nominal molecular weight cutoffs (MWCO) of 3000 Da and used the identification of the molecular weight (MW) to estimate the size of the particles. Howe & Clark (2002) presumed a correlation between MWCO and pore size based on experiments with polyethylene glycol (PEG) and supposed that 3 kDa has a size of 3 nm. Based on these results, the pore canal of the zebrafish chorion with its smallest opening of 0.2 µm (200 nm) would be approximately 66 times larger than a molecule dextran fluorescein with 3 kDa. This comparison, however, cannot be justified, since the structure of PEGs is rod-shaped and one-dimensional, whereas dextrans are spherical particles that differ in volume and diameter. The experiments of Howe & Clark (2002) were conducted under increased pressure and, thus, do not reflect the natural conditions of passive diffusion. Furthermore, the relationship between MWCO and pore size varies depending on the chemical selected for filtration due to steric, electrostatic, and chemical differences. This means that the size of particles is not the only criterion for exclusion. Nevertheless, the results of the study can be used to get an idea of the relation between the size of the opening of the pore canal and dextran with 3 kDa. However, they also

demonstrate that the pore size of the chorion by itself is not exclusively the limiting factor for crossing the chorion, but that diffusion depends on many parameters.

Finally, it should be noted that fluorescein is not the best fluorescence moiety for labeling dextran, since the observation in chapter 4.1.2 demonstrate that fluorescein in 0.01 % DMSO passes the chorion only after 48 hours. *Vice versa*, it may be supposed, that dextran fluorescein exclusively solved in water passes the chorion only very slowly or, rather, not at all. Since the signal inside the embryo was very weak after 48 hours exposure to fluorescein (100 mg/L; Figs. 3.7.3 C, D), the conclusion that dextran fluorescein with 3 kDa could not pass the chorion is not definite. For clear results, the test will have to be repeated with a water soluble fluorescence dye, which passes the chorion; e.g., dextran rhodamine b with 3 kDa.

4.4.2 Dextran fluorescein with 40 kDa

Dextran fluorescein of 40 kDa is not able to pass the chorion (Figs. 3.8.1-2). In contrast to fluorescein of 3 kDa, the image shows more plaques (Fig. 3.8.3) and the pores are not presented as precise as the ones in Fig. 3.7.4. Thus, dextran fluorescein of 40 kDa does not seem to fit into the pores.

5 Conclusion

The aim of this study was to determine the uptake and distribution of fluorescent dyes with different chemical characteristics in the egg and embryo of the zebrafish (*Danio rerio*).

Rhodamine b with its good water solubility passes the chorion and accumulates in the yolk. Most likely, due to its small polar surface and a low log P_{ow}, that rhodamine b diffuses into the yolk. Furthermore, with increased yolk consumption, rhodamine b is metabolized. Since all metabolites of rhodamine b are also fluorescent, the fluorescence signal spreading over the body can be attributed to both rhodamine b and its metabolites. The elongation of the heart and the expansion of the signal occur in parallel and demonstrate that the fluorescence dye is transported by blood and must pass the yolk syncycial layer, which is in connection with the developing heart and in direct contact with the extracellular space.

Sulforhodamine b with its charged substituents and its high water solubility does not diffuse through the chorion before 48 hours. The main distribution of sulforhodamine b is in the chorion and thus reflects the function of the chorion as a barrier for hydrophilic substances. Moreover, the observation with the CLSM shows the change of the permeability of the chorion and its thickness during development. In case sulforhodamine b actually passes the chorion, it accumulates predominately in the vascular system in the area of the duct of Cuvier. Due to parallels to the metabolism of rhodamine b, it is likely that the signal in the blood also due to metabolites of sulforhodamine b and rhodamine b. Analysis of the epi-fluorescence images with the region of interest (ROI) manager demonstrates that the ROI-manager is only a useful tool, when there is a clear delineation of the fluorescence signal, but no attachment to the chorion. Finally, the test to check if there is an uptake of sulforhodamine b in the embryo from the chorion after 48 hours demonstrates that this method is not adequate for such small amounts (0.025 µl). Thus, this test method must be repeated with, for example, radiolabeled substances.

Fluorescein, the smallest molecule tested in this study, passes the chorion and accumulates in the area around the heart and the brain, which indicates that it is transported by blood. Since no additional fluorescence dye diffuses through the chorion, most fluorescein is found in the bile and the intestine, which suggest a metabolism similar to that in humans. The strong signal in the perisyncytial space, thus in the plasma, most likely demonstrate the additional accumulation of fluorescein metabolites as monoglucuronides, which themselves have a weaker signal.

2,7-Dichlorofluorescein (DCF) is double-chlorinated, and its lipophilicity is 1.3 times higher than that of fluorescein. The bulk of DCF does not pass the chorion after 24 hours. This study does not show a linear correlation between log P_{ow} and accumulation in the embryo, but rather that the concentration ratio of undissociated and dissociated DCF might be the crucial value for distribution and subsequent toxicity. At a pH of 7.8, it is most likely that the small amount of DCF which passes the chorion by diffusion might be undissociated, whereas most of it is supposed to be dissociated and, thus, is not able to pass the chorion. The increased uptake of DCF into the embryo after 48 hours can be explained by the assumption of increasing permeability of the chorion during development. Otherwise, the distribution of DCF inside the embryo does not differ from that of fluorescein, and even the metabolism of DCF seems to be the same as for fluorescein (rather, it could even be identical if the chlorine atoms were removed first). Since DCF is red in its crystalline form, it is most likely that the red coloration of the chorion shows a chemical retention at the chorion. This precipitation must be associated with chlorine, because fluorescein does not show this effect.

5-(and-6)-Carboxy-2,7-dichlorofluorescein (Carboxy-DCF) has an additional carboxy group and is the most complex molecule tested in this study. It is a multivalent anion which neither passes the chorion after 24 hours nor after 48 hours. Most likely, the additional carboxy group causes the dissociation of carboxy-DCF, which may inhibit the passage through the chorion. Otherwise, it is shown that even after the transfer of the 24 h old dechorionated embryos directly into carboxy-DCF not increases the uptake of carboxy-DCF. Supposedly, the additional carboxy group causes a steric effect and inhibits the uptake of carboxy-DCF into the embryo as well as its passage across the pores of the chorion. The increased accumulation of carboxy-DCF in the region of the pores demonstrates an interaction within the pore canals. The distribution inside the embryo differs to that of fluorescein and DCF, since the substance rather accumulates in the yolk than in the brain. However, the accumulation in the intestinal lumen suggests that the metabolism of carboxy-DCF is the similar to that of DCF and fluorescein. Nevertheless, the distribution inside the embryo is difficult assess, since the high accumulation in the chorion disturbs the evaluation with the plot profile as well as with the ROI-manger.

An autofluorescence signal in the chorion is shown at concentration of 1 % and 0.1 % DMSO. Since no autofluorescence was found with 0.01 % DMSO, it is suggested that the higher the DMSO concentration is, the higher is the autofluorescence in the chorion. Autofluorescence is exclusively observed in the chorion. DMSO might be effective in altering

the configuration of proteins of the chorion in form of water retention. With increased water contents of the chorion, the chorion swells and is supposed to entail a different light reflection which causes the autofluorescence. However, there is also a weak fluorescence detectable without DMSO, especially after 24 hours. Nevertheless, the autofluorescence of DMSO is very weak and did not influence the results.

Different DMSO concentrations change the distribution of fluorescein in different compartments of the egg. The uptake of fluorescein was increased through the use of DMSO concentrations of 1 % and 0.1 %, whereas fluorescein which was dissolved in only 0.01 %, was not able to pass the chorion. The results suggest that increased DMSO concentrations support the passage across the chorion. Apart from its effect on proteins in the chorion in form of water retention, a steric change in the pore canals may be assumed, or an effect on lipid membranes might increase the permeability by lipid peroxidation. However, the concentration of 0.01 % DMSO seems to be too low to induce an increased permeability of the chorion. These results show that with higher concentrations of DMSO the function of the chorion as a barrier becomes less significant. Therefore, DMSO could be useful as a carrier solvent to deliver test chemicals across the chorion to the developing embryo and could be an alternative method to the dechorionation of embryos. However, to make a definite statement, there needs to be more-in-depth on how exactly DMSO influences the chorion.

Furthermore, the relative distribution inside the embryo seems not to be influenced by different concentrations of DMSO. DMSO penetrates the perivitelline space, but not the yolk compartment. Therefore, the yolk syncycial layer (YSL) seems to be a barrier to the movement of DMSO into the yolk. Consequently, DMSO might only be a vehicle to pass the chorion which directly affects the amount of fluorescein inside the egg. The direct uptake into the embryo, however, is rather influenced indirectly *via* an increased availability of chemicals inside the egg.

In contrast to fluorescein, it seems that the uptake of 2,7-dichlorofluorescein was not substantially increased with different DMSO concentrations. The increased permeability of the chorion by treatment with DMSO seems not to be sufficient for DCF to pass the chorion; therefore, the bulkiness of 2,7-dichlorofluorescein seem to be able predominant feature. There are no differences in the distribution inside the embryo observable neither after 24 hours nor after 48 hours.

Photometric determination of changes in extinction with time demonstrates that the concentration of fluorescein at all DMSO concentrations is relatively constant and does not influence the distribution.

Finally, all tests have shown that a DMSO concentration of 0.01 % does not influence the distribution nor the bioavailability of the fluorescent dyes. Thus, the present study supports the recommendation of the OECD (OECD 2000, ENV/JM/MONO (2000)6) that a maximum solvent concentration of 100 mg/L (equivalent to 0.01 %) should not be exceeded.

The test with different molecular weight dextrans demonstrates that neither dextran fluorescein with 3 kDa nor dextran with 40 kDa are able to pass the chorion. The observation with the confocal microscope indicates that dextran of 3 kDa fits into the pores of the chorion, whereas dextran of 40 kDa does not. The relation between the size of the opening of the pore canals and dextran fluorescein with 3 kDa demonstrates that the pore size of the chorion by itself is not exclusively the limiting factor for crossing the chorion and that diffusion depends on additional parameters. Nevertheless, the tests demonstrate that fluorescein is not the adequate fluorescence for labeling dextran. For better results, the test should be repeated with a water-soluble fluorescent dye which passes the chorion such as dextran rhodamine b.

In conclusion, fluorescence microscopy, epi-fluorescence as well as confocal microscopy represent a useful tool to investigate the ratio as to which fluorescent dyes cross the chorion of the zebrafish egg. On the one hand, it allows the investigation of the chorion as a barrier, on the other hand it helps to retrace pathways and to draw conclusions about metabolism. Furthermore, this method permits visualization of the accumulation of fluorescence-labeled substances in different compartments of the embryo. Based on the results of this study, new research perspectives emerge. Rhodamine b, e.g., passes the chorion and could be used as a tracer for different molecular weights. Additionally, rhodamine b in combination with different concentrations of DMSO could be a tool to demonstrate as to which order of magnitude the permeability of the chorion is increased by DMSO. Moreover, 2,7-dichlorofluorescein with its steep slope of toxicity is an interesting object to investigate changes of toxicity by changing the dissociation ratio, e.g., by decreasing the pH or by increasing the availability inside the egg by using higher concentrations of DMSO. Finally, the fact that higher concentrations of DMSO seem to decrease the barrier function may present a new approach for the investigation of the chorion´s importance in relation to embryo toxicity, and might have consequences for the evaluation of toxicity.

6 Summary

The fish embryo test (FET) with *Danio rerio* is a well-established method for the toxicological evaluation of treated waste water, chemicals and sediments and was standardized at a national level in DIN 38415-6 in 2001. In order to study the distribution of chemicals in the FET, the present study investigated the individual distribution of seven different fluorescent dyes in different compartments of the zebrafish egg (chorion, perivitelline space, different organs of the embryo). For a better assessment of the effects of side chains, rhodamine b and fluorescein were chosen as basic fluorochromes, which were then modified by diverse substituents that differed in their partition coefficient, molecular size and charge. The substances tested were rhodamine b, sulforhodamine b, fluorescein, 2,7-dichlorofluorescein and 5-carboxy-2,7-dichlorofluorescein. The permeability of the chorion was evaluated through the use of dextran fluorescein with different molecular sizes: 3 kDa and 40 kDa. Finally, the distribution of fluorescein was studied with respect to its dependancy on different concentrations of the solvent DMSO (0.01 %, 0.1 % and 1 %).

Substances with high water solubility such as rhodamine b and sulforhodamine b, accumulated in the yolk, although sulforhodamine b with its charged substituents did not diffuse through the changing chorion before 48 hours. The smallest molecule, fluorescein, accumulated in the blood and brain as early as after 24 hours, whereas the slightly larger molecules 2,7-dichlorofluorescein and 5-carboxy-2,7-dichlorofluorescein could only pass the chorion after 48 hours. Neither of the two largest molecules, dextran fluorescein with 3 kDa nor 40 kDa, was able to pass the chorion at all, and 3 kDa dextran fluorescein accumulated in the pore canals. The uptake of fluorescein was increased through the use of DMSO concentrations of 1 % and 0.1 %, whereas fluorescein which was dissolved in only 0.01 % was not able to pass the chorion.

The study thus demonstrated that the barrier function of the chorion depends on the polarity and partition coefficient of the substances tested and that the ratio of undissociated and dissociated substances might be a crucial parameter for toxicity. Furthermore, this study shows that higher DMSO concentrations decrease the barrier function of the chorion, which might present a new approach for the investigation of the chorion’s relevance for embryo toxicity.

Zusammenfassung

Der Fischembryo-Test (FET) ist eine seit 2001 auf nationaler Ebene in der DIN 38415-6 standardisierte, etablierte Methode zur Prüfung von behandelten Abwasserproben, Chemikalien und Sedimenten. Um das grundsätzliche Verteilungsverhalten von Chemikalien im FET zu beobachten, wurde im Rahmen der vorliegenden Studie die Verteilung von 7 verschiedenen Fluoreszenzfarbstoffen in den einzelnen Kompartimenten des Fischeis (Chorion, Perivitellin-Raum, verschiedene Organe des Embryos) untersucht. Zur besseren Beurteilung der Wirkung einzelner Substituenten wurden als Basismoleküle Rhodamin b und Fluorescein verwendet, die jeweils um verschiedene Substituenten erweitert wurden. Dabei wurde auf unterschiedliche Octanol-Wasser-Verteilungskoeffizienten (log K_{ow}), Molekülgrößen und Ladung geachtet. Getestet wurden Rhodamin b, Sulforhodamine b, Fluorescein, 2,7-Dichlorofluorescein und 5-Carboxy-2,7-dichlorofluorescein. Die Durchlässigkeit des Chorions aufgrund der Molekülgröße wurde mit Fluorescein markierten Dextranen von 3 und 40 kDa getestet. Zusätzlich wurde das Aufnahmeverhalten von Fluorescein in unterschiedlichen DMSO-Konzentrationen (0,01 %, 0,1 % und 1 %) untersucht.

Gut wasserlösliche Substanzen wie Rhodamin b und Sulforhodamine b akkumulierten im Dotter, allerdings diffundierte Sulforhodamine b mit seinen geladenen Substituenten erst nach 48 Stunden durch das sich verändernde Chorion. Das kleinste Molekül Fluorescein sammelte sich bereits nach 24 Stunden vermehrt im Blut und Gehirn, während 2,7-Dichlorofluorescein und 5-Carboxy-2,7-dichlorofluorescein das Chorion erst nach 48 Stunden passieren konnten. Die beiden größten Moleküle Dextran Fluorescein mit 3 und 40 kDa konnten das Chorion nicht passieren, wobei Dextran Fluorescein mit 3 kDa sich in den Poren sammelte. Die Aufnahme von Fluorescein in den Embryo wurde durch DMSO-Konzentrationen von 1 und 0,1 % gesteigert, während Fluorescein in 0,01 % DMSO das Chorion nicht passieren konnte.

Die Studie zeigt, dass die Barrierefunktion des Chorions einerseits durch die Polarität, aber auch durch den Octanol-Wasser-Koeffizienten beeinflusst wird, und dass das Verhältnis zwischen dissoziierter und undissoziierter Form der Substanzen eventuell einen wichtigen Parameter für das Auftreten von Toxizität darstellt. Außerdem wird gezeigt, dass höhere DMSO Konzentrationen die Barriereeigenschaft des Chorions herabsetzen und dadurch eventuell ein neuer Ansatz zur Erforschung der Bedeutung des Chorions in Bezug auf die Embryotoxizität gegeben wird.

7 References

Allison, A. C. (1965) Role of lysosomes in oxygen toxicity, Nature, Vol. 205, No 4967: 141-143

Bachmann, J. (2002) Entwicklung und Erprobung eines Teratogenitäts-Screening Testes mit Embryonen des Zebrabärblings *Danio rerio*. PhD thesis, Faculty of Forestry, Geo- and Hydrosciences, Dresden Techn. Univ., 214 pp.

Baldwin, I. G., Harman, M. M. I., and Neville, D. A. (1994) Performance Characteristics of a fish monitor for detection of toxic substances-I. Laboratory tails. Water Res. 28 (10): 2191-2199.

Blachnicki, K., (2006) Schematic of a fluorescence microscope. Polish original, derivative work: Mühlpfordt (2008). Illustration online at http://commons.wikimedia.org/wiki/File:FluorescenceFilters.svg, on August 12th 2009.

Black, J.J., Maccubbin, A.E. and Schiffert, M. (1985) A reliable, efficient, microinjection apparatus and methodology for the in vivo exposure of rainbow trout and salmon embryos to chemical carcinogens. J Natl Cancer Inst 75: 1123-8.

Blackman, G.E., Parke, M.H. and Garton, G. (1955) The physiological activity of substituted phenols. II. Relationships between physical properties and physiological activity. Arch Biochem 54: 55-71.

Bonsignorio, D., Perego, L., Del Giacco, L., Cotelli, F. (1996) Structure and macromolecular composition of the zebrafish egg chorion. Zygote 4, pp 101-108.

Boost, G. (1966) Syntex Institute of Clinical Medicine Reports, Syntex Cooperation, Palo Alto, Calif. Unpublished.

Braunbeck, T., Boettcher, M., Hollert, H., Kosmehl, T., Lammer, E., Leist, E., Rudolf, M. and Seitz, N. (2005) Towards an alternative for the acute fish LC(50) test in chemical assessment: the fish embryo toxicity test goes multi-species -- an update. Altex 22: 87-102.

Braunbeck, T., Lammer, E. (2006) Detailed review paper. Fish embryo toxicity assays. UBA report under conract no. 20385422. 298 pp.

Byrne, B.M.et al. (1989) The evolution of egg yolk proteins. Prog Biophys Mol Biol 53: 33-69.

Cabrita, E., Chereguini, O., Luna, M., de Paz, P., Herráez, M. P., (2003), Effect of different treatments on the chorion permeability to DMSO of turbot embryos (*Scophthalmus maximus*), Aquaculture 221: 593-604.

Cheng, J., Flahaut, E. and Cheng, S.H. (2007) Effect of carbon nanotubes on developing zebrafish (Danio rerio) embryos. Environ Toxicol Chem 26: 708-16.

Cohen, E., Gamliel, A. and Katan, J. (1988) The fungitoxicity of chlorophenols to the pathogenic fungi, *Fusarium oxysporum* and *Rhizoctonia solani*: A structure-activity relationship study. Pestic. Sci. 24, 139-146.

Colwell, R. R. and Grimes, D. J. (1966) Evidence for genetic modification of microorganisms occurring in natural aquatic environments. In: Aquatic toxicology and environmental fate (220-230). Ninth Volume, ASTM STP 91. Poston, T. M. and Purdy, R. (eds.), American Society of testing and materials, Phiadelphia, 1986, 527 pp

Connell, D. W. (1998). Bioaccumulation of Chemicals by Aquatic Organisms (439-450). In: G. Schüürmann and B. Markert (eds.), Ecotoxicology. New York and Heidelberg: Wiley and Spektrum Akadem. Publ.

Coppeta, R. (1998) Dual emission laser induced fluorescence for direct planar scalar behavior measurements. Experiments in Fluids 25: 1–15.

Cowie, J. M. G. and Toporowski, P. M. (1961) Association in the binary liquid system dimethyl sulphoxide – water. Can. J. Chem. 39 (11): 2240-2243.

Crandall, C. A. and Goodnight, C. J. (1959) The effect of various factors an the toxicity of sodium pentachlorophenate to fish. Limnol. Oceanogr. 4, 53-56.

Creton, R. (2004) The calcium pump of the endoplasmic reticulum plays a role in midline signaling during early zebrafish development. Brain Res Dev Brain Res 151: 33-41.

Dalela, R. C., Saroj Rani, Sarita Rani and Verma, S. R. (1980) Influence of pH on the toxicity of phenol and its two derivatives pentachlorophenol dinitrophenol to some fresh water teleosts. Acta Hydrochim. Hydrobiol. 8, 623-629.

Depeche, J., Billard, R. (1994) Embryology in fish, a review. Capter 1, Société Francaise d´Ichtylogie, Paris, France.

Devillers, J. and Chambon, P. (1986) Acute toxicity and QSAR of chlorophenols on *Daphnia magna*. Bull Environ Contam Toxicol 37: 599-605.

DIN (2001). German standard methods for the examination of water, waste water and sludge-subanimal testing (group T) – Part 6: Toxicity to fish. Determination of the non-acute-poisonous effect of waste water to fish eggs by dilution limits (T 6). DIN 38415-6, 2001; German Standardisation Organisation

Eicher, T.; Hauptmann, S. (2003). The chemistry of heterocycles: structure, reactions, syntheses, and applications. 2nd ed, Wiley-VCH. 572 pp.

Ertl, P., Rohde, B. and Selzer, P. (2000). Fast calculation of molecular polar surface area as a sum of fragment-based contributions and its application to the prediction of drug transport properties. Cheminformatics, Novartis Pharma AG, WKL-490.4.35, CH-4002 Basel, Switzerland

Fellers, T.J., Davidson, M.W. (2007). Introduction to Confocal Microscopy. Olympus Fluoview Resource Center. National High Magnetic Field Laboratory. online at http://www.olympusconfocal.com/theory/confocalintro.html, on August 13th., 2009.

Fetzer, J. C. (2000). The chemistry and analysis of the large polycyclic aromatic hydrocarbons. New York: Wiley & Sons, 304 pp.

Fiedler, H. and Lau, C. (1998). Environmental Fate of Chlorinated Organics (317-370). In: G. Schüürmann and B. Markert (eds.), Ecotoxicology. New York and Heidelberg: Wiley and Spektrum Akadem. Publ.

Gellert, G. and Heinrichsdorff, J. (2001) Effect of age on the susceptibility of zebrafish eggs to industrial wastewater. Water Res 35: 3754-7.

Goltz, B. (2007) Messung der Aufnahme von gelösten und partikulär gebundenen Schadstoffen im Embryo von Danio rerio mit Hilfe der radioaktiven Analytik. (not published).

Gonzalez-Doncel, M., Fernandez-Torija, C., Hinton, D.E., Tarazona, J.V. (2004) Stage-specific toxicity cypermethrin to medaka (*Oryzias latipes*) eggs and embryos usinga refined methodology for an in vitro fertilization bioassay. Arch. Eviron. Contam. Toxicol. 48: 87-98.

Gundel, U.et al. (2007) Vitellogenin cleavage products as indicators for toxic stress in zebra fish embryos: a proteomic approach. Proteomics 7: 4541-54.

Haertle, D. (2006) The principle of confocal microscopy, Swiss. Physicist at the University of Bonn, illustration online at http://en.wikipedia.org/wiki/File:Confocalprinciple.svg, on August 13th, 2009.

Hagedorn, M., Hsu, E.W., Pilatus, U., Wildt, D.E., Rall, W.R. and Blackband, S.J. (1996) Magnetic resonance microscopy and spectroscopy reveal kinetics of cryoprotectant permeation in a multicompartmental biological system. Proc Natl Acad Sci U S A 93: 7454-9.

Hagedorn, M., Kleinhans, F.W., Freitas, R., Liu, J., Hsu, E.W., Wildt, D.E. and Rall, W.F. (1997) Water distribution and permeability of zebrafish embryos, Brachydanio rerio. J Exp Zool 278: 356-71.

Hansch, C. and Dunn, W.J., 3rd (1972) Linear relationships between lipophilic character and biological activity of drugs. J Pharm Sci 61: 1-19.

Harris, D.L., Mutz, M. (2006) Debunking the Myth: Validation of fluorescein for testing the precision of nanoliter dispensing. Journal of the association for Laboratory Automation, Volume 11, Issue 4: 233-239.

Hart, N. and Donovan, M. (1983) Fine structure of the chorion and site of sperm entry in the egg of *Brachydanio*. The Journal of Experimental Zoology 227: 277-296.

Harvey, B., Kelley, R.N. and Ashwood-Smith, M.J. (1983) Permeability of intact and dechorionated zebra fish embryos to glycerol and dimethyl sulfoxide. Cryobiology 20: 432-9

Helmstetter, M. F., Alden III, R. W. (1995) Passive trans-chorionic transport of toxicants in toically treated Japanese medaka (*Oryzias latipes*) eggs. Aquatic Toxicology 32: 1-13.

Helmstetter, M. F., Maccubbin, A.E., and Alden, R. W. (1996) The medaka embryo-larval assay: an in vivo assay for toxicity, teratogenicity, and carcinogenicity (93-124). In: Ostrander, G. (eds.), Techniques in Aquatic Toxicology. Crc Press, 704 pp.

Hendrickson, J.B., Huang, P., Toczko, A.G. (1987) Molecular complexity - a simplified formula adapted to individual atoms. J. Chem. Inf. Comput. Sci. 27: 63-67.

Hermann, K., (1993) Effects of the anticonvulsant drug valproic acid and related substances on the early development of the zebrafish (*Brachydanio rerio*). Toxic. in Vitro 7, 41-54.

Herskovits, T.T. and Laskowski, M., Jr. (1962) Location of chromophoric residues in proteins by solvent perturbation. I. Tyrosyls in serum albumins. J Biol Chem 237: 2481-92.

Holocombe, G. W., Fiandt, J. T. and Phipps, G. L. (1980) Effect on pH increases and sodium chloride additions on the acute toxicity of 2,4-dichlorophenol to the fathead minnow. Wat. Res. 14, 1073-1077.

Howe, K.J. and Clark, M.M. (2002) Fouling of microfiltration and ultrafiltration membranes by natural waters. Environ Sci Technol 36: 3571-6.

ImageJ (2009) Analyze Menu, Handbook online at http://rsbweb.nih.gov/ij/docs/menus/analyze.html, on August 12th 2009

Inohaya, K., Yasumasu, S., Yasumasu, I., Iuchi, I. and Yamagami, K. (1999) Analysis of the origin and development of hatching gland cells by transplantation of the embryonic shield in the fish, Oryzias latipes. Dev Growth Differ 41: 557-66.

Inoué, S. (2006) Foundation of confocal scanned imaging in light microscopy (1 - 16). In: Pawley, J.B. (editor), Handbook of Biological Confocal Microscopy, Berlin: Springer, 988 pp.

Invitrogen ™, product information (2006) Dextran conjugates, online at http://probes.invitrogen.com/media/pis/mp01800.pdf, on August 12th., 2009.

ISO (1996) Water quality – determination of the acute lethal toxicity of substances to a freshwater fish [*Brachydanio rerio*) Hamilton-Buchanan (*Teleostei, Cyprinidae*)] – Part 1: Static method (ISO 7346-1), Part 2 – Semistatic (ISO 7346-2), Part 3 - Flow-through method (ISO 7346-3) Geneva: International Standardisation Organisation.

ISO (2007) Water quality – Determination of the acute toxicity of waste water to zebrafish eggs (Danio rerio). ISO 15088:2007.

Jansen, P.L., Chowdhury, J.R., Fischberg, E.B. and Arias, I.M. (1977) Enzymatic conversion of bilirubin monoglucuronide to diglucuronide by rat liver plasma membranes. J Biol Chem 252: 2710-6.

Jones, A. (1972) Studies on egg development and larval rearing of turbot, *Scophthalmus maximus*. J. Mar. Biol. 52: 63-66.

Kane, D. A. and Kishimoto, Y. (2001) Cell labellingand transplantation techniques. In: Zebrafish (95-120). First Volume, Nüsslein-Volhard, C. and Dahm, R. (eds), Oxford University Press, 2001, 328 pp.

Kim, D.H., Sun, Y., Yun, S., Kim, B., Hwang, C.N., Nelson, B. and Lee, S.H. (2004) Mechanical property characterization of the zebrafish embryo chorion. Conf Proc IEEE Eng Med Biol Soc 7: 5061-4.

Kimmel, C.B. und Law, R.D. (1985) Cell lineage of zebrafish blastomeres. II. Formation of the yolk syncytial layer. Dev Biol 108: 86-93.

Kimmel, C.B., Ballard, W.W., Kimmel, S.R., Ullmann, B. and Schilling, T.F. (1995) Stages of embryonic development of the zebrafish. Dev Dyn 203: 253-310.

Kishino, T. and Kobayashi, K. (1994) Relationship between the chemical structures of chlorophenols and their dissociation constants and partition coefficients in several solvent-water systems. Wat. Res. 28, 1547-1552.

Kishino, T. and Kobayashi, K. (1995) Relation between toxicity and accumulation of chlorophenols at various pH, and their absorption mechanism in fish. Wat. Res. 29, 431-442.

Kishino, T. and Kobayashi, K. (1996 a) Studies on the mechanism of toxicity of chlorophenols found in fish through quantitative structure-activity relationships. Wat. Res. Vol. 30, No. 2, pp. 393-399.

Kishino, T. and Kobayashi, K. (1996 b) Acute toxicity and structure-activity relationships of chlorophenols in fish. Wat. Res. 30, 387-392.

Kobayashi, K. and Kishino, T. (1980) Studies on the metabolism of chlorophenols in fish – XIII. Effect of pH on the toxicity and accumulation of pentachlorophenol in goldfish. Nippon Suisan Gakkaishi 46, 167-170.

Kobayashi, K., Akitake, and Manabe, K. (1979) Studies on the metabolism of chlorophenols in fish – X. Relationbetween toxicity and accumulation of various chlorophenols in goldfish. Nippon Suisan Gakkaishi 45, 173-175.

Kobayashi, K., Kimura, S. and Shimizu, E. (1977) Studies on the metabolism of chlorophenols in fish – IX. Isolation and identification of pentachlorophenyl-β-glucuronide accumulated in bile of goldfish. Nippon Suisan Gakkaishi 43, 601-607.

Lammer, E., Carr, G.J., Wendler, K., Rawlings, J.M., Belanger, S.E., Braunbeck, T. (2009) Is the fish embryo test (FET) with the zebrafish (Danio rerio) a potential alternative for the acute toxicity test? Comparative Biochemistry and Physiology, Part C 149: 196-209.

Lawson, N.D. and Weinstein, B.M. (2002) Arteries and veins: making a difference with zebrafish. Nat Rev Genet 3: 674-82.

Lee, J.W., Na, D.S., Chae, S.K., Kim, C., Kang, J.Y., Ju, B.K., Lee, H., Kim, S.U., Hwang, C.N. and Lee, S.H. (2005) Using the chorions of fertilized zebrafish eggs as a biomaterial for the attachment and differentiation of mouse stem cells. Langmuir 21: 7615-20.

Leonard, M., Vanpoucke, M., Petit-Poulsen, V., Porcher, J.M. (2005) Evaluation of thr fish embryo test as a potential alternative to the standard acute fish toxicity test OECD 203. In: International Symposium on Toxicology Assessment, Skathios, Greece.

Leonhardt, H., Gordon, L., and Livingston, R. (1971) Acid-base equilibria of fluorescein and 2,7- dichlorofluorescein in their ground and fluorescent states. J Phys Chem. 75: 245-249.

Liu, D., Thomson, K. and Kaiser, K.L. (1982) Quantitative structure-toxicity relationship of halogenated phenols on bacteria. Bull Environ Contam Toxicol 29: 130-6.

Marguerie, M., Gustafson, A., Panter, G., Stewart, J., Hutchinson, T., Alderton, W., Oskarsson, W. (2007) A pilot study on the effects of mechanical dechorionation on developmental toxicity in zebrafish embryos. Poster session presented at HESI Workshop on Alternative Assays for Developmental Toxicity, Health and Environmental Sciences Institute (HESI). February 27-28, 2007, Cary, North Carolina.

Marking, L. L. (1969) Toxicity of rhodamine b and fluorescein sodium to fish and their compatibility with antimycin a. Prog. Fish-Cult. 31 (3): 139-142).

McLeese, D. W., Zitko, V. and Peterson, M. R. (1979) Structure-lethality relationships for phenols, anilines and other aromatic compounds in shrimp and calms. Chemosphere 8, 53-57.

Nagel, R. (2002). DarT: The embryo test with the zebrafish Danio rerio – a general model in ecotoxicology and toxicology. *ALTEX 19*, 38-48.

OECD (2000) Guidance document on aquatic toxicity testing of difficult substances and mixtures. OECD Series on Testing and Assessment number 23, ENV/JM/MONO(2000)6). OECD Environment Directorate, Paris (http://www.oecd.org/ehs/), p.22

Ozoh, P.T., (1980) Effects of reversible incubations of zebrafish eggs in copper and lead ions with or without shell membranes. Bull. Environ. Contam. Toxicol. 24: 270-275.

Parker, A. J. (1962) The effects of salvation on the properties of anions in dipolar aprotic solvents. Q. Rev. Chem. Soc. 16, 163-187.

Poupard, G.et al. (2000) Apolipoprotein E gene expression correlates with endogenous lipid nutrition and yolk syncytial layer lipoprotein synthesis during fish development. Cell Tissue Res 300: 251-61.

PubChem (2009) data from National Cancer Institute (NCI) open database, online at http://pubchem.ncbi.nlm.nih.gov/help.html#Glossary on July 7th 2009.

Puig Muset, P. and Martin-Esteve, J. (1965) Physiological cell permeability and pharmacological action of DMSO. Experientia 21: 649-51.

Rammler, D.H. and Zaffaroni, A. (1967) Biological implications of DMSO based on a review of its chemical properties. Ann N Y Acad Sci 141: 13-23.

Rand, G.M. and Petrocelli, S.R. (1985): Aquatic Toxicology (1-28). In: Rand, G.M. and Petrocelli, S.R. (eds.), Fundamentals of Aquatic Toxicology. Hemisphere Publishing Corporation.

Rawson, D. M., Zhang, T., Kalicharan, D., and Jongebloed, W. L. (2000) Field emission scanning electron microscopy and transmission electron microscopy studies of the chorion, plasma membrane and syncytial layers of the gastrula-stage embryo of the zebrafish *Brachydanio rerio*: a consideration of the structural and functional relationships with respect to cryoprotectant penetration. Aquaculture Research 31: 325-336.

Ribo, J. M. and Kaiser, K. L. E. (1983) Effects of selected chemicals to photoluminescent bacteria and their correlations with acute and sublethal effects on other organisms. Chemosphere 12, 1421-1442.

Rieb, J-P (1973) La circulation sanguine chez l´embryon de Brachydanio rerio. Ann Embryol Morphol 6:43-54.

Ritter, L., Solomon, K.R., Forget, J., Stemeroff, M., O'Leary, C. (1995) Persistent organic pollutants. United Nations Environment Programme, online at http://www.chem.unep.ch/pops/ritter/en/ritteren.pdf on August 10th 2009.

Roberts, B. C. and White, R. G., (1992) Effects of angular wading on survival of trout eggs and pre-emergent fry. North American Journal of Fisheries Management, vol. 12, pp. 450-459.

Rogers, J. A. and Wong, A. (1980) The temperature dependence and thermodynamics of partitioning of phenols in the n-octanol-water system. Int. J. Pharm. 6, 339-348.

Rombough, P. (2002) Gills are needed for ionoregulation before they are needed for O_2 uptake in developing zebrafish, *Danio rerio*. J. Exp. Biol. 205: 1787-94.

Rudolf, M. (2000) Die Bedeutung unterschiedlicher Expositionswege für die Wirkung von Umweltgiften auf die Embryonalentwicklung von *Danio rerio*. Fakultät für Biologie, 175 pp.

Russell, W. M. S. and Burch, R. L. (1959). The principles of humane experimental technique. 238 pp. London: Methuen.

Saarikoski, J. and Viluksela, M. (1981) Influence of pH on the toxicity of substituted phenols to fish. Arch Environ Contam Toxicol 10: 747-53.

Scherrer, R.A. and Howard, S.M. (1977) Use of distribution coefficients in quantitative structure-activity relationships. J Med Chem 20: 53-8.

Schoots, A.F., Meijer, R.C. and Denuce, J.M. (1983) Dopaminergic regulation of hatching in fish embryos. Dev Biol 100: 59-63.

Stouthart, A.J.H.X., Spanings, F.A.T., Lock, R.A.C., Wendelaar Bonga, S.E. (1994). Effects on low water pH on lead toxicity to early life stages of the common carp (*Cyprinus carpio*). Aquat. Toxicol. 30: 137-151.

Svobodova, Z., Bulinova, J., Machova, B., Vykusova, B., and Faina, R. (1986) The toxicity of selected organic dyes to aquatic organisms. Pr. Vyzk. Ustav Ryb. Hydrobiol. Vodnany 15: 52-60.

Therapeutic Goods Administration (2007), online at http://www.novartis.com.au/PI_PDF/flu.pdf on August 8th., 2009.

Tonogai, Y., Ogawa, S., Ito, Y. and Iwaida, M. (1982) Actual survey on TLm (median tolerance limit) values of environmental pollutants, especially on amines, nitriles, aromatic nitrogen compounds and artificial dyes. J Toxicol Sci 7: 193-203.

Trinkaus, J.P. (1992) The midblastula transition, the YSL transition and the onset of gastrulation in Fundulus. Dev Suppl 75-80.

Trinkaus, J.P. (1993) The yolk syncytial layer of Fundulus: its origin and history and its significance for early embryogenesis. J Exp Zool 265: 258-84.

Tsien, R.Y., Waggoner, A. Pawley, J.B. (eds) (1995). Fluorophores for confocal microscopy. Handbook of biological confocal microscopy. Springer Netherlands. pp. 267-74.

Van Leeuwen, C.J., Griffioen, P.S., Vergouw, W.H.A., Maas-Diepeveen, J.L. (1985) Differences in susceptibility of early life stages of the rainbow trout (*Salmo gairdneri*) to environmental pollutants. Aquatic Toxicology 7: 59-78.

Villalobos, S.., Hamm, J.T., The, S.J., Hinton, D.E., (2000) Thiobencarb-induced embryotoxicity in medaka (*Oryzias latipes*): stage-specific toxicity and the protective role of chorion. Aquat. Toxicol. 48: 309-326.

Wallace, R.A. und Jared, D.W. (1969) Studies on amphibian yolk. 8. The estrogen-induced hepatic synthesis of a serum lipophosphoprotein and its selective uptake by the ovary and trasformation into yolk platelet proteins in *Xenopus laevis*. Dev Biol 19: 498-526.Byrne, B.M.et al. (1989) The evolution of egg yolk proteins. Prog Biophys Mol Biol 53: 33-69.

Webb, J.M. (1960) Studies of the metabolism of Rhodamine B (D & C Red 19). Federation Proc. 19, 125.

Webb, J.M. und Hansen, W.H. (1961) Studies of the metabolism of rhodamine B. Toxicol Appl Pharmacol 3: 86-95.

Wendemeyer, G. (1968) Uptake and distribution of ZN 65 in the coho salmon egg (*Oncorhynchus kisutch*). Comp. Biochem. Physiol. 26: 271-279.

Wendler et al. (in prep.)

Westerfield, M. (2000) The zebrafish book. A guide for the laboratory use of zebrafish (*Danio rerio*), 4. th ed., Univ. of Oregon Press, Eugene; online at http://zfin.org/zf_info/zfbook/zfbk.html, on August 9th., 2009.

Zamek-Gliszczynski, M.J., Xiong, H., Patel, N.J., Turncliff, R.Z., Pollack, G.M. and Brouwer, K.L. (2003) Pharmacokinetics of 5 (and 6)-carboxy-2',7'-dichlorofluorescein and its diacetate promoiety in the liver. J Pharmacol Exp Ther 304: 801-9.

Appendix

Pre-test Rhodamine b

Test 1			Test 2			Test 3		
	Mortality [%]			Mortality [%]			Mortality [%]	
Concentration [mg/L]	24 h	48 h	Concentration [mg/L]	24 h	48 h	Concentration [mg/L]	24 h	48 h
5	0	0	5	0	0	5	0	
75	20	20	45	0	0	45	0	
150	30	30	90	20	20	90	0	
225	90	90	130	20	20	130	0	
300	100	100	170	80	80	170	0	
400	100	100	215	100	100	215	70	
500	100	100	300	100	100	300	100	
negative control	0	0	negative control	0	0			
positive control	20	50	positive control	70	80			

Pre-test Sulforhodamine b

Test 1			Test 2			
	Mortality [%]			Mortality [%]		
Concentration			Concentration			
[mg/L]	24 h	48 h	[mg/L]	24 h	48 h	72 h
5	0	0	50	0	0	0
10	10	20	125	0	0	0
50	0	0	200	0	0	0
100	10	20	275	0	0	0
500	100	100	350	40	40	40
1000	100	100	425	100	100	100
			500	100	100	100
negative			negative			
control	-	-	control	0	0	0
positive			positive			
control	-	-	control	-	-	-

Pre-test Fluorescein

Test 1				Test 2					
		Mortality [%]				Mortality [%]			
Concentration [mg/L]	DMSO [%]	24 h	48 h	Concentration [mg/L]	DMSO [%]	24 h	48 h	72 h	120
1	0,001	0		25	0,025	0	10	10	10
10	0,01	10		50	0,05	0	0	0	0
50	0,05	0		100	0,1	0	0	0	0
100	0,1	0		200	0,2	0	0	0	0
500	0,5	0		300	0,3	0	0	0	0
1000	1	0		400	0,4	0	0	0	0
				500	0,5	0	0	0	0
				DMSO 1%		0	0	0	0
negative control		-		negative control		0	0	0	0
positive control		-		positive control		10	70	70	70

Pre-test 2, 7- Dichlorofluorescein

Test 1				Test 2			
		Mortality [%]				Mortality [%]	
Concentration [mg/L]	DMSO [%]	24 h	48 h	Concentration [mg/L]	DMSO [%]	24 h	48 h
5	0.01	0	0	50	0.17	10	10
10	0.03	30	30	65	0.22	100	100
25	0.08	0	0	85	0.28	100	100
50	0.16	0	0	100	0.33	100	100
100	0.33	100	100				
200	0.67	100	100				
300	1	100	100				
DMSO 1%	-	-	-	DMSO 1%		0	0
negative control	-	-	-	negative control		0	10
positive control	-	-	-	positive control		0	0

Pre-test 5-carboxy- 2,7-dichlorofluorescein

	Mortality [%]	
Concentration [mg/L]	24 h	48 h
10	0	0
25	10	10
50	5	5
80	0	0
negative control	5	5

Pretest dextran fluorescein 3 kDa

	Test 1		Test 2	
	Mortality [%]		Mortality [%]	
Concentration [mg/L]	24 h	48 h	24 h	48 h
50	5	5	10	10
negative control	0	0	0	5

Pre-test dextran fluorescein 40 kDa

	Test 1		Test 2	
	Mortality [%]		Mortality [%]	
Concentration [mg/L]	24 h	48 h	24 h	48 h
50	5	5	10	10
negative control	5	5	0	0